

Salt extraction by poulticing: an NMR study

PROEFSCHRIFT

ter verkrijging van de graad van doctor aan de
Technische Universiteit Eindhoven, op gezag van de
rector magnificus, prof.dr.ir. C.J. van Duijn, voor een
commissie aangewezen door het College voor
Promoties in het openbaar te verdedigen
op woensdag 23 november 2011 om 16.00 uur

door

Victoria Voronina

geboren te Sint-Petersburg, Rusland

Dit proefschrift is goedgekeurd door de promotor:

prof.dr.ir. K. Kopinga

Copromotor:

dr.ir. L. Pel

CIP-DATA LIBRARY EINDHOVEN UNIVERSITY OF TECHNOLOGY

Voronina, Victoria

Salt extraction by poulticing: an NMR study / by Victoria Voronina. -

Eindhoven : Eindhoven University of Technology, 2011. -

Proefschrift. ISBN 978-90-386-2849-3

Cover design: Tamara Druzhinina and Victoria Voronina

Printed by: Ipskamp Drukkers B.V., Enschede, The Netherlands

The work described in this thesis has been carried out in the group Transport in Permeable Media at the Eindhoven University of Technology, Department of Applied Physics. Part of this work is supported by the EC Desalination project (FP6 022714).

To my family

SUMMARY

The crystallization of salts is widely recognized as one of the most significant causes of damage to many cultural objects consisting of porous materials, such as monuments, sculptures, historic buildings, wall paintings, etc. A common response to salt damage problems are treatments aimed at reducing the salt content of the affected object, most typically through the application of poultices. Poultices are applied to porous materials in order to extract soluble salts. The process of poulticing is relatively simple in theory, but in practice the efficiency of the salt extraction is more difficult to predict. This study aims to develop a better understanding of the physical principles of the salt and moisture transport by which poultices function.

A desalination treatment by poultice includes two main phases. The first is the wetting phase: water is transported from the poultice into the wall, where it starts to dissolve the salts. The second phase is the salt extraction. The dissolved salt ions travel in the form of an aqueous saline solution from the substrate into the poultice. This salt migration can be the result of two different processes. The first is generated by the existence of a concentration gradient between the substrate and the poultice. In this case the salt ions diffuse through the solution. The other one is realized by the capillary water flow from the substrate to the poultice (generally resulting from drying). In this case the salt ions are transported by the moving solution (advection).

If salt ions are advected from the substrate into the poultice by capillary moisture flow, a concentration gradient will be established. Because of this salt concentration an osmotic pressure will develop.

One of the aims of this study was to investigate the potential contribution of osmotic pressure to salt extraction during drying of the poultice. For this purpose we have conducted a series of experiments to investigate the influence of osmotic pressure on ion transport processes. Nuclear Magnetic Resonance (NMR) techniques were used to obtain information on the water and salt distribution in the poultice/substrate system during desalination. The results of the experiments show that the contribution of the osmotic pressure can have a significant influence on the desalination process.

Poultices which contain different mixes of clay and sand were studied in order to understand the influence of each component on the drying behavior of the poultice. Desalination experiments in controlled environmental conditions were carried out on substrates with well known pore size distributions. NMR was used to obtain information on the water and salt distribution in the poultice/ substrate system during desalination.

The study demonstrates the relation between salt extraction and pore structure parameters of the poultice/substrate system. It also shows the influence of

some additional factors, such as an interventional layer between substrate and poultice, on the salt extraction during the desalination treatment.

SAMENVATTING

De kristallisatie van zouten is een van de meest belangrijke oorzaken van schade aan veel culturele objecten bestaande uit poreuze materialen, zoals monumenten, sculpturen, historische gebouwen, muurschilderingen, etc. Een gebruikelijke aanpak van de problemen ten gevolge van zoutschade bestaat uit het verminderen van de hoeveelheid zout in het aangetaste object. Dit gebeurt meestal door het aanbrengen van zogeheten poultices, een soort natte kompressen, waarmee een deel van de in water oplosbare zouten uit een poreus materiaal verwijderd kan worden.

In theorie is het proces van zoutonttrekking via poultices relatief eenvoudig, maar in de praktijk is de efficiëntie van dit proces zeer moeilijk te voorspellen. Het doel van het in dit proefschrift beschreven onderzoek is het ontwikkelen van een beter begrip van de fysische principes van het vocht- en zouttransport waarop de werking van poultices is gebaseerd.

Een zoutonttrekking met behulp van poultices bestaat uit twee fasen. De eerste is de bevochtigingsfase; hierbij wordt water vanuit de poultice aan het object toegevoerd, zodat de daar aanwezige zouten kunnen oplossen. De tweede fase is de feitelijke zoutonttrekkingsfase, waarbij de poultice droogt. De opgeloste zout-ionen verplaatsen zich dan van het object naar de poultice. Deze zoutmigratie kan veroorzaakt worden door twee verschillende processen. Het eerste proces is diffusie van de zout-ionen door de oplossing ten gevolge van een zoutconcentratiegradint tussen het object en de poultice. Het tweede proces is capillaire stroming van het object naar de poultice (doorgaans een gevolg van het drogen van de poultice). Hierbij bewegen de zout-ionen mee met de stromende oplossing (advectie).

Als zout-ionen ten gevolge van capillair vochttransport van het object naar de poultice verplaatst worden, zal een concentratiegradint ontstaan. Hierdoor zal een osmotische druk optreden. Een van de doelstellingen van de hier beschreven studie is een onderzoek naar de mogelijke bijdrage van de osmotische druk aan de zoutonttrekking tijdens het drogen van de poultice. Voor dit doel hebben we een reeks experimenten uitgevoerd om de invloed van de osmotische druk op het transport van ionen in kaart te brengen. Nuclear Magnetic Resonance (NMR) technieken werden gebruikt om informatie te verkrijgen over de ruimtelijke verdeling van water en zout in een aantal poultice/ondergrond systemen tijdens de zoutonttrekking. Uit de resultaten van deze experimenten blijkt dat de osmotische druk een belangrijke invloed kan hebben op dit proces.

Poultices bestaand uit verschillende mengsels van klei en zand werden bestudeerd om de invloed van elke component op het drooggedrag van de poultice te begrijpen. Zoutonttrekkings experimenten onder gecontroleerde omgevingscondities zijn uitgevoerd aan ondergronden met bekende poriegrootte verdelingen.

NMR werd gebruikt om informatie over de verdeling van water en zout te verkrijgen in de het poulitice/ondergrond systeem tijdens dezoutontrekking.

Deze studie toont een duidelijk verband aan tussen de zoutonttrekking en de eigenschappen van de poriestructuur van het poulitice/ondergrond systeem. Ook is informatie gekregen over de invloed op de zoutonttrekking van een aantal andere factoren, zoals een extra "interventie" laag tussen ondergrond en poulitice.

CONTENTS

1. <i>Introduction</i>	1
1.1 Introduction	1
1.2 Characteristics of poultices	4
1.3 Efficiency of poultice treatment	4
1.4 Scope of the thesis	6
1.5 Outline of this thesis	6
2. <i>Theory:working principles of poultices</i>	7
2.1 Introduction	7
2.2 Diffusion based methods	9
2.2.1 Diffusion	9
2.2.2 Salt extraction by diffusion	9
2.2.3 Efficiency	10
2.3 Advection-based methods	13
2.3.1 The ideal case: only advection	13
2.3.2 The non-ideal case: as in practice	17
2.3.3 Combined poultice: wetting and desalination	19
2.4 Discussion and conclusion	20
2.4.1 Wetting phase	20
2.4.2 Salt extraction phase	21
3. <i>Osmotic pressure in a two layered porous material system</i>	23
3.1 Introduction	23
3.2 Theory	25
3.2.1 Capillary pressure	25
3.2.2 Capillary pressure and osmotic pressure	28
3.3 Experimental setup	29
3.3.1 Nuclear Magnetic Resonance (NMR) analysis	29
3.3.2 Materials	33
3.4 Results and discussions	33
3.4.1 Moisture saturated samples	33
3.4.2 Saline solution saturated samples	35
3.4.3 Discussion and Conclusion	37
4. <i>Experimental techniques</i>	41
4.1 NMR	41
4.1.1 NMR basics	41
4.1.2 Spin echo detection	44

4.1.3	NMR and pore size distributions of porous materials . . .	45
4.1.4	NMR measurement setup	46
4.2	Methods of measuring the capillary pressure curve	47
4.2.1	Pressure plate	47
4.2.2	Mercury intrusion porosimetry	49
4.2.3	Ion Chromatography (IC)	50
5.	<i>Osmotic pressure in a poultice/substrate system</i>	53
5.1	Introduction	53
5.2	Theory	54
5.2.1	Capillary pressure	54
5.2.2	Capillary pressure and osmotic pressure	58
5.2.3	Shrinkage and osmotic pressure	58
5.2.4	Peclet number and desalination	60
5.3	Experimental setup	62
5.3.1	Sample materials	62
5.3.2	Experimental design	62
5.4	Results and Discussion	63
5.4.1	Poultice (saline solution)/Substrate (water)	63
5.4.2	Poultice (water)/Substrate (saline solution)	65
5.4.3	Poultice (saline solution)/Substrate (saline solution) . . .	67
5.5	Discussion and Conclusions	67
6.	<i>Poultice composition</i>	69
6.1	Introduction	69
6.2	Results and discussions	70
6.2.1	Poultice/fired-clay brick	70
6.2.2	Poultice/Dutch limestone	78
6.3	Conclusions	83
7.	<i>Intervention layer</i>	87
7.1	Introduction	87
7.2	Results and Discussion	88
7.3	Conclusions	94
8.	<i>Conclusions and outlook</i>	95
8.1	Conclusions	95
8.2	Outlook	96
	<i>Appendix A. Boltzmann's transformation</i>	99
	<i>Appendix B. Water velocity</i>	101
	<i>References</i>	103
	<i>List of Publications</i>	109
	<i>Acknowledgement</i>	111

Curriculum Vitae 115

1. INTRODUCTION

1.1 *Introduction*

It has been known since ancient times that the presence of salt can cause damage in porous building materials. Herodotus already reported in his book "The histories": "salt exudes from the soil to such an extent it affects even the pyramids" (about 440BC, translation from 1972) [Her420].

Historical monuments, buildings, and wall paintings are a significant part of the world cultural heritage. One of the most common causes of the deterioration of these objects is salt weathering [Gou97], [Lew80]. Salt weathering reveals itself in both physical and aesthetic damage. This process is influenced by environmental conditions and the characteristics of the salts present in the environment or the object.

Historical buildings and monuments are mostly made of porous materials. Because of this characteristic feature moisture can enter the object and carry various soluble salts inside or dissolve and displace salts that are present. Moisture can enter into a porous material through capillary rise from ground water, rainwater, and vapor condensation. When environmental conditions change, the salt solution inside a porous material can dry. During drying salts can crystallize in the porous network and may cause stresses inside the pores. These stresses are responsible for internal cracking of the porous material. A typical example of salt damage is shown in figure 1.1.

Attempts to restore damaged buildings and monuments were made already centuries ago. However, in the XVIII–XIX centuries the damaged buildings were often repaired by replacement of damaged parts or they were rebuilt completely. Such a restoration is destructive, both for the ancient material with its archeological interest and for the whole historical monument with its character of age. In the middle of the XIX century it became clear that loss of historical heritage implies the risk to lose the values that represent the past culture and traditions of our society. Therefore, as a result of the accumulation of systematic knowledge in the field of art history, materials structures, and engineering, conservation became a field of science in the XIX–XX centuries. During this time scientists began to study the damaging effects of the environment to works of art. The first scientific study on salt crystallization and pressure was done by Lavalle. In 1853 he published a paper [Lav53] where he described experiments which indicated the ability of salts to push away a certain weight. Due to this force crystals can damage porous materials.

A common response to salt damage problems is salt content reduction. Consequently, desalination of the material has become a crucial step in conservation and restoration. The first document about desalination of a porous material was

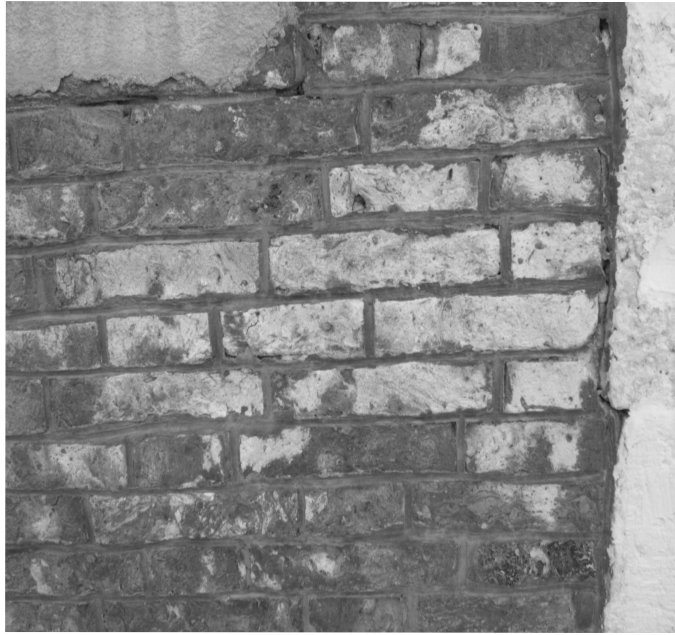


Fig. 1.1: A typical example of salt damage observed for masonry.

published by Rathgen [Rat15] in 1915. In this publication he reported about the desalination of ancient Egyptian art by a so-called bath method, which was performed in 1890. In this bath method the object is immersed in water which is refreshed continuously. Because of a difference in salt concentration between the porous material and the water in the bath, salt is transported from the object by diffusion. Nowadays the bath method is mostly used to desalinate small movable objects. However, problems can arise due to the fragility of the object's surface or the presence of materials that can be affected by water (e.g., pigments and binding media). Therefore, for such materials other methods should be used.

Later another method was invented which enables the removal of salts from non-moveable and fragile objects. This method involves the use of a poultice. The term poultice has its origin in the field of medicine where it refers to the application of a cleaning pack to the body to relieve infection [Woo00]. The advantage of this method is that it introduces less moisture into the object to be desalinated. Moreover, this method is fast, i.e., the time period for salt extraction is of the order of days and the object is dry after desalination.

The desalination by poultices consists of the application of a wet poultice material to the surface of the object to be treated. This material is kept in place for some time before being removed. Because of drying and differences in salt concentration between the material and the poultice, the salt is transported from the object to the poultice.

Cleaning of the surface of limestone by a lime poultice was pioneered and developed by Robert Baker in the 1950's. Hot lime was applied to the surface of the limestone. Once the hot lime had been applied it was covered with scrim, wet sacking, and polythene. It was essential that the cover remained wet and no



Fig. 1.2: An example of poultice application on a test wall in Venice.

drying was allowed. After some time the poultice with dirt was removed from the surface. Later in 1975 Bowley [Bow75] demonstrated that it was possible to extract a considerable quantity of salt from masonry through the repeated use of clay poultices. Today poulticing is one of the most common approaches in conservation to extract salt from a masonry, because this method can be applied in situ. An example of poultice application on a test wall is shown in figure 1.2.

Since the method of salt extraction by poultices was introduced it has widely been used by conservators and practitioners. However, the parameters which control the desalination efficiency are not exactly known [Ver05]. A survey among practitioners in the field has shown that details of the treatment may vary from one practitioner to another and the efficiency of the salt extraction is rather difficult to predict. Therefore, such studies are only of limited use to identify the key parameters which govern the desalination efficiency [Her08],[Saw08]. A better understanding of the physical phenomena of water and salt transport in the poultice and the material on which the poultice is applied, the substrate, is needed to describe the parameters controlling the desalination process and to achieve a better poultice performance.

1.2 Characteristics of poultices

A poultice typically consists of a porous hydrophilic mixture of materials wetted with liquid. The desalination poultice mixtures available on the market are predominantly based on cellulose, paper pulp, clay, and aggregate materials. The ratio of the components can vary in order to comply with specific properties of the substrate. This mixture of materials is blended with liquid in such a way, that it can be easily applied to a vertical surface such as a wall. When poultice is applied on a surface, it should not shrink too much during drying and should have a good adhesion and workability.

The shrinkage, adhesion, and workability are determined empirically. The shrinkage of a poultice is frequently measured by a method used in soil science. The wet poultice is put on a cylindrical glass petri dish, and is dried at constant temperature and air flow. The diameters of the poultice sample in the wet and dry state are used to calculate the shrinkage [Bou08b]. Ideal poultice does not shrink. However, all materials available on the market have a certain degree of shrinkage. In order limit the risk of poultice detachment, the shrinkage should be small.

In order to characterize the workability of a poultice a flow test for a mortar can be used. This is possible because a poultice has many characteristics in common with fresh mortars. The standard flow test uses a mortar sample with a conical frustum shape. The sample is placed on a flow table and thrown several times within a certain period of time. The thrown mortar spreads out on the flow table. The initial and final diameters of the mortar sample are used to calculate the mortar flow. The flow values are related to the workability properties [Bou08b].

Until now there is no standardized adhesion test available. A new test method has been proposed by A. Bourgès and V. Vergès-Belmin [Bou08b]. In this method the researchers use a table, to which a porous substrate is fixed in a vertical position. The fresh poultice is applied to the substrate and a certain amount of mechanical shocks are delivered via the table. The adhesion, expressed as a percentage, is related to the number of shocks the poultice resists before it detaches and the fraction of the poultice that detaches from the substrate. The researchers claim that this method can be adapted to various categories of substrates.

1.3 Efficiency of poultice treatment

The selection of a poultice in terms of adhesion, shrinkage, and workability does not necessarily imply a high efficiency of the subsequent salt extraction treatment. The salt extraction efficiency for a particular poultice/substrate system can be characterized by means of dimensionless efficiency value ε :

$$\varepsilon = \frac{|\Delta m|}{m_0} \times 100\%, \quad (1.1)$$

where Δm [kg] is the mass difference of the amounts of salt in the substrate before and after extraction, and m_0 [kg] is the mass of the initial salt content.

We assume that because of the treatment there is a net decrease in the object's soluble salt content, and no increase (the latter might occur when dissolved salts react to form new salts).

The efficiency value can be used to classify the efficiency of the treatment. For example, within the EU-project Desalination (FP6 022714) the following classification system for different ranges of efficiency has been adopted:

Quality	Efficiency (%)
very high	90 – 100
high	75 – 90
medium	50 – 75
low	25 – 50
very low	0 – 25
dangerous, salt enrichment	< 0

Depending on the dominant salt migration process, poulticing treatments can be divided into methods based on diffusion (i.e. the transport of a salt from the substrate to the poultice because of a concentration gradient) and advection (i.e., the transport of a salt within flowing water).

Diffusion based extraction methods can reach an efficiency of 100%, but they are extremely slow. It can take weeks or months to achieve an acceptable extraction efficiency [Pel10]. Moreover, the method requires the substrate to remain completely water saturated for a long time. Hence this method may result in additional damage due to dissolution of the material, swelling of organic components, chemical alteration of pigments and binding media, bio-deterioration, and other water related decay processes [Saw08].

In order to speed up salt extraction using a poultice, a faster ion transport by water advection is required. Advection is realized by capillary water flow from the substrate to the poultice (generally induced by drying), where dissolved ions move together with the flow. In the case of advection based salt extraction (i.e., drying of poultices) the efficiency of salt extraction strongly depends on the pore-size range of the substrate compared to that of the poultice. Therefore, the poultice materials have to be adapted to the pore-size distribution of the substrate. However, since the pore-size distribution of the poultice materials may vary due to shrinkage during drying, such an optimization is far from straightforward [Saw10].

If salt ions are advected from the substrate into the poultice by capillary moisture flow, a concentration gradient will be established. As a consequence of this salt concentration gradient an osmotic pressure will develop. The influence of the osmotic pressure on water movement is well known in soil science [Whe25], [Let69], [Nas89]. Basically, the solvent (water) tends to flow from a region with a less concentrated solution to a region with a more concentrated solution. The osmotic pressure has already been taken into account in the modeling of water and salt transport during poulticing [Ngu08]. However, these authors did not recognize the effect of osmotic pressure on water flow during desalination.

1.4 Scope of the thesis

This thesis focuses on moisture and salt transport in poultice/substrate systems during drying. One of our aims is to investigate the contribution of the osmotic pressure on salt extraction by poultices. Until now the influence of osmotic pressure on water flow in the poultice/substrate system has not been described. We investigated the effect of osmotic pressure on water flow resulting from concentration gradients in the system during desalination. A model describing water transport in a two layered porous system was developed to examine the drying behavior of the poultice/substrate system.

The main experimental tool used in this study to examine the drying of the poultice/substrate system is Nuclear Magnetic Resonance (NMR). NMR is non-destructive technique widely used in medicine [And84] and chemistry [Man03]. NMR can also be used to study moisture and ion transport in porous media in situ. It has been shown that NMR is a powerful technique for measuring the combined transport of water and sodium in porous building materials [Pel00]. Therefore, using NMR it is possible to monitor the distribution of water and dissolved sodium ions in the poultice/substrate system during drying.

1.5 Outline of this thesis

In chapters 2 and 3 the theory of moisture and salt transport in a poultice/substrate system is introduced. In chapter 2 the physical principles of salt and moisture transport which are relevant for poultices are reviewed. It will be shown how, depending on the application methodology, the treatment by poulticing can be divided into diffusion and advection based methods. In chapter 3 the potential contribution of the osmotic pressure to salt extraction during poulticing treatments will be demonstrated.

The experimental techniques used for the experiments and the characterization of porous building materials are discussed in chapter 4. The measurements of the transport of moisture and salt in various poultice/substrate system are presented in chapter 5. Chapter 6 describes the influence of poultice composition on the desalination. In chapter 7 studies of water and salt transport in poultice/substrate systems with a so-called intervention layer are presented. Finally, in chapter 8 the general conclusions and suggestions for future research are given.

2. THEORY:WORKING PRINCIPLES OF POULTICES

The crystallization of soluble salts plays a significant role in the deterioration of porous cultural property. A common response to salt damage problems is to undertake treatments aimed at reducing the salt content of the affected object, most typically through the application of poultices. The process of poulticing is in theory relatively simple: the wet poultice material is applied to the surface of the object to be treated, and is kept in place for some period of time before being removed. However, in practice the efficiency of the salt extraction, or even the location of salt accumulation post treatment is more difficult to predict. This chapter examines the physical principles of salt ion and moisture transport by which poultices function, and shows how depending on the application methodology, these treatments can be divided into diffusion and advection based methods. The maximum salt extraction efficiency, the depth to which this can be achieved, and the time scale required is estimated for each type of poulticing system, to gain a better understanding of their working properties and performance. Finally, the pros, cons and limitations of desalination treatments are discussed.¹

2.1 Introduction

The crystallization of salts in porous media is widely recognized as one of the primary causes of irreversible damage to many cultural objects such as wall paintings, sculpture, historic buildings, and other artworks. Moreover, contemporary buildings and civil constructions also suffer from salt-related deterioration processes. Salt crystallization can therefore be regarded as a common deterioration problem with significant cultural and economic implications. Currently, most methods of treating salt damage problems are aimed at reducing the salt content of the affected object. While the removal of water soluble salts sounds easy, nevertheless this can prove difficult in practice, particularly in the case of objects that are monumental in scale. While small objects can be immersed in water, and so complete salt extraction is theoretically more possible, nevertheless, even here problems can arise due to the fragility of the object's surface, or the presence of materials that are adversely affected by water (e.g. pigments and binding media). More difficult is the removal of salts from large nonmoveable objects such as architectural surfaces (e.g. wall paintings and stone masonry) forming a constituent part of a building or monument. Such objects therefore require treatment in situ, one of the most common approaches

¹ The contents of this chapter have been published in Journal of Cultural Heritage, 11: 59-67, 2010

to which is to use a poultice.

In general the application methodology for poulticing is relatively simple: the wet poultice material is applied to the surface of the object to be treated, and is kept in place for some period of time before being removed. However, a recent survey of practitioners in the field has demonstrated the extent to which the precise details of the treatment method can vary from one practitioner to another, and in relation to the type of object undergoing treatment (e.g., in terms of the selection of poultice materials, intervention layers and the use of auxiliary materials to aid adhesion, conformance, bioresistance and alter drying rates, as well as the timing and sequence of poultice applications) [Saw08] and [Her08]. Nevertheless, the treatment itself can be summarized as having two main steps. The first is the wetting phase: water is transported from the poultice into the wall where it starts to dissolve the salts. The second phase is that of extraction, whereby the dissolved salt ions travel in the form of an aqueous saline solution from the wall back into the poultice. The cause of this salt migration is due to two different processes: it can either be generated by the existence of a concentration gradient between the object and the poultice, in which case the salt ions diffuse through the solution, or by capillary water flow from the object to the poultice (generally due to drying) in which the ions are advected within the solution [Ver05].

To evaluate the efficiency of salt extraction, it is important to compare the amounts of salt present before and after the extraction treatment. The desalination efficiency for a particular poultice/substrate system can be characterized by means of a dimensionless efficiency value ε [-]:

$$\varepsilon = \frac{|\Delta m|}{m_0} \times 100\%, \quad (2.1)$$

where Δm [kg] is the mass difference of salt before and after extraction, and m_0 [kg] is the total initial salt content. Here we assume that due to the treatment there is a net decrease in the object's soluble salt content, and no increase (as it can be in the case when dissolved salts react to form new salts).

The efficiency value can then be used to classify the efficiency of the treatment. However, it is important to note that the efficiency of a salt extraction treatment is dependent on the solubility of the salt, and also on the depth. For example, the degree of salt extraction achieved is generally higher at the object surface than at depth, resulting in a different degree of desalination efficiency. This leads to difficulties when trying to compare the findings of one researcher with those of another. Consequently, it is convenient to divide practical efficiency values into two categories: those that characterize the efficiency of desalination with respect to fixed depth intervals, and those that are concerned with whole length of substrate (i.e., the entire object).

One should also be aware of the confusion which can arise when discussing the *efficiency* of a salt extraction treatment versus its *effectiveness*. The term *effectiveness* also takes into account the effects of the treatment over a certain time period. Hence, a treatment could have a high efficiency approaching 100%, but if over time the treatment was observed to fail, then its effectiveness is low.

It can be demonstrated that the mechanism by which salts are transported during poulticing will strongly influence the efficiency of the treatment. Therefore, knowledge of physical principles governing the extraction process is needed in order to optimize treatment methods. The aim of this chapter is to categorize poulticing methods according to their physical mechanism of salt extraction, and to come to an understanding of how the maximum treatment efficiency can be achieved and the time required for this. We will first discuss desalination based on diffusion. Secondly, methods based on advection will be discussed. Finally, the pros and cons of each method will be evaluated with regard to practical treatment options.

2.2 Diffusion based methods

2.2.1 Diffusion

A good example of diffusion is the spreading out of a drop of ink in a glass of water. This is due to the Brownian motions of the water and ink molecules, and will continue until equilibrium has been reached such that the ink concentration is the same throughout. This process can be described by a simple diffusion equation, which is also referred to as Fick's second law:

$$\frac{\partial C}{\partial t} = D \frac{\partial^2 C}{\partial x^2}, \quad (2.2)$$

where C [mol/l] is the concentration and D [m²/s] is a diffusion coefficient of, for example, ink in water or dissolved salt ions in water, t [s] is the time and x [m] is the distance.

In porous materials particles cannot diffuse freely in all directions, but are instead restricted by the pore structure, and so the length of the effective diffusion pathway becomes longer. This is often referred as the tortuosity of a porous material. Hence, for a porous material the diffusion can be described by:

$$\frac{\partial C}{\partial t} = D_{eff} \frac{\partial^2 C}{\partial x^2}, \quad (2.3)$$

where D_{eff} [m²/s] is the effective diffusion coefficient for a given porous material. For a porous material the effective diffusion coefficient is given by:

$$D_{eff} = -\phi\chi D, \quad (2.4)$$

where ϕ [-] is the porosity of the material and χ [-] is the tortuosity. The porosity and the tortuosity together represent the influence of the pore structure on the diffusion process [Bea90], [Dul91]. For many porous building materials the diffusion coefficient is in the order of $0.1 - 1 \times 10^{-9}$ m²/s [Ahl04]. Here we have ignored any interactions, such as, for example, ion exchange between the solid matrix of the porous material and the solution.

2.2.2 Salt extraction by diffusion

In order to remove salts from an object by diffusion the object is brought into contact with an aqueous solution with a lower salt concentration, i.e., in

general close to zero. For the purposes of this argument, we will assume the concentration of the desalinating material remains constant (i.e., in the case when the object is flushed continuously with clean water, or the poultice is renewed very frequently).

In order to gain a better insight into the extraction process by diffusion it is helpful to first do some simulations. We shall consider a semi-infinite sample with the initial conditions $C = C_0$ at $x > 0$ and $t = 0$ (i.e. the sample is unsaturated), and the boundary conditions $C = 0$ at $x = 0$, $C = C_0$ for $x \rightarrow \infty$, $t > 0$. In this case the diffusion equation given in equation 2.5 can be reduced to an ordinary differential equation (see appendix A.1):

$$-\frac{\lambda}{2} \frac{dC}{d\lambda} = D_{eff} \frac{d^2C}{d\lambda^2}, \quad (2.5)$$

with the initial and boundary conditions $C = 0$ for $\lambda = 0$, and $C = C_0$ for $\lambda \rightarrow \infty$, λ being a Boltzmann variable which is defined as:

$$\lambda = \frac{x}{\sqrt{t}}. \quad (2.6)$$

Using the specified initial and boundary conditions, equation 2.5 has only one solution. Consequently, this demonstrates that the progress of the diffusion process is proportional to the square-root of time.

As an example, a simulation of salt extraction by diffusion is given in figure 2.1, which illustrates the change in the salt concentration profile of a porous material, over daily time intervals. As can be seen the rate of salt extraction becomes slower with time. In the same figure 2.1 the same profiles are given, but scaled according to the square root of time. As can be seen these scaled profiles all collapse onto one master curve, further illustrating the square root of time dependency of diffusion-based desalination processes.

2.2.3 Efficiency

In order to gain some indication of the extraction efficiency as a function of depth and time, a second simulation was performed. Here we have taken a masonry wall 100 mm thick and as a rough estimate a diffusion coefficient for the salt ions of 1×10^{-9} m²/s. However, it should be noted that given the degree to which the diffusion coefficient in many porous materials can vary, these simulations will in general give an underestimation of the time needed in practice. In figure 2.2 the efficiency of salt extraction over the first 20, 40, 60, 80 mm and the total thickness of 100 mm are given. As can be seen, to achieve 100% desalination of the sample at any given depth will take more than 200 days. It can also be seen that to achieve 80% desalination of the first 20 mm will take in the order of 10 days, and the first 40 mm around 30 days.

Hence, while it is possible to completely desalinate an object by diffusion, in general this is a slow process. Also, it should be noted that for the purposes of this discussion we have taken a relatively high ion diffusion coefficient, while for many porous building materials the ion diffusion coefficient will be lower. Therefore, to speed up the salt extraction process using a poultice, a faster ion transport process is required.

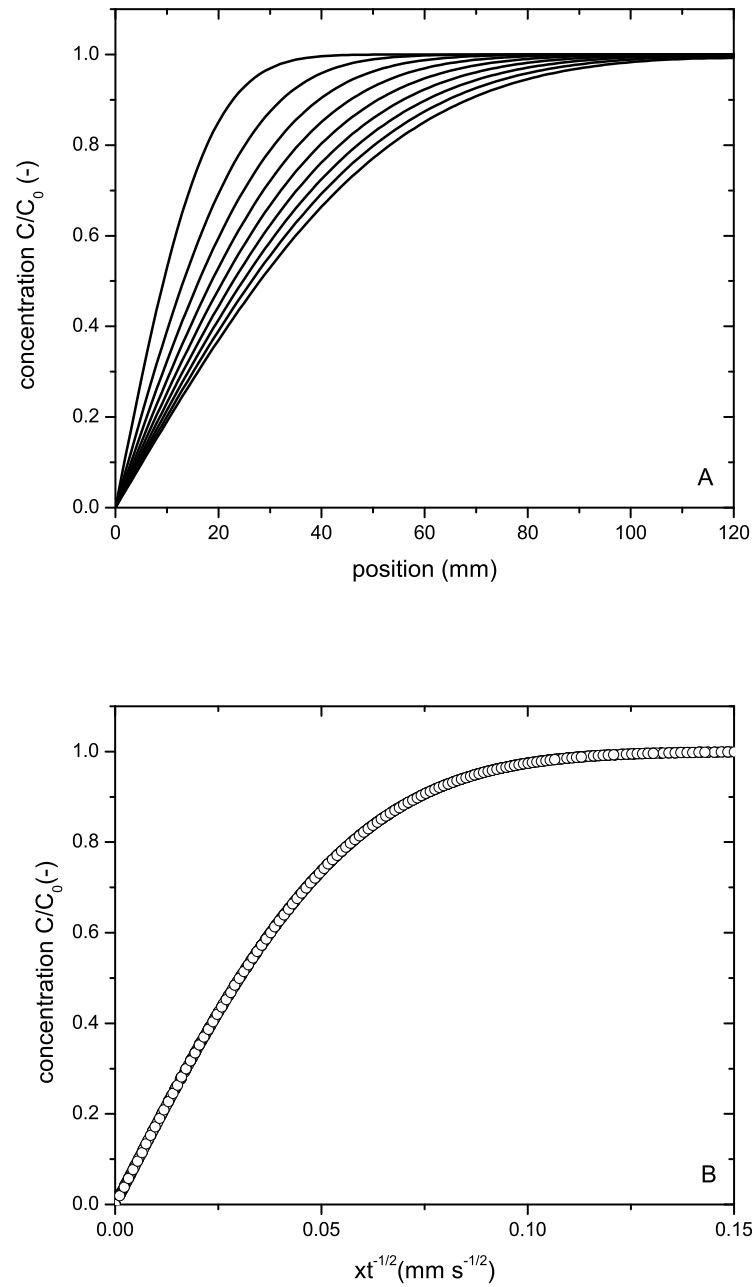


Fig. 2.1: A: simulated concentration profiles taken at daily intervals over 10 days using a diffusion coefficient of $1 \times 10^{-9} \text{ m}^2/\text{s}$. B: the same profiles after applying the Boltzmann-Matano transformation, i.e., scaling the simulated profiles with $t^{1/2}$.

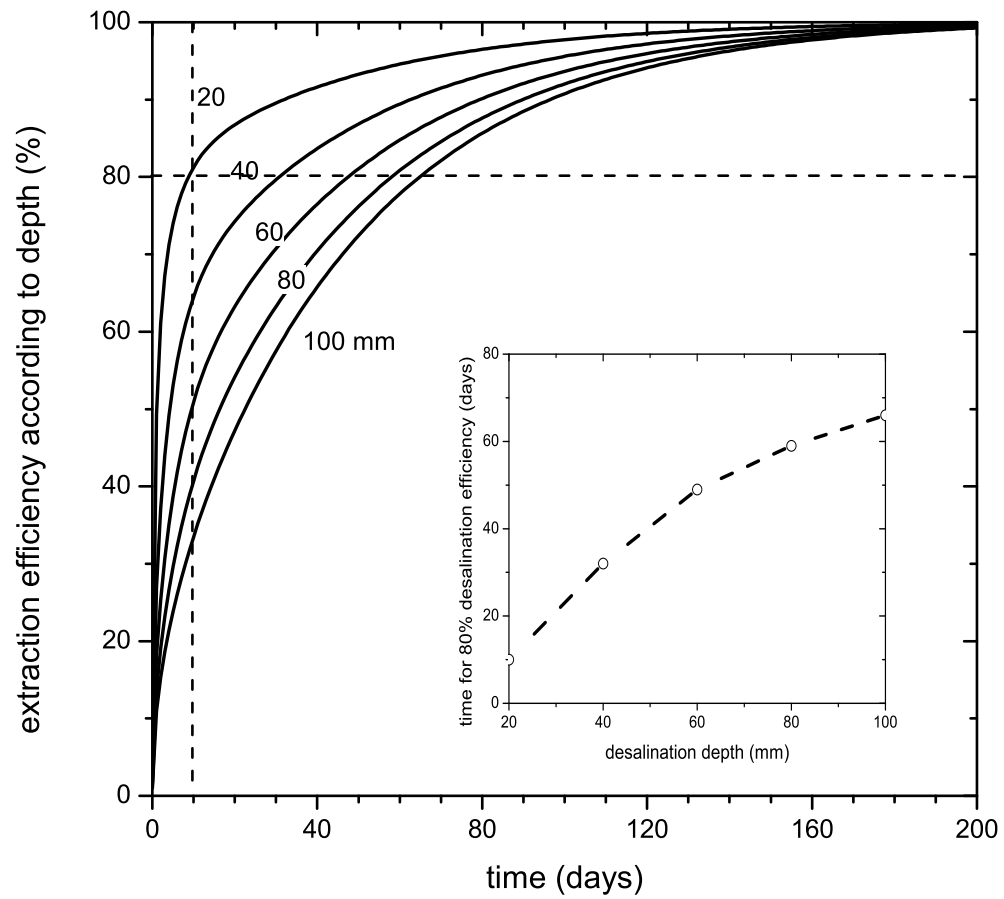


Fig. 2.2: The calculated desalination efficiency at a depth of 20, 40, 60, 80 and 100 mm as a function of time for diffusion based salt extraction. In the inset, the time required for 80% desalination is given for various depths.

2.3 Advection-based methods

The term 'advection' refers to the transport of mass by a moving medium. A good example of advection is the transport of pollutants in a river: the flow of water carries the impurities downstream. This can also take place in a porous material, i.e., dissolved ions can be transported by the moisture flow. Hence, if there is a flow of moisture from the substrate into the poultice, then the substrate can be desalinated by advection. As advection is generally more rapid than diffusion, desalination treatments based on advection can be much faster. However, in order for advection from the substrate into the poultice to take place, certain requirements regarding the pore size distribution of the poultice and of the substrate need to be fulfilled, in particular that the poultice contains a sufficient quantity of pores that are smaller than the majority of those in the substrate [Bou08a], which we will discuss in this section.

2.3.1 The ideal case: only advection

In general, the drying of a homogeneous, uniformly wet, porous material has two identifiable stages: first a uniform or constant rate drying period, followed by a receding drying front period. During the first period, moisture transport is fast and takes place solely through the liquid water network. During the second period, the pattern of liquid water migration is affected by the porous structure of the material, due to different capillary forces exerted by pores of varying size. Water is preferentially drawn into the micropores due to capillary pressure gradients, while the surface macropores begin to empty of liquid water. Consequently, water near the receding drying front starts to form isolated clusters, capillary flow in this region becomes discontinuous and transport occurs through the vapor phase. The water clusters evaporate due to the large difference in relative humidity between the air near the clusters and that at the surface of the material. During drying, air will invade the largest pores, where the capillary pressure (p_c) is lowest, as can be seen from the following equation [Bea90], [Dul91]:

$$p_c = -\frac{2\gamma \cos \varphi}{r_m}. \quad (2.7)$$

In this equation r_m [m] is pore radius that distinguishes between the pores filled with water ($r < r_m$) and the empty pores ($r > r_m$). γ [Nm^{-1}] is the surface tension of the liquid/vapor interface and φ [-] is the contact angle between the liquid/air and liquid/solid interface. With increasing moisture content the radius of the widest pore just filled with water, r_m , increases and therefore p_c decreases.

In order to understand the water transport and thereby the advection of the ions during the drying of a two-layer system (i.e. substrate + poultice) we will make the following assumptions:

- the two materials are in perfect hydraulic contact
- the water network is a percolating network (i.e., the drying front has not receded below the surface of either the substrate or the poultice)

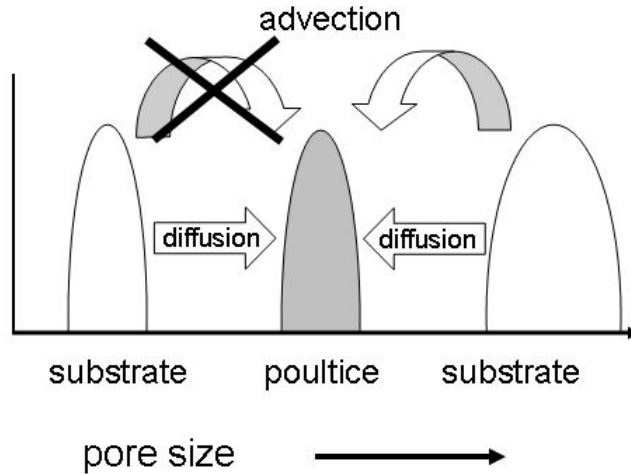


Fig. 2.3: Schematic diagram illustrating the possible transport mechanisms (i.e., diffusion and advection) by which aqueous ions can travel from a substrate into a poultice, depending on the substrate pore sizes relative to those of the poultice.

In a two-layer system with a given moisture content, water is present in the pores with diameters smaller than r_m in each material. Therefore, during drying water is removed first from the material with the largest pores. Consequently, in the case of poultice/substrate systems, the poultice will dry first if it has larger pores than the substrate, as is schematically represented in figure 2.3. Furthermore, in this case there is no advection of water and dissolved salt ions from the substrate into the poultice. Hence the salts can only move if there is a concentration gradient between poultice and substrate (i.e., by diffusion). If, on the other hand, the poultice has smaller pores than the substrate, the substrate will dry first and there will be moisture flow, and thereby an advection of ions, from the substrate into the poultice. However, there is a limit to the speed of ion transport by advection. Within a poultice, advection primarily takes place through the macro pores (as long as they are smaller than those within the substrate) while the micro pores make only a minor contribution, due to their smaller volume, higher surface to volume ratio and hence higher viscosity/friction effects.

The effect of the substrate/poultice pore size relationship on drying behavior is demonstrated in figure 2.4, which shows what happens when the same salt accumulating plaster is applied to two different substrates: one with very fine pores (calcium silicate brick), and another with coarse pores (Bentheimer sandstone) [Pet07], [Pet05]. In both cases drying takes place from the plaster surface. As can be seen, the drying behavior is as expected: the porous substrate dries first only in the case of the plaster on top of the Bentheimer sandstone.

Since salt is transported with water, we can make an estimate of the efficiency value based on the moisture content. In order to do this, in addition to the assumptions already made, we have to further assume that:

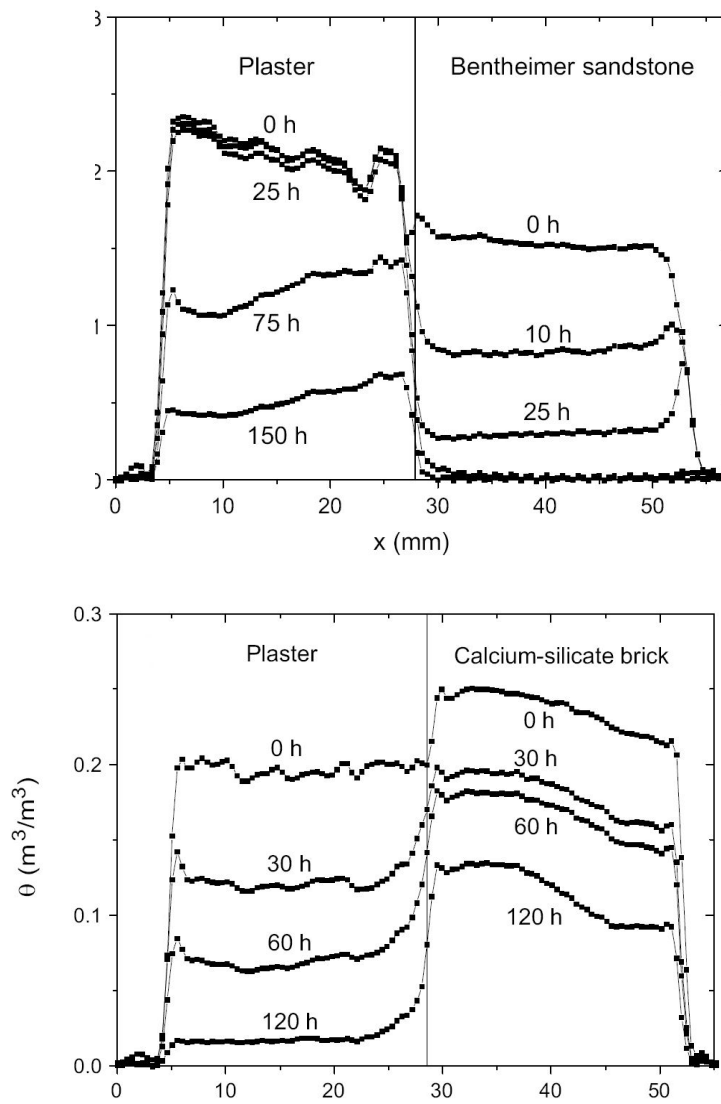


Fig. 2.4: Measured moisture profiles (using NMR) for the same salt accumulating plaster applied on a substrate with larger pores coarse pores (Bentheimer sandstone) and on a substrate with smaller pores (calcium-silicate brick).

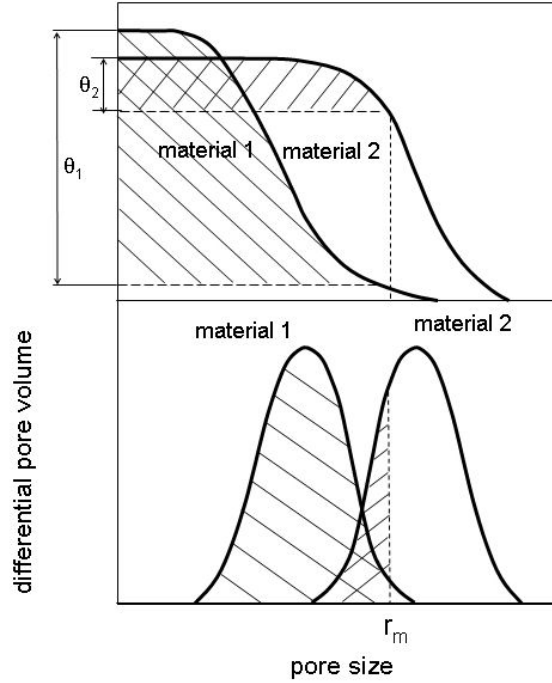


Fig. 2.5: The cumulative and differential pore volumes versus pore radius (here shown for two arbitrary materials) can be used for estimating the salt extraction efficiency. During the second stage of desalination water is present in pores with pore radii $r < r_m$, which corresponds to a moisture content θ_1 in material 1 and θ_2 in material 2.

- this is the second stage of salt extraction (i.e. no more moisture is entering the sample)
- all salts have completely been dissolved

Under these conditions the transport of salt is equivalent to the transport of moisture. Therefore the efficiency value can be estimated from the transport of moisture from the substrate to the poultice/desalination mortar as [Pet07], [Pet05]:

$$\varepsilon \simeq \varepsilon_w = \frac{\Delta V}{\Delta V_0} = \frac{\Delta \theta}{\Delta \theta_0}, \quad (2.8)$$

where ε_w is the efficiency value calculated on the basis of the water quantity. V_0 and θ_0 are the initial volume of water and moisture content in the substrate. ΔV and $\Delta \theta$ are the volume of water and moisture content that has exited the substrate after a definite period of time. Here the extraction efficiency is calculated on basis of the wetted part of the substrate, which in this case is the entire substrate. Hence the efficiency is related to the total sample length. In cases where the substrate has only been partly wetted, the estimated efficiency is only valid for the part that is wet.

Since, as shown above, water transport in a two-layer system is characterized by the pore size differences between the two materials, the efficiency value can

also be estimated from the capillary pressure law. The volume of water that leaves the substrate while the plaster completely dries out equals the volume of the pores in the substrate with a radius larger than that of the smallest pores in plaster. Hence ε_p can be calculated from the total pore volume V_p of the substrate and the volume of the pores $V_{p'}$ in the substrate with a radius larger than that of the smallest pores in the plaster:

$$\varepsilon_p = \frac{V_{p'}}{V_p}. \quad (2.9)$$

Hence by measuring the cumulative pore volume of both materials as a function of pore size with, e.g., mercury intrusion porosimetry one can infer the likely efficiency of desalination as shown schematically in figure 2.5.

However, as ions will only be advected from substrate pores larger than those of the poultice, salt will remain in the smaller substrate pores. After treatment the salt in these pores will act as a reservoir capable (in the case of wetting, or automigration due to high humidity and deliquescence) of redistributing to the larger desalinated pores.

2.3.2 The non-ideal case: as in practice

As has been shown in the previous section, ions can be advected by the capillary moisture flow from the substrate into the poultice. However, as soon as the advected ions start to accumulate, back-diffusion will counteract this by leveling off any concentration gradient. Moreover, the increasing accumulation of salt affects the drying rate by lowering the vapor pressure of the saline solution within the poultice, hence reducing the rate of moisture loss. At very low drying rates diffusion based transport becomes increasingly dominant, and the salt concentration tends to become more uniform throughout the sample. Hence there will be a competition between advection and diffusion during transport. This can be described by a combined advection-diffusion equation [Bea90]:

$$\frac{\partial(C\theta)}{\partial t} = \frac{\partial}{\partial x} \left[\theta \left(D_{eff} \frac{\partial C}{\partial x} - CU \right) \right]. \quad (2.10)$$

Here C is the salt concentration, θ is the moisture content, D_{eff} the effective diffusion coefficient of the salt in the porous material and U [m/s] the moisture velocity. Therefore the term on the left refers to the change in the total salt content $C\theta$ over time. The term on the right refers to the transport of salt in the presence of moisture by diffusion (given by the term $(D_{eff}\partial C/\partial x)$, or by advection (given by the term CU).

From this equation, the competition between two mechanisms of transport, advection and diffusion, can be characterized by a Peclet number, Pe [Hui02]:

$$Pe = \frac{|U|L}{D_{eff}}, \quad (2.11)$$

where L is the length scale of interest. If $Pe \gg 1$, advection dominates and ion transport takes place due to capillary water flow. For $Pe \ll 1$, diffusion

dominates and ion transport proceeds according to the concentration gradient. It should be noted that the Peclet number is defined at the macroscopic scale of the bulk porous material and not, as is often done, within the pores of material.

As a result, salts can be extracted by advection only from the part of the substrate where $Pe > 1$. This has important consequences for our understanding of how salt extraction takes place. Let us assume we have the same situation as in the previous section, i.e., a sample saturated homogeneously with a saline solution, which is dried from one side. As the sample starts to dry we need to take into account the moisture velocity. The initial moisture velocity is zero. Moisture starts to move from the back of the substrate, slowly increasing in speed as it approaches the drying surface. As a consequence, at the back of the substrate where the moisture velocity is very low, there is an area where diffusion is always dominant over advection. Consequently, this part of the sample cannot be desalinated by an advection based transport process. Moreover, as was shown in section 2.2, due to its location at the back of the substrate it will take an extremely long time to desalinate this part by diffusion. Consequently, in this area, the efficiency of desalination is likely to be very low.

We can attempt to estimate the effect of increasing moisture velocity on the desalination efficiency on a sample with length l as follows. When a porous material initially starts to dry, i.e., during the constant rate drying period, the moisture content is virtually homogeneous throughout the sample and decreases linearly with time. Hence one can as a first order approximation estimate the moisture velocity for a sample with length l as follows (see appendix A2):

$$U(x) = \frac{-\alpha}{\theta_0 - \alpha}(l - x), \quad (2.12)$$

Here θ_0 is the initial moisture content of the sample, t the time, α [-] a constant related to the drying rate of the sample ($\alpha = \partial\theta/\partial t$) and l [m] the length of the substrate. As can be seen, the moisture velocity increases linearly from the closed end of the sample (at $x = l$) to the substrate/poultice interface ($x = 0$). As a result the balance of competition between advection and diffusion changes throughout the sample, as is schematically illustrated in figure 2.6.

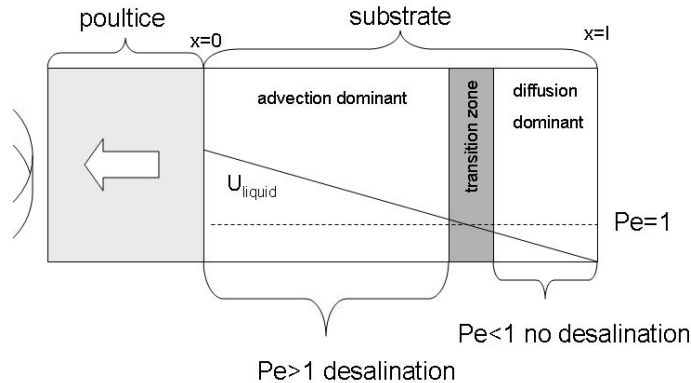


Fig. 2.6: A schematic representation of the effect of linearly increasing moisture velocity on the salt transport mechanism within the substrate [Pel10].

At the closed end of the sample there is a region where diffusion is dominant over advection. This effect will be present for all advection based salt extraction methods.

Based on this idea, the Peclet number at the substrate/poultice interface can be used to estimate the efficiency, since this is proportional to the ratio of the part of the substrate where advection is dominant and the total substrate length, i.e.,

$$\varepsilon_{ad} = \frac{Pe - 1}{Pe} \times 100\%. \quad (2.13)$$

Hence for $Pe \gg 1$ the efficiency approaches 100%. Conversely, when $Pe = 1$ at the surface, then diffusion is dominant throughout the sample and desalination does not take place by advection.

Here we have assumed that in the part where $Pe > 1$ all the salt will be advected out of the substrate. However, as shown above, the effect of the substrate/poultice pore size distribution needs also to be taken into account. By combining the estimated effect of the increasing moisture velocity with that due to the substrate/poultice pore size distribution, we obtain an estimate of the total efficiency, i.e.,

$$\varepsilon_{total,ad} = \frac{Pe - 1}{Pe} \times \varepsilon_p \times 100\%. \quad (2.14)$$

This shows that in general the efficiency of salt extraction treatments based on advection will always be less than 100% for any given substrate.

2.3.3 Combined poultice: wetting and desalination

As stated previously, in general terms salt extraction comprises two steps. In the first, water penetrates from the poultice into the porous material and dissolves the salt. In the second, the salt ions are transported from the object into the poultice. In many situations it would be preferable if the second step is advection-based, as this is much faster than diffusion. However, to achieve this, the wetting and desalination processes demand totally different poultice properties. In the case of wetting, the poultice must have pores larger than the object so that the substrate can absorb water, as given schematically in figure 2.7. However, for desalination the poultice needs to have pores smaller than those of the object for advection to take place. Hence if the poultice is intended to have the dual purpose of both wetting and desalination, it must have a wide pore size distribution incorporating large pores that can act as reservoirs for wetting and small pores to ensure that advection from the substrate to the poultice takes place, and the object dries before the poultice. Moreover, potential changes in the porosity and pore size distribution of the poultice material during drying need also to be considered (as evidenced by the shrinkage and cracking of clay/cellulose poultice materials commonly observed in the field), as these may affect the efficiency of extraction.

A further issue encountered in practice that must also be taken into account is that of the degree of contact that the poultice material has with the substrate surface. The experimental results of Petkovic [Pet05], and those given in figure

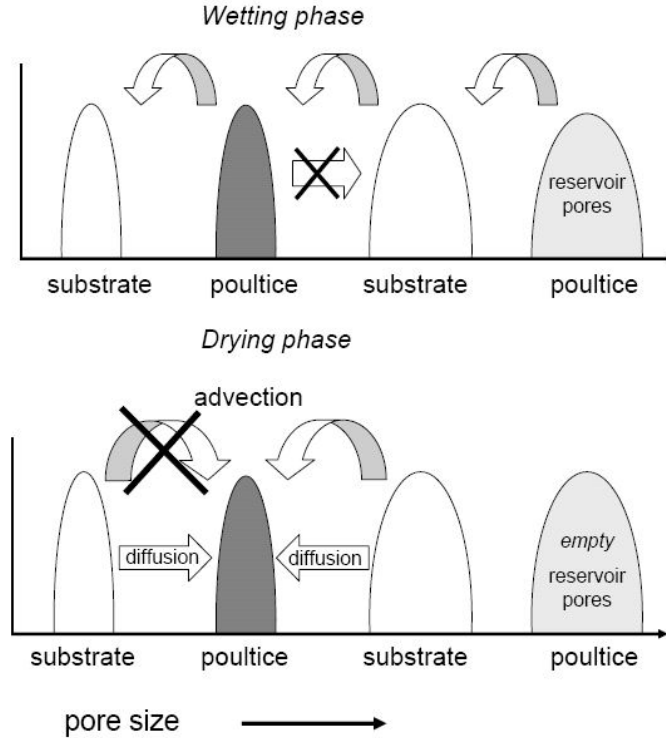


Fig. 2.7: A schematic representation of the combined demands on a poultice with a pore size distribution suited for both wetting and desalination by advection.

2.4 illustrate the situation where there is very good capillary contact between the substrate and the poultice material. Consequently, in such situations moisture transport is not significantly impeded at the substrate/poultice interface by factors other than the substrate/poultice pore size relationship. However, in the field, the degree of conformance (and hence contact with the substrate surface) achieved on application is known to vary from one poultice material to another, and their subsequent shrinkage on drying leads to well-known problems of detachment, particularly in the case of clay and cellulose-based poultices [Bou08a]. Moreover, the effect of variable drying conditions can also play a significant role in determining the rate of moisture transfer between the substrate and poultice [Bou08c].

2.4 Discussion and conclusion

The two stages of desalination treatment using poultices (wetting of substrate and salt extraction) will now be discussed.

2.4.1 Wetting phase

During the wetting phase, moisture is introduced into the object in order to dissolve the salts. While many practitioners opt to prewet the object using water sprays, nevertheless in certain situations a more controlled and slower

introduction can be desirable. For example, during wetting one runs the risk of transporting surface accumulated salts by advection deeper within the material. Moreover, many cultural objects comprise moisture sensitive materials (e.g., pigments and binding media) that will not tolerate the introduction of copious amounts of water. Controlled wetting of the substrate can be achieved through the use of a poultice. However, as stated above, if the poultice is intended to act as a reservoir for water for this phase, it should have pores that are larger than those of the object.

2.4.2 Salt extraction phase

The extraction of salts from the substrate to the poultice is effected by two different transport mechanisms, diffusion and advection.

Diffusion-based desalination methods

Pros

- When sufficient time is available, diffusion-based extraction methods can have an efficiency of 100%.
- The method functions independently of pore size. Consequently, the same poultice will work on any porous material.

Cons

- Slow method: in general, it will take weeks or months for this method to be effective.
- One has to renew the poultice frequently in order to keep on extracting salts.
- Good hydraulic contact between poultice and object has to be maintained throughout the treatment period.
- The object has to remain completely saturated with water for a very long time period. Hence this could result in additional damage due to dissolution of the material, swelling of organic components, chemical alteration of pigments and binding media, biodeterioration, and other water related decay processes.
- At the end of the treatment the object is wet, and has to be dried, during which any remaining salt may be transported back to the surface.

Advection-based desalination methods

Pros

- Fast method, i.e., the time period for salt extraction is of the order of days.

- Less moisture is introduced to the object
- The object surface is dry after desalination although there is residual moisture remaining at depth within the substrate, and so further salt and moisture transport to the surface can potentially occur.

Cons

- The method is pore-size dependent, i.e., it will only work if the poultice contains a significant quantity of pores that are smaller than those of the object. Accordingly, the poultice has to be adapted to suit the material on which it is to be used.
- Requires good hydraulic contact between poultice and object.
- Due to the nature of advective transport, salts will only be removed from the surface region of the object.
- During the extraction the increasing accumulation of salt will influence the drying rate by lowering the vapour pressure of the saline solution within the poultice, hence reducing the rate of moisture loss by evaporation. As a result the rate of advection decreases.
- Increasing salt accumulation in the poultice also promotes the rate of back diffusion from the poultice into the substrate (i.e., both poultice and substrate are still wet but the Peclet number has dropped to below 1). Hence renewed poultice application is necessary, the timing of which will have to be determined by tests, i.e., one could not leave the poultice on the substrate until both are completely dry.

From this discussion it is therefore clear that there is no single ideal poulticing method for extracting salts, and that in practice one can never achieve complete desalination of a nonmoveable object. Indeed, it is therefore more accurate to refer to such interventions as 'salt content reduction' rather than 'desalination' treatments. Given that poulticing measures often result in only a partial and relatively superficial removal of salts, in the absence of adequate measures to ensure that the supply of salts and moisture to the object is no longer ongoing, their long-term effectiveness is likely to be limited. Consequently, regardless of the salt extraction efficiency achieved immediately after treatment, the effectiveness of the intervention has to be evaluated over time, and if necessary repeated, adapted or abandoned in favour of an alternative approach.

3. OSMOTIC PRESSURE IN A TWO LAYERED POROUS MATERIAL SYSTEM

*The crystallization of salts is widely recognized as one of the most significant causes of irreversible damage to many cultural objects such as wall paintings, stone sculptures, historic buildings. The removal of salts from these non-moveable objects is however difficult and often poultices are used. In these methods a wet poultice is applied to the surface of the substrate to be treated and is kept in place for some period of time before being removed. Many studies up to now on poulticing have focused on the salt and moisture transport solely in terms of advection and diffusion. The objective of this study is to demonstrate the potential contribution of osmotic pressure to salt extraction during poulticing treatments. To this end we have conducted a series of experiments where we have measured the moisture and salt transport during poulticing for some well defined materials. Here we have used Nuclear Magnetic Resonance (NMR) to measure non-destructively the moisture and ion transport during these experiments. This study shows that osmotic pressure can exert a significant influence on salt extraction by poulticing methods during drying. Importantly, as salt is transported from the substrate and into the poultice, this results in a build-up of osmotic pressure within the poultice decreasing the effective pore-size of the poultice. Therefore the build-up of osmotic pressure enhances the salt extraction and thus increases the efficiency of the poulticing treatment.*¹

3.1 Introduction

The crystallization of salts is widely recognized as one of the most significant causes of irreversible damage to many cultural objects comprised of porous materials such as wall paintings, stone sculptures, historic buildings and other artworks [Arn91], [Gou97], [Lew80]. Salt phase transitions occur in response to the moisture content (water vapor pressure) and temperature of their surroundings, and are therefore environmentally activated. The damage caused by salts can to some extent be avoided by preventive methods, which include (in line with the generally accepted approach of minimal intervention in conservation) passive measures using environmental control. This approach relies on the selection and maintenance of optimum environmental conditions under which salt damage can be minimized. However, environmental control is difficult to implement, and in many situations is not feasible (e.g. when objects are exposed to exterior conditions, or there are conflicts with the requirements of

¹ The contents of this chapter have been submitted in Journal of Materials and Structures 2011

building users or other objects housed therein). In such instances an alternative approach (and indeed one which is commonly taken in conservation practise) is direct intervention to reduce the salt content of the affected materials, either by mechanical means (dry brushing) and/or by using water as an extraction medium.

While the removal of water soluble salts from porous materials in theory sounds easy, nevertheless this can prove difficult in practice. For small objects (providing they are not composed of water sensitive materials), can be treated using a water bath, whereby the object is immersed in water that is periodically refreshed. In such cases, given sufficient time almost complete salt extraction is at least theoretically possible.

The removal of salts from large non-moveable objects is however more difficult, to which end the use of water containing poultices to reduce the salt content is very common [Ver05], [Her08]. The application methodology for poulticing is in principle relatively simple: the wet poultice is applied to the surface of the substrate to be treated and is kept in place for some period of time before being removed. However, in practice there are a large number of variables that exert a significant effect on the salt extraction process. The extraction of water soluble salts by poulticing involves two main phases. The first is the wetting phase during which water is transported from the poultice into the wall where it starts to dissolve the salts. The second phase is the salt extraction, during which the dissolved salt ions are transported in the form of a saline solution from the substrate into the poultice. This salt migration can be the result of two different processes, i.e., diffusion and advection [Pel10]. The diffusion process is generated by the existence of a concentration gradient between the substrate and the poultice. In this case the salt ions diffuse through the solution from the substrate to the poultice. This is however a slow process and the salt extraction even for small objects can take weeks or months. Another process is realized by capillary water flow from the substrate to the poultice (generally due to drying) and is accompanied by ion advection within the solution. In the case of advection based salt extraction (i.e., drying poultices) the efficiency of salt extraction is strongly dependent on the relative pore-size range of the substrate and the poultice. This extraction process is potentially considerably faster than diffusion based methods. However, it carries a significant drawback in that in order to have advection the poultice materials have to suit the pore-size distribution of the substrate. While this can to some extent be achieved through the inclusion of clay minerals (such as kaolin) in poultice mixtures [Aur08], [Lub10], nevertheless these materials pose significant problems in that they are difficult to remove and result in staining. Accordingly they are not suitable for use on colored materials or painted surfaces [Saw10].

Many studies up to now on poulticing have focused on the moisture transport solely. However in salt extraction, as there are salt gradients present so too will there be osmotic pressure gradients present. The influence of osmotic pressure on water movement is well known in the soil science [Whe25], [Let69], [Nas89]. The influence of osmotic pressure in salt accumulation plasters was taken into account in a numerical model by Nguyen et al [Ngu08].

The objective of this study is to demonstrate the potential contribution of

osmotic pressure to salt extraction during drying poulticing treatments. To this end we have conducted a series of experiments to investigate the influence of osmotic pressure on ion transport processes during poulticing. For these experiments, generic porous materials were used to avoid complicating effects such as poultice shrinkage which often occurs in practice. In the following sections the fundamental aspects of capillary transport and osmotic pressure relating to the two generic porous materials selected for the study will first be discussed. Following this, the Nuclear Magnetic Resonance (NMR) setup used to measure non-destructively the moisture and ion transport during the experiments and the materials used will be described. Finally the results of the experiments showing the influence of the osmotic pressure on the desalination process will be discussed.

3.2 Theory

In this section the fundamental equations to describe the desalination process by advection during drying are discussed. First the drying of a combination of two different porous materials that are saturated with water and placed in contact with each other is discussed. Secondly the influence of the osmotic pressure on this process in the case where the water is replaced with a saline solution is considered.

3.2.1 Capillary pressure

For a single capillary pore the capillary pressure P_c is given by:

$$P_c = -\frac{2\gamma \cos \varphi}{r}. \quad (3.1)$$

where γ [N/m] is the surface tension of the liquid/vapor interface, φ [-] is the contact angle between the liquid/air and liquid/solid interface, r [m] is pore size. In most porous materials the pores are not uniform, and therefore there is a pore size distribution. Thus the overall macroscopic capillary pressure ψ_c of the material is a function of its pore size distribution. To illustrate this point, the capillary pressure curves and pore size distributions as measured for Migne limestone (a fine porous material) and Bentheimer sandstone (a coarse porous material) are given in figure 3.1. From this it can be seen that the fine porous Migne limestone has pores in the range 0.5-3 μm in diameter, whereas the coarse porous Bentheimer sandstone has pores in the range 30-40 μm in diameter. This difference in pore size distribution is reflected in the respective capillary pressure curves for these two materials.

At any given moisture content, the distribution of water within the material is dependent on the pore size distribution. For any moisture content θ [m^3m^{-3}], there will be a critical pore radius, r_m , that discriminates between the pores filled with water and the empty pores. Hence macroscopic capillary pressure ψ_c will be a function of the moisture content θ which can be described thus:

$$\psi = \psi_c(\theta), \quad (3.2)$$

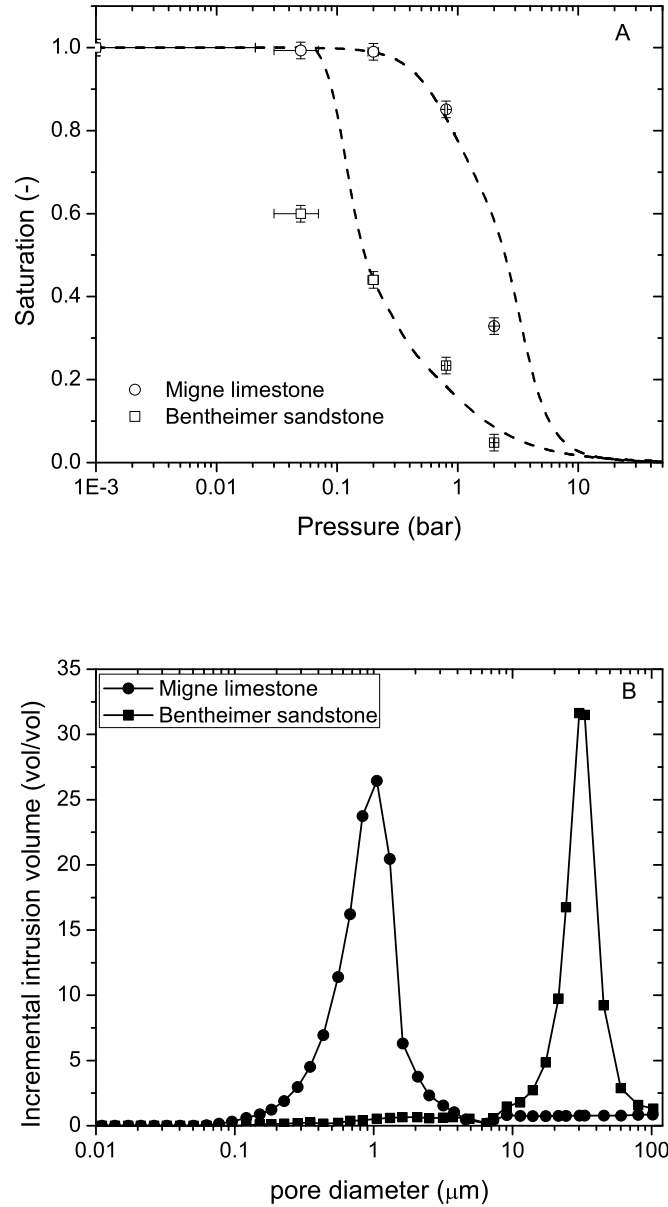


Fig. 3.1: A. The capillary pressure curve for Migne limestone and Bentheimer sandstone as measured by pressure plate. The dashed line is a fit through this data points using the pore size distribution as determined by means of mercury intrusion porosimetry. B. The pore size distribution as obtained by mercury intrusion porosimetry.

When a poultice is placed in contact with a porous substrate, there are two interfaces: an air/material; and a material/material interface. If we assume a perfect hydraulic contact at the poultice/substrate interface, the capillary pressure will be continuous at this interface, i.e.:

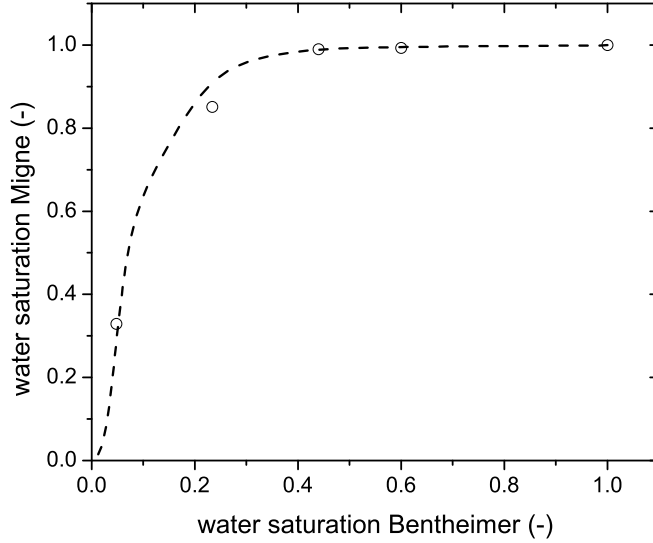


Fig. 3.2: The water saturation of the Bentheimer sandstone as a function of the water saturation of the Migne limestone as determined by the pressure plate. The dashed line is the relation as determined from the measured pore size distribution.

$$\psi_p(\theta_p) = \psi_s(\theta_s), \quad (3.3)$$

where ψ_p is the capillary pressure of the poultice, ψ_s the capillary pressure of the substrate and θ_p and θ_s the moisture content of the poultice and substrate at the interface. Hence as a result due to differences in the porosity and pore size distribution between the two materials there will be a jump in moisture content across the interface. The relationship between the moisture contents either side of the interface can be described thus:

$$\theta_p = \psi_p^{-1}\psi_s(\theta_s) = f(\theta_s). \quad (3.4)$$

As an example the relationship between the moisture content across the interface between Bentheimer sandstone and Migne limestone is shown in figure 3.2.

During drying, the pattern of liquid water migration is very much affected by the different capillary forces exerted by pores of varying size. Where micropores are interconnected with macropores, water is preferentially drawn into the micropores due to capillary pressure gradients. Thus, the surface macropores begin to empty of liquid water, while the micropores remain full [Uem87]. Hence when two different porous materials are placed in hydraulic contact with each other, the material with the largest pores will start to drain first. For example, in the case of the Migne/Bentheimer combination, because the pores of Migne limestone are considerably smaller than those of the Bentheimer, they remain

filled with water until the moisture saturation of the Bentheimer sandstone falls below 0.4 (see figure 3.2). Consequently, for poultice/substrate systems, if the substrate has larger pores than the poultice during drying there will be a capillary moisture flow (and thereby a possible advection of ions) from the substrate into the poultice. Thus for salt extraction by advection, the choice of poultice materials suitable for use on a particular substrate material is constrained to those which possess a certain pore size distribution (for an extended discussion see [Pel10]).

3.2.2 Capillary pressure and osmotic pressure

When the substrate/poultice system contains a saline solution there is an additional contribution to the macroscopic capillary pressure of each porous material due to the osmotic pressure, i.e.:

$$\psi = \psi_c(\theta) + \psi_s, \quad (3.5)$$

where the osmotic pressure, ψ_s , is given by:

$$\psi_s = \frac{RT}{V_w} \ln(a_w), \quad (3.6)$$

where R is the universal gas constant, T is the absolute temperature and a_w is the water activity (for pure water $a_w = 1$ and hence osmotic pressure is zero).

When the well known Pitzer's activity coefficient model is applied the osmotic pressure can be calculated as [Eng88]:

$$\psi_s = \nu RT m_l \left(1 + z_+ z_- A_1 + m_l \left(\frac{2\nu_m \nu_n}{\nu} \right) A_2 + m_l^2 \left(\frac{(2\nu_m \nu_n)^{3/2}}{\nu} \right) \beta_2 \right), \quad (3.7)$$

where

$$A_1 = -\frac{A_\phi I^{1/2}}{1 + 1.2I^{1/2}} \quad (3.8)$$

$$A_2 = \beta_0 + \beta_1 \exp(-2I^{1/2}) \quad (3.9)$$

A_ϕ is the Debye-Huckel coefficient, m_l is the molality of the solution, z_+ and z_- ion charges, I ionic strength of the solution, ν_m and ν_n are the number of moles of ions produced by one mole of the electrolyte (i.e., 2 for NaCl) and β_0 , β_1 , β_2 are the given parameters for Pitzer's activity coefficient model.

As an example, the osmotic pressure of a NaCl solution is given in figure 3.3 as calculated using the Pitzer model. The osmotic pressure reaches almost 350 bar for a saturated sodium chloride solution. Even at low concentration, i.e., in the order of 1 molal, the osmotic pressure is already of the order of the maximum capillary pressure as reached in the Bentheimer sandstone. Hence due to the presence of soluble salts in a porous material, its effective pore size (i.e., the equivalent pore size for a water saturated system) will decrease as the total macroscopic capillary pressure is increased by the osmotic pressure of the salt. As an example in figure 3.4 the total pressure is given for the

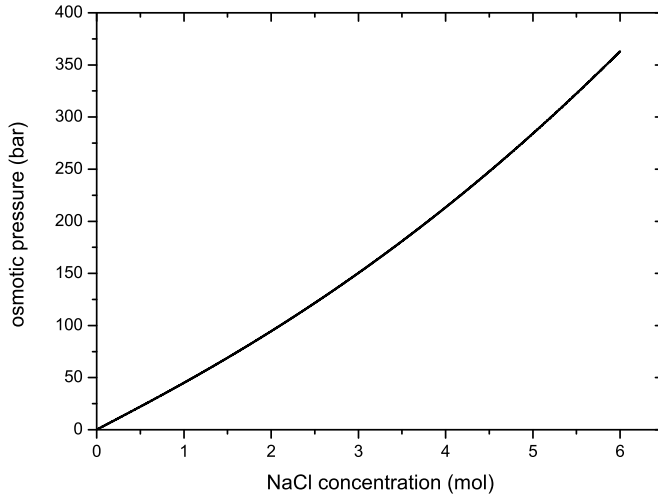


Fig. 3.3: Osmotic pressure of NaCl solution calculated by Pitzer's model.

Bentheimer sandstone and Migne limestone for various NaCl concentrations. As can be seen, at higher salt concentrations the macroscopic capillary pressure is predominantly determined by the osmotic pressure. Hence the overall pressure curves change significantly and no longer solely reflect the pore size distribution.

The osmotic pressure will also have a large influence on the moisture content relationship between the two materials when they are in contact. To illustrate this effect, figure 3.5 shows the moisture content relationship between a Migne limestone and Bentheimer sandstone when placed in hydraulic contact, at various saline solution concentrations in either of the materials. As can be seen the salt concentration has a large influence on the moisture distribution between the two materials. When salt is present in the Migne limestone the moisture will have an increased tendency to remain in this material, whereas this situation can be completely reversed by the introduction of salt into the Bentheimer sandstone. This further indicates that adding salt to a material decreases its effective pore size. However, it must be noted that all the examples so far given have considered only a static salt content, and do not account for net salt transport from one material into the other. In order to see these effects we need to measure non-destructively the moisture and ion transport taking place within the porous materials.

3.3 Experimental setup

3.3.1 Nuclear Magnetic Resonance (NMR) analysis

When attempting to study salt and moisture transport processes within porous materials one of the major difficulties to overcome is the problem of interstitial measurement. To this end Nuclear Magnetic Resonance (NMR) analysis was used to non-destructively study the transport of salt and moisture within

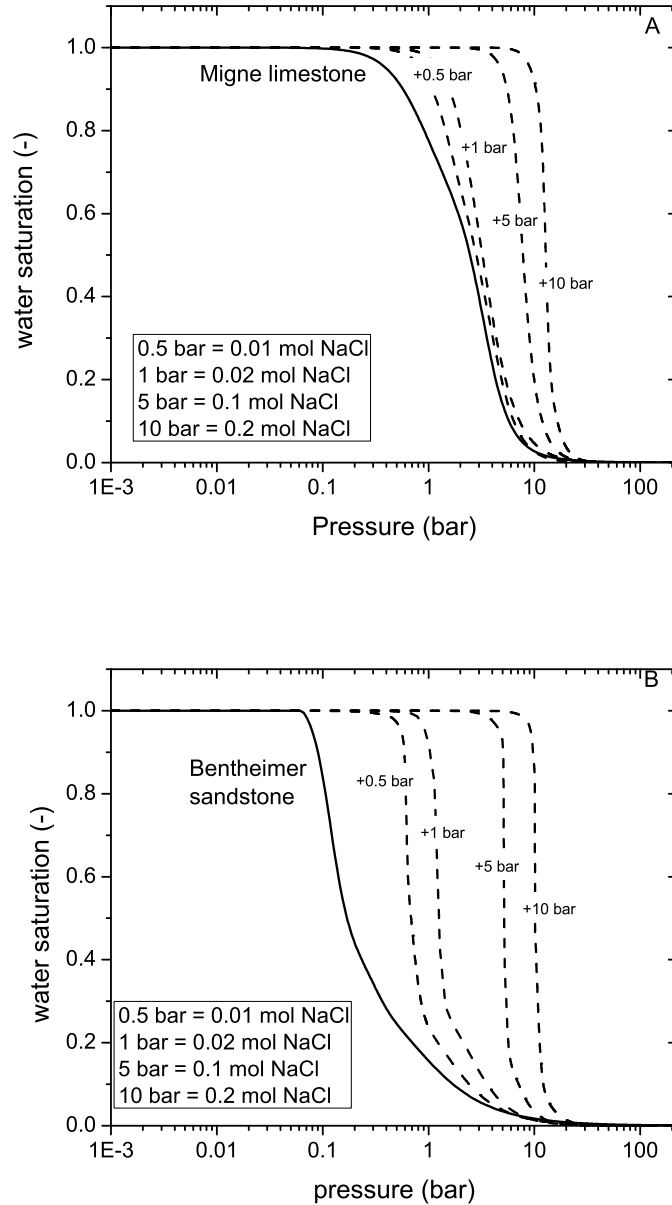


Fig. 3.4: The total pressure curves, i.e., capillary pressure + osmotic pressure, for Migne limestone and Bentheimer sandstone saturated as a function of NaCl concentration. The corresponding osmotic pressure was calculated on basis of the Pitzer model and are given in the insets.

combinations of different porous materials containing saline solutions. Using a purpose-built NMR scanner, designed for imaging porous building materials [Pel95], [Pel02], [Pet07], it is possible to follow the distribution of water and dissolved sodium ions in real time both quantitatively and quasi-simultaneously.

During nuclear magnetic resonance (NMR) analysis the magnetic moments

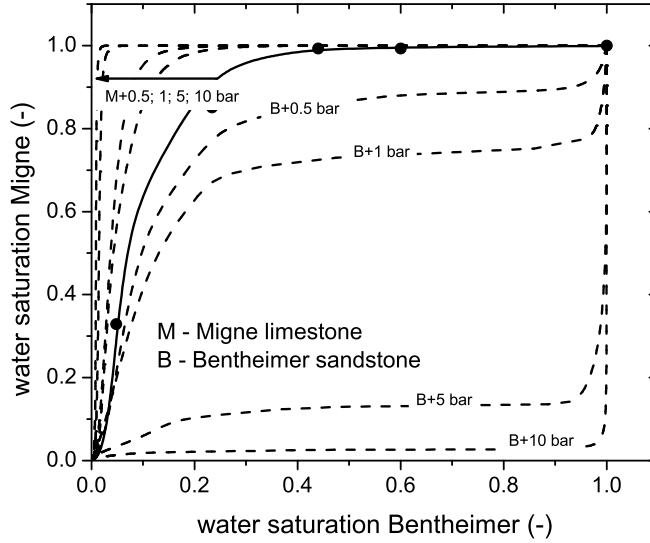


Fig. 3.5: The water saturation of Migne (M) limestone as a function of water saturation of Bentheimer (B) sandstone. The various curves represent the moisture content relationship between a Migne limestone and Bentheimer sandstone when placed in hydraulic contact, at various NaCl concentrations in either of the materials.

of the nuclei are manipulated by suitably chosen radio frequency fields, resulting in a so-called spin-echo signal. The amplitude of this signal is proportional to the number of nuclei excited by the radio frequency field. The selectivity of NMR for measuring specific species is due to the resonance condition for each nucleus, which is given by:

$$f = \gamma B_0, \quad (3.10)$$

where f is the frequency of the radio frequency field, γ is the gyromagnetic ratio ($\gamma = 42.6$ MHz/T for 1H and 11.3 MHz/T for ^{23}Na) and B_0 is the strength of externally applied static magnetic field. Accordingly this method can be tuned to detect specific nuclei such as (in this case) hydrogen (and therefore water) and sodium ions.

For the experiments described here a purpose-built NMR scanner was used, which incorporates an iron-cored electromagnet operating at a field of 0.78 T. In order to perform quantitative measurements, a Faraday shield was placed between the tuned circuit of the probe head and the sample. In addition, the quality factor of the LC circuit chosen was rather low ($Q \approx 40$), to suppress the effects of the (electrically conducting) NaCl solution. A constant magnetic field gradient of up to 0.3 T/m was applied using Anderson coils, giving a one-dimensional resolution of the order 1 mm for water, and 3.5 mm for Na. The spin-echo experiments were performed at a fixed frequency, corresponding to the center of RF coil. The sample holder is schematically depicted in figure 3.6. The sample was moved vertically through the magnet with the help of a

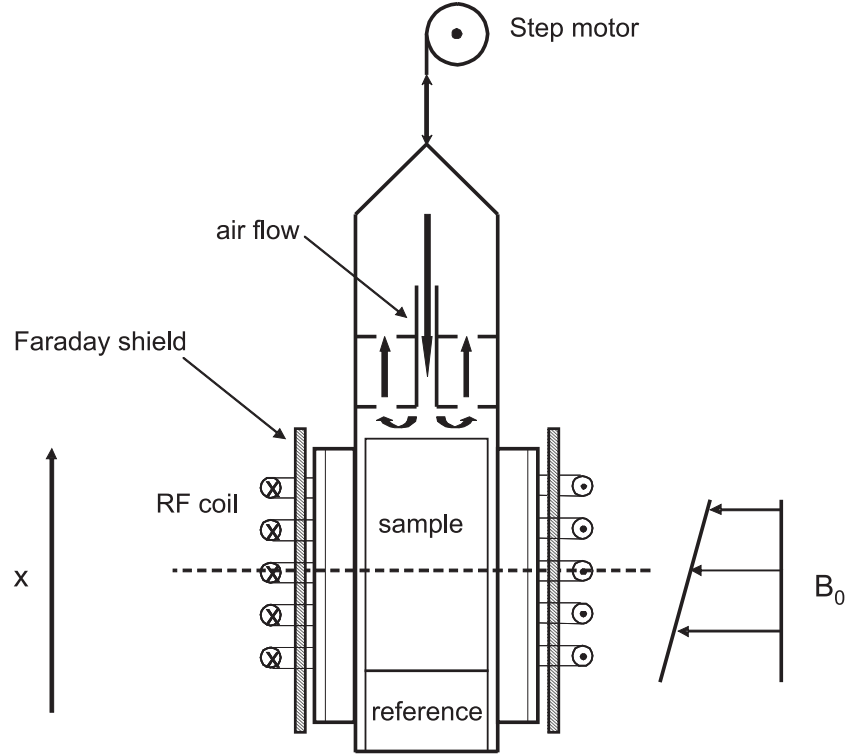


Fig. 3.6: A schematic diagram of the NMR setup for drying experiments. The Teflon holder with the sample and the reference is moved in the vertical direction by means of a step motor.

step motor. The sample, a cylinder with a length in the order of 50 mm and a diameter of 19 mm, was sealed on all sides apart from the top surface with Teflon tape. Over the exposed top surface air (with a relative humidity of 5%) was blown, thus creating a one-dimensional drying effect. While the sample was drying, first the moisture content within the small region of the sample located at the center of the RF coil was measured. Next, the frequency was changed from 33 MHz (1H) to 9 MHz (^{23}Na) and the Na concentration in that region was measured. With the NMR settings used in these experiments only the Na nuclei within the solution (dissolved aqueous sodium ions) are measured, i.e., no signal is obtained from NaCl crystals.

The time taken for each moisture content measurement was 1 minute, whereas it took 4 minutes to measure the Na content with a similar signal to noise ratio. This procedure was repeated until a complete moisture and Na profile was measured. A time step is attributed to each measurement point. In addition measurements of an external 4M NaCl solution reference were also performed, thus allowing the calibration of the H and Na signal intensities in reference to a known volume of water [cm^3] and quantity of Na [mol]. Before drying was started, i.e., prior to switching on the air flow, a water and a Na profile was first measured, to provide a $t=0$ reference base line for the experiment. The moisture and Na profiles for $t > 0$ were obtained by interpolating the successive experimental profiles measured at different elapsed times.

3.3.2 Materials

In order to study the effect of osmotic pressure on salt and moisture transport between different porous materials during drying, experiments were conducted using rigid porous materials. These were selected in preference to commonly used poultice materials, as their soft malleable nature tends to result in a significant degree of shrinkage during drying. This shrinkage not only affects the pore-size distribution of the material during drying, but can also result in a loss of contact between the poultice and the substrate. Consequently, the experiments described here were conducted using different combinations of two non-shrinking materials with very different pore size distributions: a Bentheimer sandstone; and a Migne limestone (as already introduced in the theory section above). For the purposes of the following experiments the Bentheimer sandstone represented the substrate (i.e., the underlying porous layer) and the Migne limestone the poultice (i.e., the overlying porous layer). Accordingly, the drying took place at the surface of the Migne limestone.

3.4 Results and discussions

In order to study the effects of osmotic pressure on salt and moisture transport within composite porous material systems comprising two different material layers, experiments were first conducted on composite samples containing water only. Following this, further experiments were undertaken in which either the underlying or the overlying porous layer was saturated with a saline solution, while the other contained only water.

3.4.1 Moisture saturated samples

Both sample materials were first vacuum saturated with water. Before the materials were brought into contact, a very thin layer of kaolin clay was applied at the interface of the materials to ensure a good hydraulic connection. The sandwiched sample materials were wrapped in Teflon tape sealing all sides except the top surface, and placed within the sample chamber of the NMR scanner. Dry air (at 5% RH) was blown across the exposed top surface thus creating a one-dimensional drying experiment.

In figure 3.7 the results are given for the water saturated Migne/Bentheimer combination. For comparison, results are shown for the case where the layer structure is reversed (i.e. the Bentheimer is placed on top of Migne, and drying takes place from the surface of the Bentheimer). As can be seen the measured moisture profiles reflect the pore size distributions. In both cases the material with the largest pores dries first. These results conform to the general idea that in order to extract salts by advection using drying poulticing methods, the pore size distribution of the poultice should be smaller than that of the substrate ([Pel10], [Saw10]).

In figure 3.8 we have also plotted the moisture contents at the Migne/Bentheimer interface for both of these experiments. As can be seen, these correspond well to the curve determined from capillary pressure curves measured for these ma-

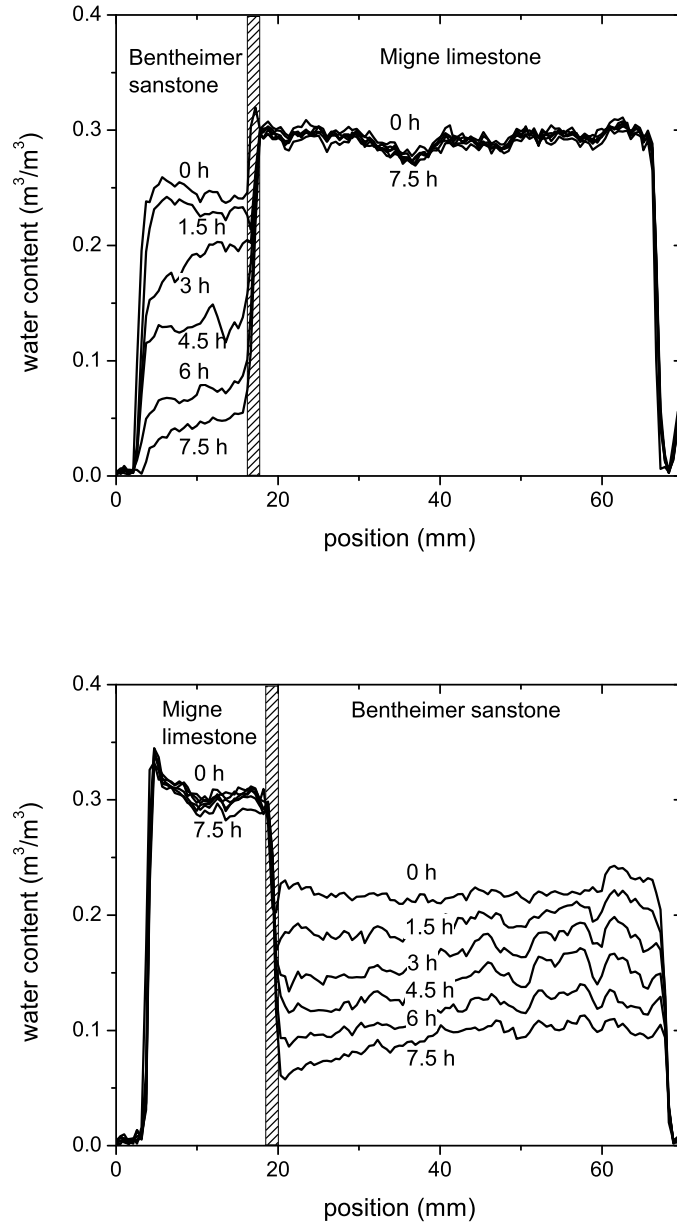


Fig. 3.7: The moisture profiles as measured during drying at various times. The samples are dried at the left side where as the righside is sealed off. A. Migne limestone on Bentheimer sandstone. B. Bentheimer sandstone on Migne limestone.

materials shown in figure 3.2. This also demonstrates that in these experiments there is a good hydraulic contact between the two materials.

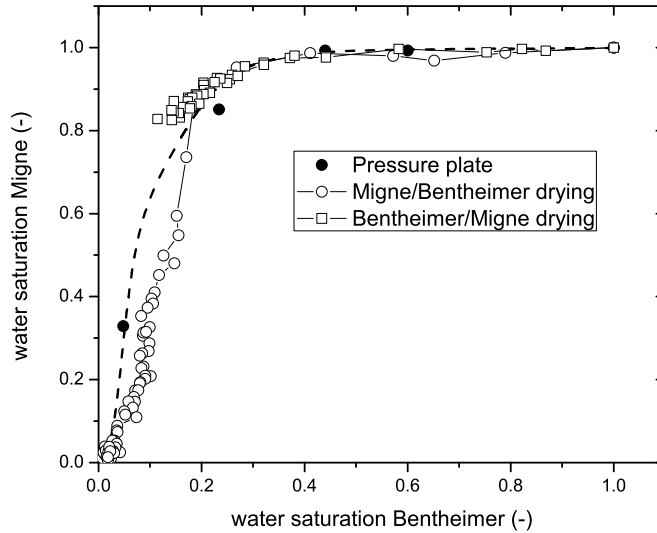


Fig. 3.8: The water saturation of Migne limestone at the interface as a function of water saturation of Bentheimer at the interface as determined from the drying experiments (see figure 3.7). The dashed line represents the relation as determined by the measured capillary pressure curve (see figure 3.1).

3.4.2 Saline solution saturated samples

In order to study the potential effect of osmotic pressure on salt and moisture transport during poulticing treatments the experiments described in the previous section were repeated, but with the modification that either the Migne limestone or Bentheimer sandstone were saturated with a saline solution instead of water. In the first experiment, the Bentheimer sandstone (representing the substrate), was vacuum saturated with a 3 molal salt solution, and then placed in contact with the Migne limestone (representing the poultice) which had been similarly saturated with water. The sample sandwich was then wrapped in Teflon tape on all sides apart from the top surface, and drying was performed in the NMR scanner as before.

In the second experiment, the Bentheimer sandstone (representing the substrate), was vacuum saturated with water and brought into contact with the Migne limestone (representing the poultice) which had been vacuum saturated with a 3 molal salt solution. Again the sample sandwich was then wrapped in Teflon tape on all sides apart from the top surface, and drying was performed in the NMR scanner as before.

Migne(saline solution)/Bentheimer(water)

In figure 3.9 we have plotted both the measured and calculated relation between the moisture content of the Migne and Bentheimer at the interface for a water saturated Bentheimer sample in contact with a 3 molal NaCl solution

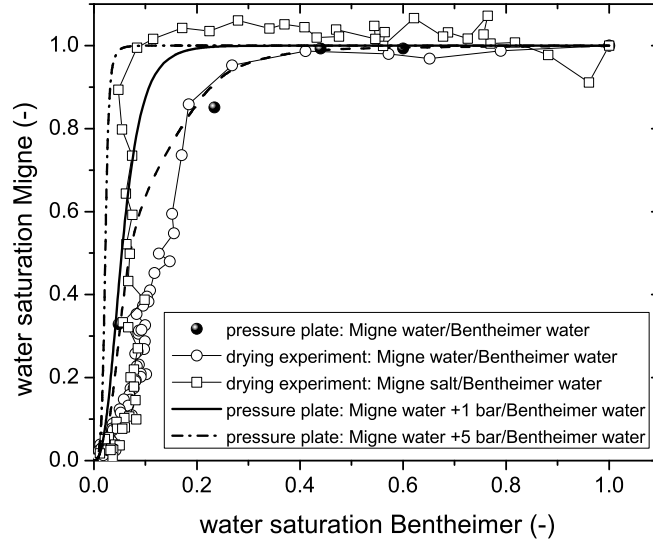


Fig. 3.9: The water saturation of Migne limestone as a function of water saturation of Bentheimer sandstone for the water Migne/water Bentheimer and solution Migne/water Bentheimer systems. The dashed lines represent the relation as determined from the measured capillary pressure curves (solid line) and the osmotic pressure.

saturated Migne sample. For comparison we have also plotted the relation for a drying experiment with both materials saturated with water. As can be seen initially as drying starts, the Bentheimer loses moisture, while the Migne stays saturated. However, once the moisture saturation of the Bentheimer falls below 0.4, the influence of the osmotic pressure becomes apparent. As the osmotic pressure reduces the effective pore size of the Migne limestone, the stone remains saturated until the Bentheimer sandstone reaches much lower moisture saturation levels than before. However, as soon as the moisture saturation of the Migne starts to decrease a slight increase in the Bentheimer saturation is observed. This can be explained on the basis of drying and the salt transported. As the moisture content decreases in the Migne the drying rate will drop and as a result salt will start to diffuse into the Bentheimer as it is no longer advected away from the interface. Hence the osmotic pressure difference between the two materials decreases. Therefore the macroscopic capillary pressure of the Migne is reduced, while that of the Bentheimer is correspondingly increased. Accordingly, the moisture content relation between the two materials shifts towards that for water saturated samples.

Migne(water)/Bentheimer(saline solution)

In figure 3.10 both the theoretically derived and measured moisture content relation at the interface between the Migne and Bentheimer are shown for a 3 molal NaCl solution saturated Bentheimer sample in contact with a water

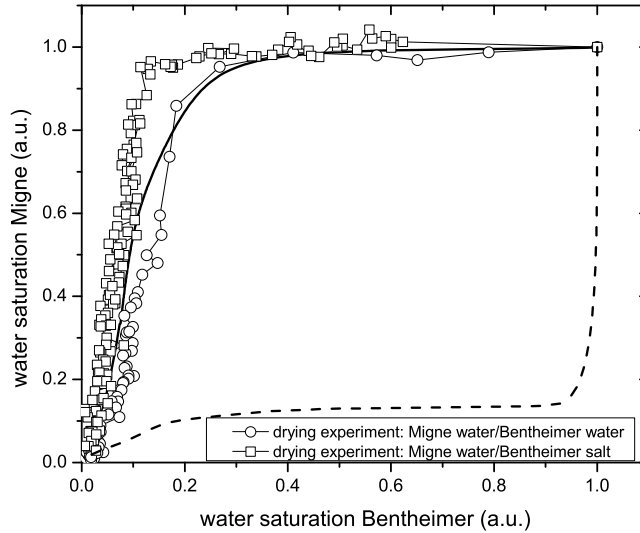


Fig. 3.10: The water saturation of a Migne limestone as a function of water saturation of a Bentheimer sandstone for a drying experiments. The dashed line represents the relation as determined from the measured capillary pressure curves (solid line) and the calculated osmotic pressure.

saturated Migne sample.

As can be seen, the theoretical and measured curves do not correspond with each other. However in order to understand this discrepancy, ion advection has to be taken into account. Therefore, in figure 3.11 we have also plotted the salt concentration profiles as measured during this experiment. As can be seen as soon as the experiment commences, salt is transported from the Bentheimer into the Migne stone. As a result there is an immediate build up of osmotic pressure in the Migne limestone, which correspondingly reduces its effective pore size. At the same time, the macroscopic capillary pressure of the Bentheimer decreases. Accordingly the moisture content relation between the two materials shifts to favour increased moisture (and salt) transport from the Bentheimer sandstone to the Migne limestone.

3.4.3 Discussion and Conclusion

These drying experiments demonstrate the effect that osmotic pressure has on salt and moisture transport within porous materials. Essentially, a saline solution in a porous material will exert an osmotic pressure that acts to reduce the effective pore size of the material. Moreover it has been shown that to correctly interpret the experimental results presented here, the movement of salt ions within a composite poultice/substrate porous system has to be taken into account. In general due to the transport and accumulation of salt from the substrate to the poultice, the effective pore size of the poultice will decrease. Hence while the pore size distribution of the poultice needs to be smaller than

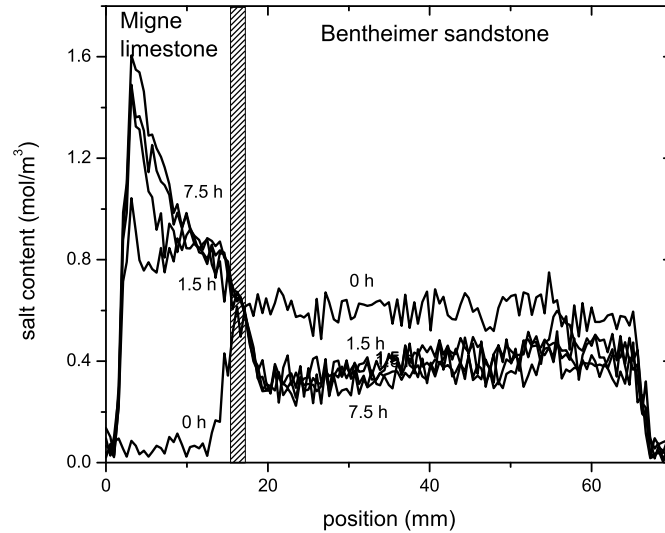


Fig. 3.11: The salt profiles in the Migne water /Bentheimer solution system plotted several times during drying.

that of the substrate for capillary flow and advection to commence, as salts accumulate in the poultice its effective pore size decreases, thereby facilitating the ongoing salt extraction process.

This study shows that contribution of osmotic pressure can exert a significant influence on salt extraction by poultice method during drying. Importantly, as salt is transported from the substrate and into the poultice, this results in a build-up of osmotic pressure within the poultice, thereby enhancing the extraction.

In order to show that this is purely an effect due to the osmotic pressure we have conducted an additional experiment in which a Bentheimer saturated with 5M NaCl solution was put on top of a 2 M NaCl solution saturated Bentheimer. In this case due to the larger concentration the effective pore size of the Bentheimer with 5 M NaCl solution will be smaller. The resulting moisture profiles and the corresponding moisture content at the interface are plotted in figure 13 and 14. As can be seen the Bentheimer with 5 M NaCl solution dried more slowly indicating that its effective pore size is smaller. After some time there was a deviation from the relationship as predicted on basis of the calculated osmotic pressure. This is due to the salt transport in the Bentheimer saturated 2 M NaCl solution towards the interface of which as a result the concentration difference will decrease.

These findings have potential practical implications for the optimization of poulticing treatments. While the pore size requirements for advection to take place at the start of the process remain, nevertheless, these constraints need not be quite so severe, as they are gradually overcome by the build up of an osmotic pressure due to the ongoing migration of salt from the substrate to

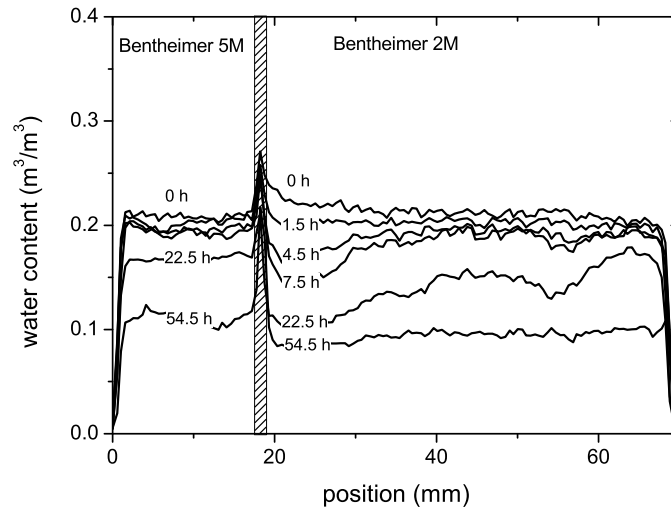


Fig. 3.12: The water profiles in the Bentheimer/Bentheimer system plotted several times during drying. Bentheimer on the top was saturated with 5M NaCl solution, the substrate Bentheimer was saturated with 2M NaCl solution.

the poultice. Moreover, it is clear that the longer a poultice stays in contact with the substrate, the more it will accumulate salt, and thereby the osmotic pressure is increased and its effective poresize will become smaller.

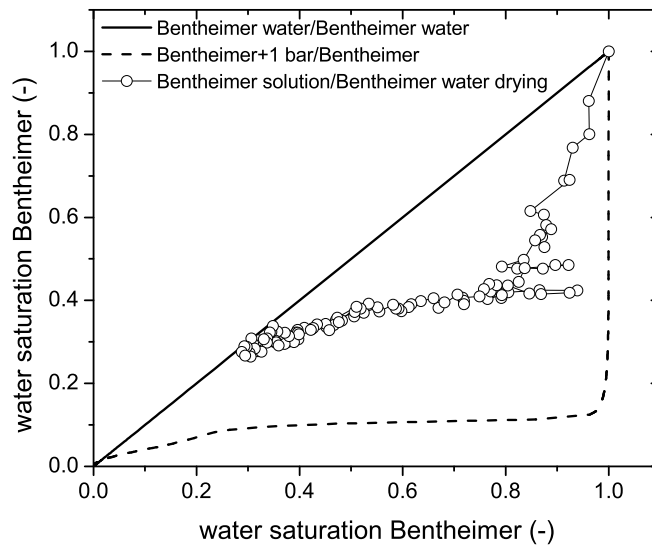


Fig. 3.13: The water saturation of the 2M NaCl solution saturated Bentheimer as a function of water saturation of the 5M NaCl solution saturated Bentheimer.

4. EXPERIMENTAL TECHNIQUES

4.1 NMR

4.1.1 NMR basics

Nuclear Magnetic Resonance (NMR) imaging is a non-destructive technique for quantitative mapping of certain chemical elements in materials. In this section the NMR technique used for the experiments reported in this thesis is discussed briefly. A quantum mechanical approach is necessary to describe some peculiar properties of NMR, but in most cases it is easier to explain the NMR technique using a semi classical model.

The NMR phenomenon is based on the fact that nuclei of atoms have a magnetic moment. In the presence of an external magnetic field \vec{B}_0 which is applied in z direction, the magnetic moment $\vec{\mu}$ of a nucleus precesses around the direction of the external field with the Larmor frequency [Cal91]:

$$f = \frac{\gamma B_0}{2\pi}, \quad (4.1)$$

where γ is the gyromagnetic ratio of the nucleus. For a given magnetic field, different types of nuclei have different Larmor frequencies. Therefore, the various types of nuclei can be differentiated on basis of these frequencies.

In an NMR experiment the ensemble of all nuclei of a certain type should be considered. The magnetic moments of these nuclei yield a net magnetization \vec{M} :

$$\vec{M} = \sum_i \vec{\mu}_i. \quad (4.2)$$

The direction of this net magnetization can be manipulated by applying a radio frequency magnetic field $\vec{B}_{rf}(t)$ perpendicular to \vec{B}_0 . In order to explain what happens when \vec{B}_{rf} is applied a coordinate frame is introduced that rotates at an angular frequency ω around the z -axis of the laboratory frame. To distinguish between the rotating frame and the laboratory frame, the rotating frame is denoted by x', y', z' , whereas the laboratory frame is x, y, z .

The motion of the magnetization \vec{M} in the laboratory frame is given by the Bloch equation [Cal91]:

$$\frac{d\vec{M}(t)}{dt} = \gamma \vec{M}(t) \times \vec{B}(t) - \mathcal{R} \left(\vec{M}(t) - \vec{M}(0) \right), \quad (4.3)$$

where $\vec{B}(t)$ is the total magnetic field, which consists of the sum of the static magnetic field \vec{B}_0 and the time varying magnetic field $\vec{B}_{rf}(t)$, and \mathcal{R} is a tensor representing the relaxation mechanisms.

In a frame rotating at the same frequency as $\vec{B}_{rf}(t)$, \vec{B}_{rf} is fixed and equation 4.3 can be written as:

$$\frac{d\vec{M}(t)}{dt} = \gamma\vec{M}(t) \times \vec{B}_1 - \mathcal{R}(\vec{M}(t) - \vec{M}(0)), \quad (4.4)$$

if the frequency of \vec{B}_{rf} corresponds to the Larmor frequency. In this equation \vec{B}_1 is the RF magnetic field vector.

In the presence of the static field B_0 in the z -direction there will be an equilibrium magnetization $\vec{M}(0)=(0, 0, M_0)$. Upon applying an RF field the magnetization changes from its equilibrium value and it will precess around \vec{B}_1 in the rotating frame. This precession is illustrated in figure 4.1.

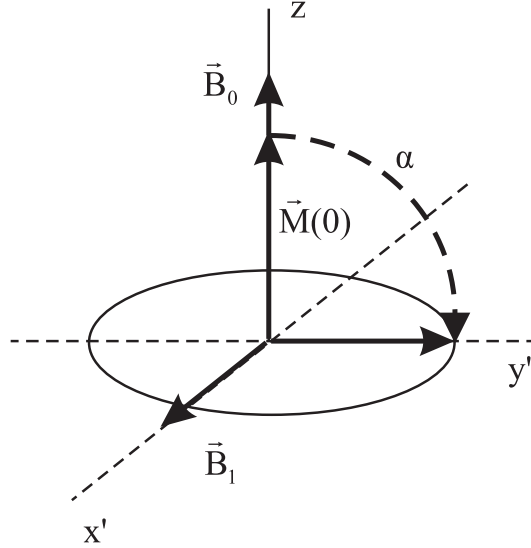


Fig. 4.1: Rotation of the net magnetization vector \vec{M} during a 90° RF pulse.

If the RF field is turned on for a time period t_{rf} and the RF frequency is equal to the Larmor frequency, the magnetization is rotated from the z axis towards the xy plane by an angle α (so-called flip angle):

$$\alpha = \gamma B_1 t_{rf}. \quad (4.5)$$

The flip angle is proportional to $B_1 t_{rf}$. If we increase the strength of the RF field or increase the time during which the RF field is applied, the flip angle increases. If $\alpha = \pi/2$ (a so called 90° pulse) the magnetization moves from the z direction into the xy plane and becomes equal to $(0, M_0, 0)$. In the laboratory frame the magnetization will now rotate around the z axis at the Larmor frequency. The system will return towards the equilibrium situation $(0, 0, M_0)$ because of two relaxation processes. The z component of \vec{M} will return to its equilibrium value $\vec{M}(0)$ by so-called spin-lattice relaxation or longitudinal relaxation. This process is characterized by a relaxation time T_1 . During this relaxation process the energy of the nuclear spins is transferred to the local environment. The magnetization components $M_{x'}$ and $M_{y'}$ will decay to zero by

so-called transverse relaxation or spin-spin relaxation. This process is characterized by a relaxation time T_2 . In this process the spin system will not exchange energy with the environment. During this relaxation process spins dephase due to interactions with their neighbors and the presence of fast changing molecular fields.

In equations 4.3 and 4.4 both the spin-spin and spin-lattice relaxation processes are taken into account by the relaxation matrix \mathcal{R} :

$$\mathcal{R} = \begin{pmatrix} 1/T_2 & 0 & 0 \\ 0 & 1/T_2 & 0 \\ 0 & 0 & 1/T_1 \end{pmatrix}. \quad (4.6)$$

Because often the magnetic field \vec{B}_0 is not perfectly homogeneous, a distribution of Larmor frequencies exists. Therefore, the dephasing of the spins in the xy plane is often faster than the longitudinal and transverse relaxation. This dephasing has a characteristic time T_2^* . Following the RF pulse, a signal can be detected as a result of the voltage induced in a pick-up coil by the rotating magnetization. This signal is called the free induction decay (FID). After some time the spins have dephased and the magnetization in the xy plane is canceled out.

In practice, when the FID has decayed significantly, a 180° RF pulse is applied, during which all spins are rotated over 180° around \vec{B}_1 . Because a 180° pulse does not change the phase accumulation itself (if only reverses the accumulated phase), it will result in a rephasing effect. This rephasing of the spins is again followed by a dephasing. The signal obtained from such a rephasing and successive dephasing is called a spin echo.

4.1.2 Spin echo detection

There are many pulse sequences leading to spin echoes [Ber04]. One of the sequences used for the measurements reported in this thesis is the Hahn sequence [Hah50]. This sequence consists of a 90° RF pulse and 180° RF pulse (figure 4.2).

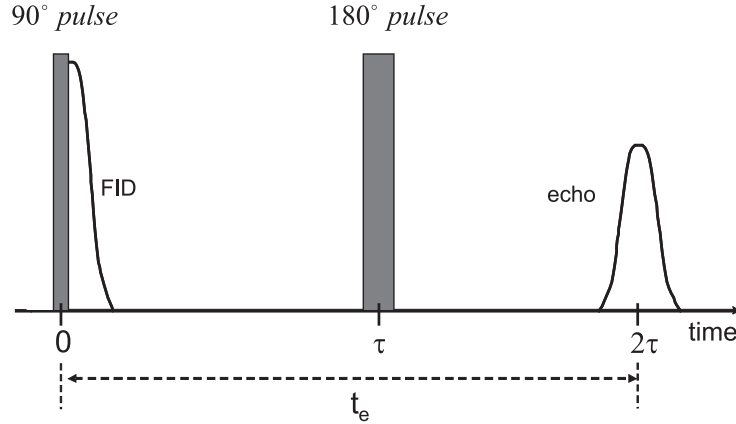


Fig. 4.2: Diagram of a Hahn spin-echo sequence. A 90° pulse is followed by a 180° pulse and the spin echo. τ is the period between the 90° and 180° pulses and $t_e = 2\tau$ is the echo time.

The time between the two RF pulses is called the inter pulse delay time τ . An echo occurs at a time $t_e(2\tau)$ after the initial 90° RF pulse. The signal to noise ratio of the measurements can be improved by averaging the signals obtained from successive measurements. After each measurement, however, one has to wait until the transverse relaxation process has destroyed the transverse magnetization and the longitudinal relaxation process has restored the longitudinal magnetization to the equilibrium situation. The latter process is generally the limiting factor. The time between successive spin-echo sequences is called the repetition time t_r .

If a magnetic field gradient is superimposed on \vec{B}_0 , the Larmor frequency becomes position dependent. Since the pulse sequence sketched in figure 4.2 only excites spins within a small range of Larmor frequencies, only a small slice of the sample will contribute to the spin-echo signal. In this way, the Hahn spin-echo sequence can be used to measure the amount of hydrogen and/or sodium in a slice of a material. The position of the selected slice can be changed by moving a sample along the direction of the field gradient.

For moisture and ions in a porous material $T_2 \ll T_1$. In that case the signal intensity of the spin echo is given by [Cal91]:

$$S = k\rho \left(1 - \exp\left(-\frac{t_r}{T_1}\right) \right) \exp\left(-\frac{t_e}{T_2}\right). \quad (4.7)$$

In this equation k is the sensitivity of the nuclei, ρ is the density of the nuclei, t_r is the repetition time of the pulse sequence and t_e is the echo time.

From the signal intensity of the individual slices, hydrogen or sodium profiles in the whole sample can be composed.

Another sequence used for the measurements is the Carr Purcell Meiboom Gill pulse sequence (CPMG) [Car54]. The CPMG sequence consists of a 90° pulse followed by many 180° pulses (figure 4.3). A 90° pulse puts the magnetization in the xy plane. After each 180° pulse, the spins rephase, giving rise to a spin-echo signal, and dephase again. The timing of the CPMG sequence is such that the 180° pulses are applied at $(2n - 1)\tau$, ($n = 1, 2, 3, \dots$) and the signals appear at $t = 2n\tau = nt_e$.

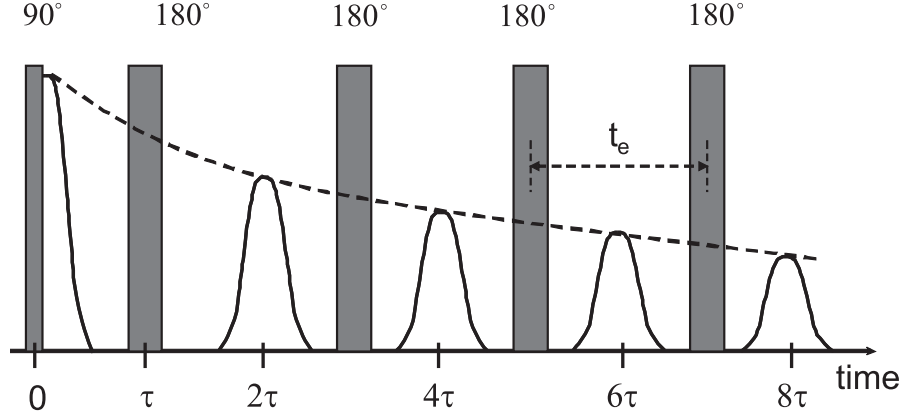


Fig. 4.3: Diagram of a CPMG sequence. A 90° pulse is followed by number of 180° pulses. A spin echo forms after each 180° pulse.

By measuring the amplitude of the spin echoes in the CPMG sequence we can obtain the transverse magnetization decay. If dephasing due to movement of the spins can be neglected, this decay is governed by the transverse relaxation time T_2 . In that case the magnetization decay $S(t)$ is given by:

$$S(t) = S(0) \exp\left(\frac{-t}{T_2}\right), \quad (4.8)$$

where $S(0)$ is the equilibrium magnetization. The transverse relaxation of the spins in a liquid in a porous material is rather fast (microseconds to milliseconds) and depends on the pore size of the material. The relation between the transverse relaxation time and the pore size of the material will be discussed in the next section.

4.1.3 NMR and pore size distributions of porous materials

When performing NMR measurements on water in a porous material the NMR relaxation of hydrogen nuclei can be used to determine the distribution of water within a porous medium in relation to pore size.

Consider a spherical pore with a volume V and a surface S , which is completely filled with water. The water molecules in this pore will move randomly due to Brownian motion. This random motion is characterized by the self-diffusion coefficient D_{self} . Near the pore wall the transverse relaxation of the nuclei of the water is fast, in the order of microseconds. The relaxation of the hydrogen nuclei in bulk water, characterized by $T_{2,bulk}$, is much slower, in the

order of seconds. Brownstein and Tarr [Bro79] have shown that in the so-called fast diffusion limit the overall relaxation time, $T_{2,meas}$, is given by:

$$\frac{1}{T_{2,meas}} = \frac{1}{T_{2,bulk}} + \frac{S}{V}\rho_{2,surf}, \quad (4.9)$$

where $\rho_{2,surf}$ is the surface relaxivity. This fast diffusion limit generally holds for pore sizes in the nanometer and micrometer range. Because the bulk relaxation time is much larger than the surface relaxation time, the first term at the right hand side of equation 4.9 can usually be neglected. Therefore, the measured relaxation time is proportional to (V/S) which is a measure of the pore size. Assuming cylindrical pores with radius r , the volume to surface ratio $V/S = r/2$ and therefore:

$$T_{2,meas} = \frac{r}{2\rho_{2,surf}}. \quad (4.10)$$

4.1.4 NMR measurement setup

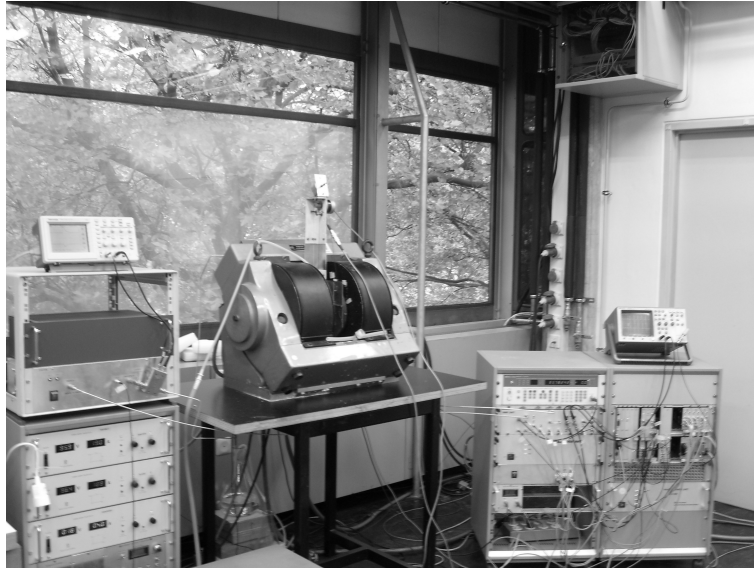


Fig. 4.4: The NMR apparatus used in the experiments described in this thesis.

The NMR scanner used in the experiments is a home built 0.78 T scanner. A picture of the NMR setup is shown in figure 4.4. In our experiments the main magnetic field B_0 and the field gradient G were 0.7 T and 0.33 T/m, respectively. The RF circuit was specially designed in order to measure quantitatively both H and Na contents at different positions within the sample [Pel00].

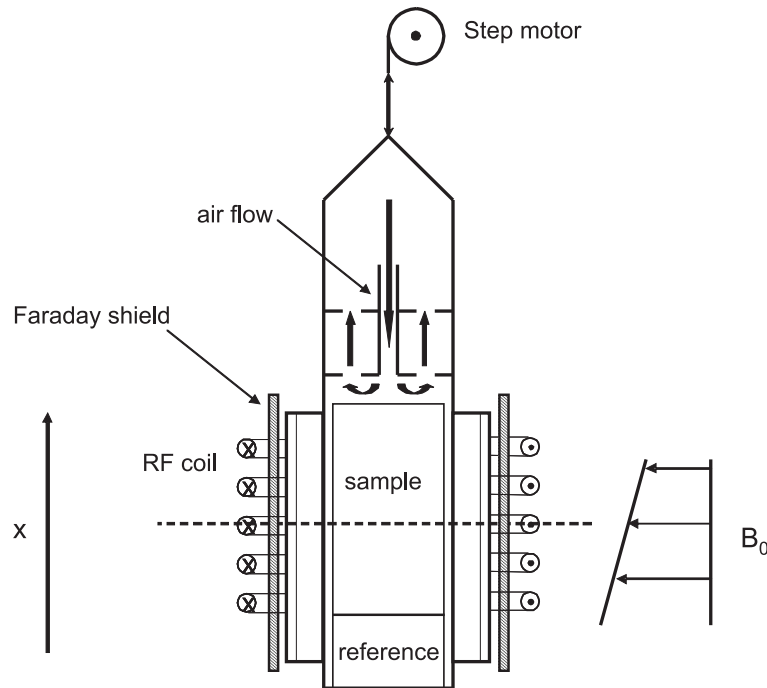


Fig. 4.5: Schematic diagram of the NMR setup for drying experiments. The Teflon holder with the sample and the reference is moved in the vertical direction by means of a step motor.

To determine the H and Na profiles over the whole sample, the sample holder (figure 4.5) was moved in the vertical (x) direction by means of a step motor. The time to measure both a H and Na profile within the sample was about 1.5 h. The echo times for measuring hydrogen and sodium were 0.2 and 0.45 ms, respectively. Due to the short transverse relaxation time of Na in the solid phase in our equipment only dissolved Na ions were measured. The Na signal was obtained from 256 successive spin-echo measurements which were averaged to obtain a sufficient signal to noise ratio.

Using a reference, the H and Na signal intensities can be related to the amount of water and the amount of sodium, respectively. This reference contained a NaCl solution ($c = 4 \text{ mol/kg}$).

4.2 Methods of measuring the capillary pressure curve

The relation between the applied pressure and the water saturation in a porous medium, the so-called capillary pressure curve, is useful to characterize the pore structure of the medium. To find a capillary pressure curve two experimental methods are described: pressure plate (direct method) and mercury intrusion porosimetry (indirect method).

4.2.1 Pressure plate

A key element in considering immiscible fluids in a pore is the presence of a curved meniscus between the fluids. This leads to a pressure difference between

the fluids related to the curvature of the interface. This pressure difference, called capillary pressure P_c , is inversely proportional to the radius of curvature, which is related to the pore radius [Won99]. In case of a water-air mixture, the capillary pressure drives water into the pore. If we counteract this process with an applied pressure difference δP_a , the pore will be emptied when $\delta P_a > P_c$ and filled with water when $\delta P_a < P_c$. However, in a porous material generally a distribution of pore sizes is present. Therefore, not all pores will be emptied or filled at the same applied pressure difference. The larger pores with larger throats will be emptied at low values of δP_a , whereas smaller pores with narrow throats will be emptied at higher δP_a . Therefore, the moisture content θ will be a function of the applied pressure difference:

$$\theta = \theta(\delta P_a). \quad (4.11)$$

The relation between the water saturation and the applied pressure difference δP_a can be measured directly by the so-called pressure plate method.

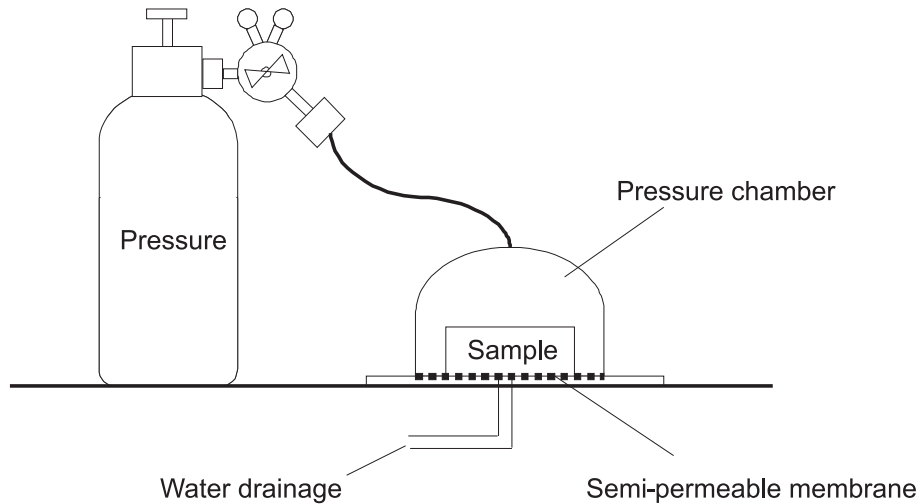


Fig. 4.6: General schematic of a pressure plate apparatus.

The pressure plate originates from soil physics. A pressure plate apparatus for the measurement of water retention curves was first used by Richards [Ric48]. Later this method was adopted for use on wood and building materials [For79], [Clo91].

In figure 4.6 a schematic diagram of a pressure plate apparatus is shown. A pressure plate consists of a pressure chamber with a semi-permeable membrane. This membrane allows water to pass through but is air tight. The sample is placed in the pressure chamber on this membrane. Before the start of the measurements the sample is saturated with water and placed in the pressure chamber. By slowly increasing the pressure in the chamber the moisture saturation in the sample will decrease. As each experimental data point should represent an equilibrium situation where no moisture transport within the sample occurs it takes on average 2 weeks. Therefore, the pressure plate method is very time consuming.

The applied pressure difference δP_a is related to the hydraulic radius of the pores in the material that are being emptied according to the Kelvin equation, describing the capillary pressure:

$$\delta P_a = \frac{2\gamma_w \cos\theta_w}{r}, \quad (4.12)$$

where r is the radius of the pore, γ_w is the surface tension of the water, and θ_w is the contact angle between the air-water interface and the pore wall. This angle is generally assumed to be zero because of the complete wetting of porous materials by water [Kru97]. Equation 4.12 is often used to determine a pore size distribution from the measured capillary pressure curve. One should note that the resulting values of r are only accurate for cylindrical pores. For a real porous system the values of r obtained from equation 4.12 may not reflect the actual pore sizes. An example is the so-called ink-bottle effect, which occurs when larger channels or pores are interconnected by smaller throats. When a certain pressure is applied on a such system water from the larger channels can flow out only through the smaller throats. As a result, the larger channels or pores will be underestimated in size.

4.2.2 Mercury intrusion porosimetry

The determination of the capillary pressure curve of water is often based on the capillary pressure curve of mercury measured by MIP. Mercury intrusion porosimetry was first used by Washburn [Was21] and has been used as a reliable method to determine the total pore spaces and pore size distribution for a wide variety of porous solids [Rit45].

Mercury is non-wetting for most porous materials. In contrast to water, it does not enter the pores spontaneously. Intrusion of mercury into the pores occurs only when external pressure P_m is applied on the mercury. The radius of the pores being intruded by mercury can be deduced again from the Kelvin equation:

$$r = -\frac{2\gamma_m \cos\theta_m}{P_m}. \quad (4.13)$$

In this equation γ_m is the surface tension of the mercury, θ_m is the contact angle between the mercury and the pore wall. This contact angle is 140° on average [Rit45].

Since equations 4.12 and 4.13 both originate from the Kelvin equation, the equivalent pore radius should theoretically be equal for the both the pressure plate and the MIP measurements:

$$r = \frac{2\gamma_w \cos\theta_w}{\delta P_a} = -\frac{2\gamma_m \cos\theta_m}{P_m}. \quad (4.14)$$

The capillary pressure curve of water can be related to the experimental mercury intrusion data by rewriting equation 4.14 to:

$$\delta P_a = \frac{\gamma_w \cos\theta_w}{\gamma_m \cos\theta_m} P_m. \quad (4.15)$$

A typical mercury intrusion test involves placing a sample into a chamber. The sample needs to be dry, therefore the chamber is evacuated to remove contaminant gas and vapor. After evacuating the chamber is filled with mercury. Next, pressure is applied, and the volume of mercury forced into the sample is measured, for instance, by an electrical capacitance method [Web97].

The advantage of MIP is that it is fairly rapid (few hours) in comparison with the pressure plate (several weeks). The pore size range that can be detected by MIP is from about 10 nm to a few 100 μm . Limitations of MIP originate also from the "ink-bottle" effect, in which case the calculated size of the internal pores is determined by the pore-throats used to access these pores. Moreover, a sample has to be dry before the measurements, which in some cases gives rise to inaccurate results, because of, e.g., shrinkage of the material.

A number of researchers have compared capillary pressure curves obtained by MIP with capillary pressure curves obtained by pressure plate measurements. Some researches reported that the capillary pressure curve determined by MIP is closely related to the pressure plate results [Aun01]. However, some results have shown significant deviations between these capillary pressure curves [Kro99]. These deviations were explained by the ink-bottle effect.

The MIP measurements presented in this thesis have been obtained using an Autopore IV9500 (Micromeritics Instrument Corporation). The derivative of the mercury content of the sample with respect to pressure was used to obtain the pore size distribution.

4.2.3 *Ion Chromatography (IC)*

The salt accumulated at the drying surface of a porous material will crystallize and cannot be determined by NMR. In order to validate the total amounts of sodium and chloride in the sample an ion chromatograph was used. The IC measurements data presented in this thesis have been performed using an ICS-90 (Dionex Corporation).

Ion chromatography (IC) is a technique for the separation of many ionic species. Once separated, the individual ions are detected, identified and quantified. This technique with different modifications is used very frequently since it has been introduced in 1975 by Small [Sma75].

Several ion separation methods are available in IC. Ion exchange is the primary method of separation. For inorganic anions and cations this method allows ions to be separated based upon specific properties, e.g. their charge. The ion-exchange processes occur between a mobile phase and ion-exchange groups bonded to a support material. The support material consists of polystyrene, ethylvinylbenzene, or methacrylate resins co-polymerized with divinylbenzene and modified with ion-exchange sites. Separation of anions is accomplished with quaternary ammonium groups attached to the polymer, whereas sulfonate-, carboxyl-, or phosphonate groups are used as ion-exchange sites for the separation of cations. Different types of ions migrate through the resin at different rates, depending upon their interactions with the ion-exchange sites.

In order to validate the amount of ions after a drying process a part of the sample was powdered and diluted with a certain amount of pure water.

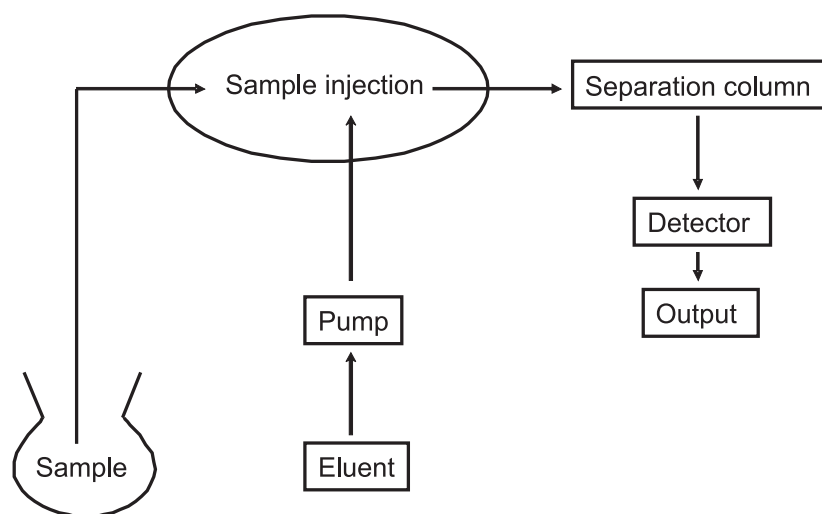


Fig. 4.7: General schematic of an IC system.

The total amount of ions in this solution was measured quantitatively by ion chromatography.

In general an IC system consists of a liquid eluent, a high pressure pump, a sample injector, an analytical separator column and a detector (figure 4.7). The eluent pumped continuously through the system at a fixed rate. The sample is introduced into the system by a sample loop on the injector. Next, the sample with the eluent is pumped into the separation column. The sample ions are attracted to the charged stationary phase of the column. Because the different sample components progress through the column at different rates they enter the detector at different times. The detector monitors the electrical conductance of a solution of the sample ions and produces the chromatogram.

5. OSMOTIC PRESSURE IN A POULTICE/SUBSTRATE SYSTEM

Salts are widely recognized as a cause of deterioration of porous building materials. A general approach to slow down salt damage problems is reducing the salt content of the affected object. One of the most common treatments is the application of poultices. Desalination by poultices may result from two different salt transport processes: diffusion and advection. In this study we consider only the advection process. In the case of advection based desalination the efficiency of salt extraction strongly depends on the pore-size range of the substrate and the poultice. For advection to be effective, the poultice materials should be adapted to the pore-size distribution of the substrate. However, the poultice can shrink during drying, which affects the pore-size distribution of the poultice material. The salt transport from the poultice to the substrate by water advection results from a capillary pressure gradient, but upon drying a salt concentration gradient may appear in the poultice/substrate interface. Because of this concentration gradient an osmotic pressure arises, which may change the drying behavior of the poultice/substrate system. We have investigated the effect of the pore size distribution of the poultice and the osmotic pressure on the drying behavior of a poultice/substrate system. To this end, we have measured the time evolution of moisture and salt concentration profiles in such a system, using a specialized NMR setup. Comparison of the results with a model based on capillary pressure equilibrium at the poultice/substrate interface shows that the accumulation of salt from the substrate in the poultice may improve the salt extraction process, because the osmotic pressure decreases the effective pore size of the poultice.

5.1 Introduction

It is well known that the decay of historic buildings and monuments made of porous materials is caused by the presence of soluble salts [Arn91], [Gou97], [Lew80]. One of the common approaches to protect historic buildings and monuments from further decay is desalination by poulticing [Ver05]. Desalination by poulticing means the transport of soluble salts from the affected object into the poultice material. The salts that are dissolved in water can move from the object into the poultice by two mechanisms: diffusion and advection. Because salt transport by diffusion is relatively slow (it can take several months) [Pel10], in this study we only consider advection, which is a considerably faster mechanism.

Salt transport by advection requires a capillary pressure gradient as the driving force during the drying process. During drying the largest pores, where the capillary pressure is lowest, will empty first. In a porous system consisting of two layers water will flow from the material with larger pores to the material

with smaller pores. Consequently, in a poultice/substrate system the poultice should have smaller pores than the substrate in order to provide water flow from the substrate into the poultice. Therefore, in order to improve the salt extraction efficiency, the pore sizes of the poultice should be adapted to the pore sizes of the substrate.

During drying of a poultice/substrate system salts migrate from the substrate to the poultice and a concentration gradient develops in the poultice/substrate interface. The presence of a concentration gradient in this interface creates an osmotic pressure, which can significantly influence the water flow. In [Vor11] the influence of osmotic pressure on the water flow in a layered system of two porous materials has been shown. It was demonstrated that the osmotic pressure generated by a saline solution in a porous material will reduce the effective pore size of that material. During drying salt will be transported from the substrate into the poultice, and hence the effective pore size of the poultice will decrease. Since for salt extraction by advection [Pel10] the pores of the poultice have to be smaller than those of the substrate, the accumulation of salt in the poultice can effectively decrease the pore sizes and improve the salt extraction process. However, in that study the experiments were conducted using rigid porous materials in order to create a pure osmotic pressure effect. These materials were selected to avoid shrinkage effects which are commonly inherent to poultice materials.

The objective of the present research is to investigate both the effects of osmotic pressure and varying pore size distribution of the poultice on the water flow in a poultice/substrate system during drying. To this end a series of drying experiments on a kaolin/sand poultice and fired-clay brick substrate have been done. First, the theoretical aspects related to the moisture and ion transport in a poultice/substrate system will be discussed. Second, the experimental methods and the main characteristics of the poultice and substrate material will be given. Next, the moisture transport measurements during drying will be presented. The paper ends with a discussion and some conclusions.

5.2 Theory

5.2.1 Capillary pressure

For a single pore the capillary pressure p_c is given by:

$$p_c = -\frac{2\gamma \cos \varphi}{r_m}. \quad (5.1)$$

where γ [N/m] is the surface tension of the liquid/vapor interface, φ [-] the contact angle between the liquid/air and liquid/solid interface and r_m [m] the pore size. In a porous material a distribution of pore sizes is present and hence the overall macroscopic capillary pressure of the material ψ , is a function of its pore size distribution. At any given moisture content, the distribution of water within the material depends on its pore size distribution. For any moisture content θ there will be a critical pore radius, r_m , which discriminates between the pores filled with water and the empty pores.

The capillary pressure curve and pore size distribution measured for a fired-clay brick are plotted in figure 5.1. As can be seen from this figure the fired-clay brick contains pores with diameters in the range of 3-10 μm .

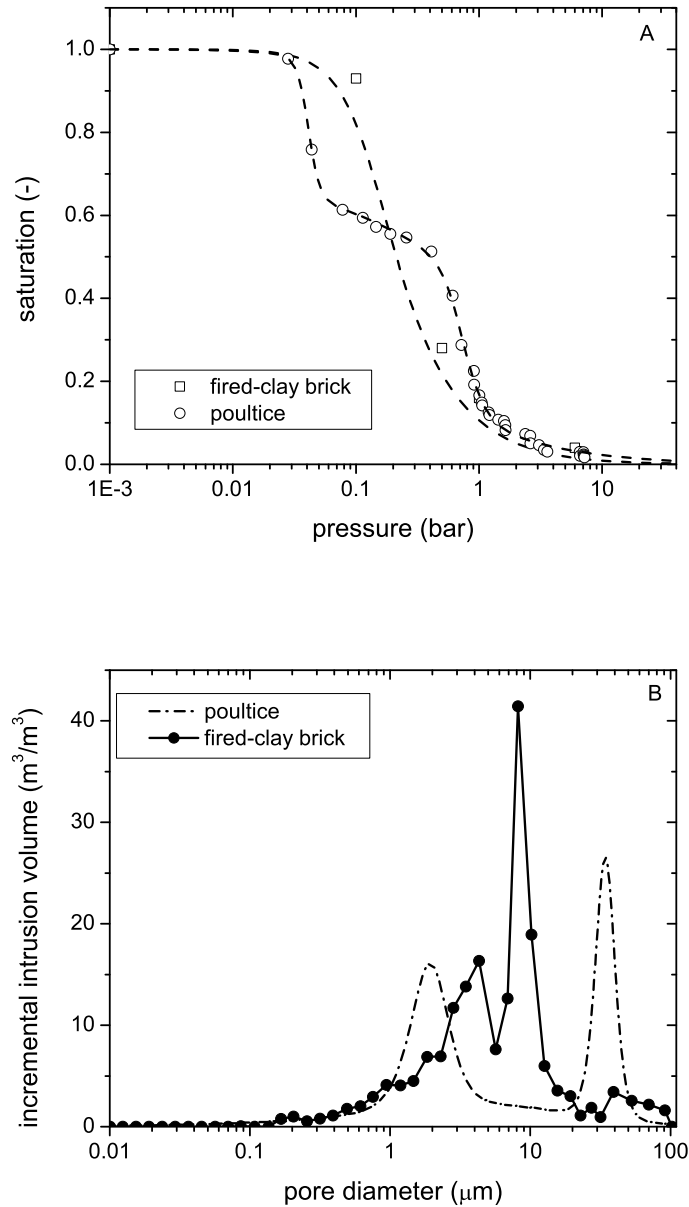


Fig. 5.1: A. Capillary pressure curve of fired clay brick measured by a pressure plate and the capillary pressure curve of poultrice determined from drying experiments. The dashed curve is a pressure curve fit through the measured data points. B. Pore size distribution of fired-clay brick obtained by mercury intrusion porosimetry and that of poultrice obtained from drying experiments.

In case of a combination of two materials like a poultrice/substrate system

we will have an two air/material and one material/material interface. If we assume a perfect hydraulic contact at the material/material interface the capillary pressure will be continuous at this interface, i.e.:

$$\psi_p(\theta_p) = \psi_s(\theta_s). \quad (5.2)$$

where ψ_p is the capillary pressure of the poultice and ψ_s is the capillary pressure of the substrate. θ_p and θ_s are the moisture content of the poultice and the substrate, respectively. Because of differences between the pore-size distributions and, consequently, the capillary pressure curves of both materials, generally a jump in moisture content across the interface will occur. The relation between the moisture contents on both sides of the interface can be described by:

$$\theta_p = \psi_p^{-1}\psi_s(\theta_s) = f(\theta_s). \quad (5.3)$$

As an example the moisture profiles measured during drying of a fired-clay brick/poultice combination are plotted in figure 5.2(A). These profiles have been measured using an NMR based method described in section 5.3. As already mentioned above, during drying the largest pores, where the capillary pressure (p_c) is lowest, will empty first. In the present system three drying stages can be observed. During the first stage (up to about 4 hours) the poultice dries significantly, whereas the fired-clay brick remains almost saturated. The brick starts to dry during the second stage. During the third stage (after about 15 hours) the brick is almost dry and the poultice still contains water.

From these experiments, a relation can be derived between the moisture contents in the brick and the poultice at the interface between these two materials. This relation is plotted in figure 5.2(B), where the moisture contents in both materials are scaled to the respective saturation values at $t = 0$. Using this relation and the capillary pressure curve of the fired-clay brick, the capillary pressure curve of the poultice can be determined. This curve is included in figure 5.1.

This drying behavior of the fired-clay brick/poultice system can be explained as follows. If a poultice would have one pore size which is equal to the pore size of fired-clay brick, equation 5.3 predicts a linear relation between the moisture contents of both materials at the interface. If a poultice would have one pore size which is smaller or larger than the pore size of fired-clay brick, it can be derived from equation 5.3 that an inflection point will occur in this relation. In the present system (figure 5.2(B)) we have observed two inflection points. This indicates that the poultice has two dominant pore sizes, one in the range smaller than 3 μm and one in the range larger than 10 μm . If the pores of the substrate are considerably smaller than those of the poultice, the pores of the substrate remain filled with water. If, on the other hand, the pores of the substrate are considerably larger than those of the poultice, the pores of the substrate will be emptied first.

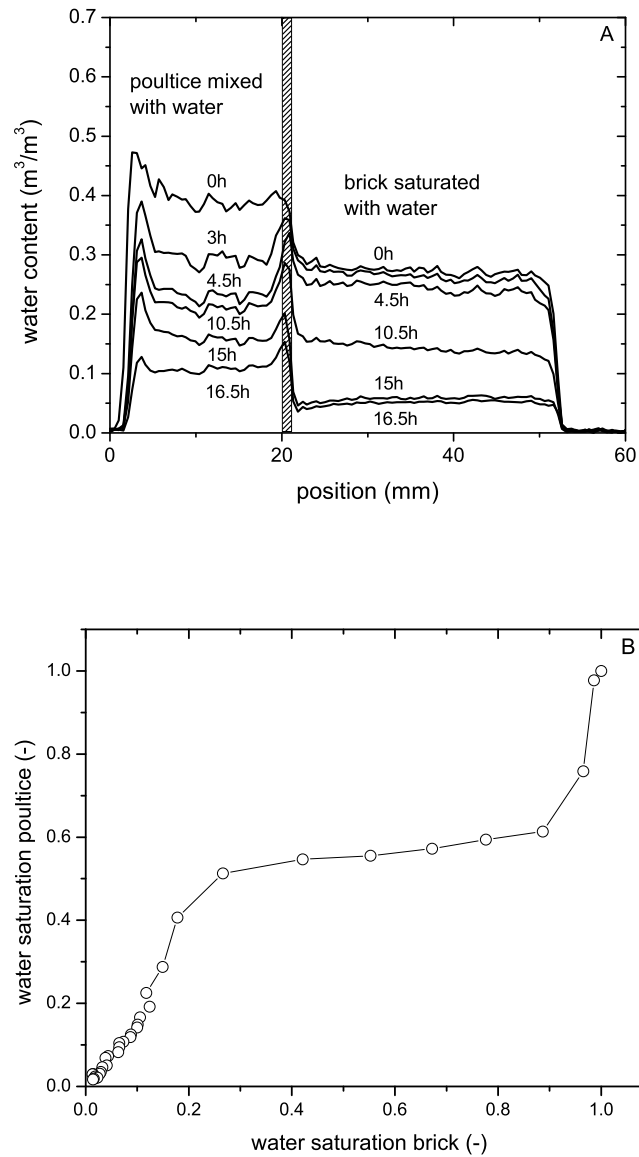


Fig. 5.2: A. Water profiles in a fired-clay brick/poultice system measured during drying. The brick was initially saturated with pure water and the poultice materials were mixed with water. B. Saturation of the fired-clay brick as a function of the water saturation of the poultice determined from the drying experiments.

5.2.2 Capillary pressure and osmotic pressure

When the substrate/poultice system contains a saline solution, there is an additional contribution to the macroscopic capillary pressure of each porous material resulting from the osmotic pressure, i.e.:

$$\psi = \psi_c(\theta) + \psi_s, \quad (5.4)$$

where the osmotic pressure, ψ_s , is given by:

$$\psi_s = \frac{RT}{V_w} \ln(a_w). \quad (5.5)$$

Here R is the universal gas constant, T the absolute temperature and a_w the water activity (for pure water $a_w = 1$ and hence the osmotic pressure is zero). As a result of the presence of soluble salt in a porous material, its effective pore size will decrease, since the total macroscopic capillary pressure is increased by osmotic pressure of the salt [Vor11]. As an example the water retention curves for the fired clay brick and the poultice are plotted in figure 5.3 for various NaCl concentrations.

As can be seen from this figure, at higher salt concentrations the macroscopic capillary pressure is predominantly determined by the osmotic pressure. At increasing values of the osmotic pressure the water retention curve significantly changes and does no longer reflect the actual pore size distribution. As a result the relation between the moisture contents of both materials at the interface will significantly change. This is illustrated in figure 5.3 for the presence in either the poultice (p) or the substrate (s). This figure shows that the moisture will have a tendency to remain in the material where salt is present. This indicates that an increasing salt content of a material significantly decreases its effective pore size. However, one should note that this model is quite simple, because it considers only static salt contents. During drying salt is transported by water advection through the interface and therefore the salt concentrations can change. To study the effect of osmotic pressure in such a dynamic situation, drying experiments are needed.

5.2.3 Shrinkage and osmotic pressure

We have shown that the poultice used in this study has mainly two dominant pore sizes, smaller pores in the diameter range of a few microns and larger pores of several tens of microns. However, we also have observed that the poultice shrinks during drying.

In figure 5.4 the thickness of the poultice is plotted as a function of the drying time. This figure shows that during the first drying stage mentioned in section 5.2.1, i.e., up to about 4 hours, the thickness decreases. Consequently, the pore size distribution of the poultice materials will change. Since during this drying stage the smaller pores of the poultice are still filled with water, we assume that the shrinkage is mainly associated with a collapsing of the larger pores when they are emptied. This assumption is supported by the observation that the thickness of the poultice decreases by about 5 %, corresponding to

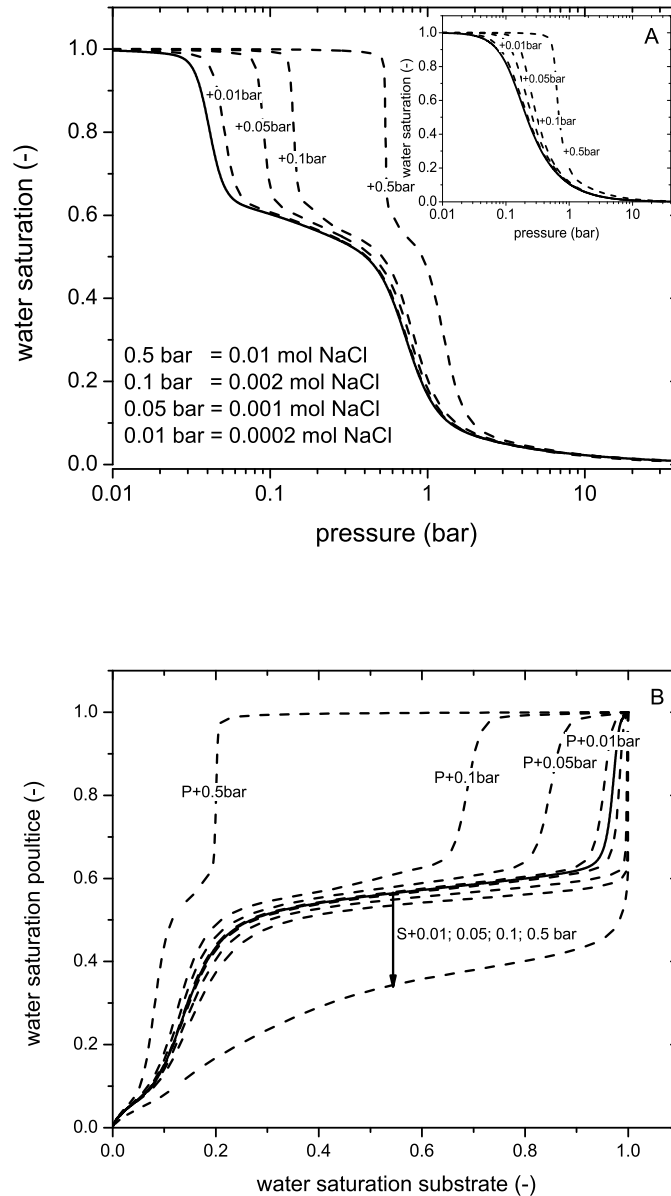


Fig. 5.3: A. Water retention curves of a fired-clay brick and a poultice for various NaCl salt contents. B. Water saturation of the poultice as a function of water saturation of the fired clay brick. The various curves represent the relation for various salt contents in either the fired-clay brick or the poultice.

a volume shrinkage of about 15 %. This agrees very well with the water loss of $0.15 \text{ m}^3/\text{m}^3$ of the poultice during the first drying stage, associated with emptying of the large pores. Since during this drying stage hardly any water is transported from the fired clay brick to the poultice and after this stage the large pores have collapsed, we will not consider these pores in the description

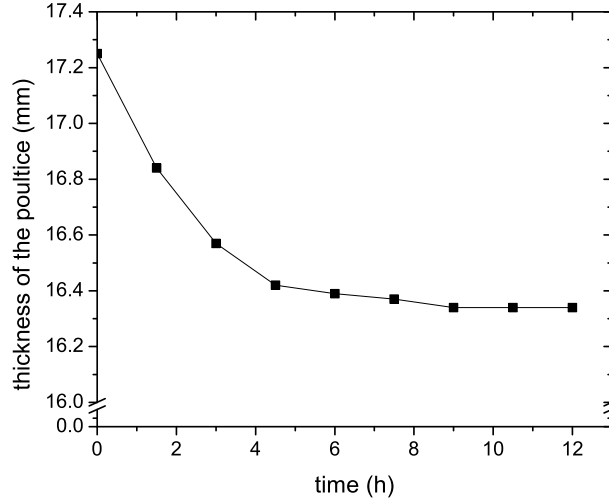


Fig. 5.4: Thickness of the poultice vs. drying time determined from the moisture profiles.

of the advection based desalination process. We will return to this point in section 5.4.1.

A first consequence of this approach is that the water retention and saturation curves for the fired clay brick and the poultice plotted in figure 5.3 should be modified. Some examples of such modified curves are shown in figure 5.5. The latter curves will be used to describe the osmotic pressure effects during desalination in the poultice/fired clay brick system.

5.2.4 Peclet number and desalination

Ions can be transported both by advection and by diffusion. As already mentioned in the introduction, in this study we focus on salt extraction by advection. Because the driving force for salt transport is water transport, it is important to maintain the drying process as long as possible. However, at very low drying rates salt transport by diffusion can become dominant and a competition between two mechanisms of transport, advection and diffusion, will take place. The salt transport can be described by a combined advection-diffusion equation [Bea90]:

$$\frac{\partial(C\theta)}{\partial t} = \frac{\partial}{\partial x} \left[\theta \left(D_{eff} \frac{\partial C}{\partial x} - CU \right) \right]. \quad (5.6)$$

where C is the salt concentration, D_{eff} is the effective diffusion coefficient of the salt in the porous material and U is the moisture velocity. Therefore the term at the left hand side refers to the change in the total salt content $C\theta$ over time. The terms at the right hand side refer to the transport of salt in the presence of moisture by diffusion (given by the term $D_{eff}\partial C/\partial x$) or by advection (given by the term CU), respectively. From this equation, the competition between

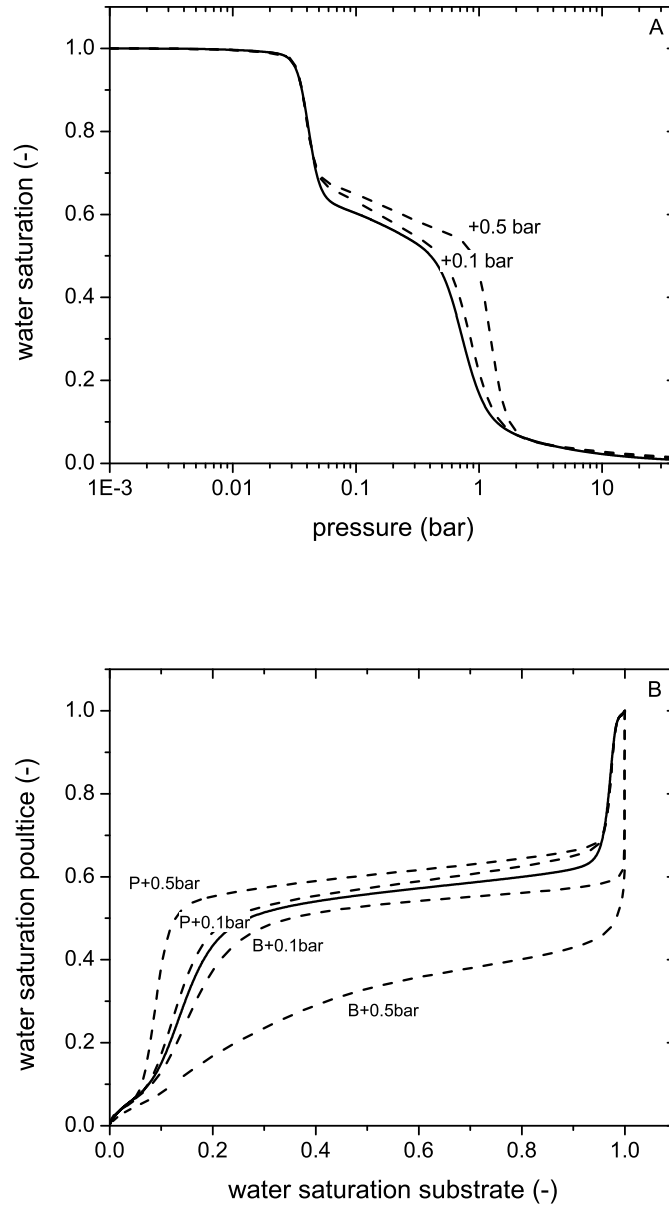


Fig. 5.5: A. Water retention curves of the poultice in which the collapsing of the larger pores during drying has been accounted for. B. Water saturation of the poultice as a function of the water saturation of the fired-clay brick. The various curves represent the relation for various salt contents in either the brick or the poultice.

two mechanisms of transport, advection and diffusion, can be characterized by a Peclet number, Pe [Hui02]:

$$Pe = \frac{|U|L}{D_{eff}}, \quad (5.7)$$

where L is the length scale of interest. If $Pe \gg 1$, advection dominates and ion transport takes place due to capillary water flow. For $Pe \ll 1$, diffusion dominates and ion transport depends on the concentration gradient. As a result, salts can be extracted by advection only from that part of the substrate where $Pe > 1$. It is important to keep the drying rate sufficiently high as long as possible to satisfy this condition, in order to extract the maximum amount of salt from an affected object.

5.3 Experimental setup

5.3.1 Sample materials

In order to study the effect of osmotic pressure on salt and moisture transport between substrate and poultice during drying, experiments were conducted using a rigid porous material as substrate and various poultice materials. The substrate used in this study is a fired clay brick with pore sizes in the diameter range 3-10 μm (figure 5.1), as was already discussed in section 5.2. Cylindrical substrates were drilled with a diameter of 19 mm and a total length of 31 mm. The poultice mixture selected for the test is kaolin/sand/water (1:5:0.2) by weight. The sand was siliceous sand (standard sand CEN-NORMSAND DIN-EN 196-1). This mixture was selected on the basis of a characterization survey, including pore-size distribution measurements, of a large range of different poultice mixtures, the results of which are presented in [Lub10]. The selection of the ratio of the component has been primary made based on good adhesion and workability and easy application to a vertical surfaces such as a wall.

5.3.2 Experimental design

The hydrogen and sodium profiles have been measured with a home-built NMR scanner especially designed for this purpose. An extensive description of this set up can be found in [Pel95], [Pel02]. In our experiments the main magnetic field B_0 and the field gradient G were 0.7 T and 0.33 T/m, respectively. The RF circuit was specially designed in order to measure quantitatively both H and Na contents at different positions within the sample [Pel00]. To determine the H and Na profiles over the whole sample, the sample holder was moved in the vertical (x) direction by means of a step motor. A standard Hahn spin-echo sequence was used. The time to measure both a H and Na profile within the sample and the poultice was about 1.5 h. The echo times for measuring hydrogen and sodium were 0.2 and 0.45 ms, respectively. Due to the short transverse relaxation time of Na in the solid phase, in our equipment only dissolved Na ions were measured. The Na signal was obtained from 256 successive spin-echo measurements of which the signals were averaged to obtain a sufficient signal to noise ratio. Using an external standard containing a NaCl solution ($c = 4$

mol/l)., the H and Na signal intensities can be related to the volume of water and the quantity of Na.

Experiments were performed in which initially either the substrate or the poultice was saturated with a saline solution, while the other contained only water. The substrate was first vacuum saturated with water or a 3M salt solution. All sides of the substrate except the top were wrapped in Teflon tape to prevent water evaporation at these surfaces. The poultice composition mixed with water or with a 3M NaCl solution was applied on top of the substrate and next the system was placed within the sample chamber of the NMR scanner. Dry air (at 5% RH) was blown over the exposed poultice top surface, thereby creating a one-dimensional drying experiment.

5.4 Results and Discussion

5.4.1 Poultice (saline solution)/Substrate (water)

In order to study the potential effect of osmotic pressure on salt and moisture transport during poulticing treatments the experiments discussed in section 5.2 were repeated, but with the modification that now either the poultice or the substrate was saturated with a saline solution instead of water.

In the first experiment the poultice materials was mixed with a 3M salt solution and then applied on top of the substrate which had been saturated with water. In figure 5.6 we have plotted both the measured and calculated relation between the moisture content of the poultice and that of the substrate at the interface.

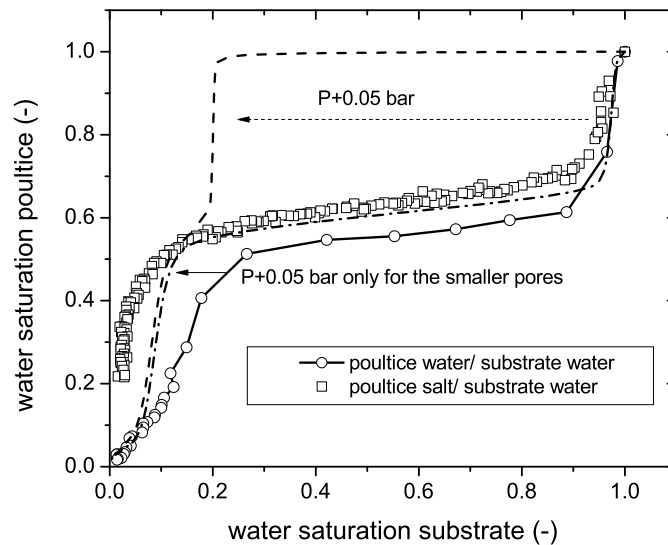


Fig. 5.6: Water saturation of the poultice as a function of the water saturation of the fired-clay brick. The experimental results are compared with the theoretical model.

Initially, as the drying starts, the poultice loses moisture, while the substrate remains saturated. However, once the moisture saturation of the substrate drops below 0.9, the influence of the osmotic pressure in the saline saturated poultice becomes evident. During the next drying stage, the moisture content of the substrate decreases, while the moisture content of the poultice remains almost constant. Once the moisture saturation of the substrate has decreased below 0.3, the effect of the osmotic pressure becomes very significant. As the osmotic pressure reduces the effective pore size of the poultice, the water saturation of the poultice remains rather high (about 0.6) until the substrate reaches much lower moisture saturation levels than for the poultice(water)/substrate(water) combination.

The dashed curve in figure 5.6 lines represents the calculated relation between the moisture contents of the poultice and the substrate at the interface. This relation, which includes the influence of osmotic pressure on all pores that are initially present in the poultice, does not correspond well to the curves determined by drying measurements. However, the relation which includes only the influence of the osmotic pressure on the small pores of the poultice (dashed-dotted curve) corresponds well to the results from the drying experiment. This confirms the assumption in section 5.2.4 that the large pores disappear due to shrinkage of the poultice before moisture transport from the substrate to the poultice occurs. Their contribution can be neglected after the initial stage of the drying process. Therefore, the osmotic pressure is only effective for the small pores of the poultice.

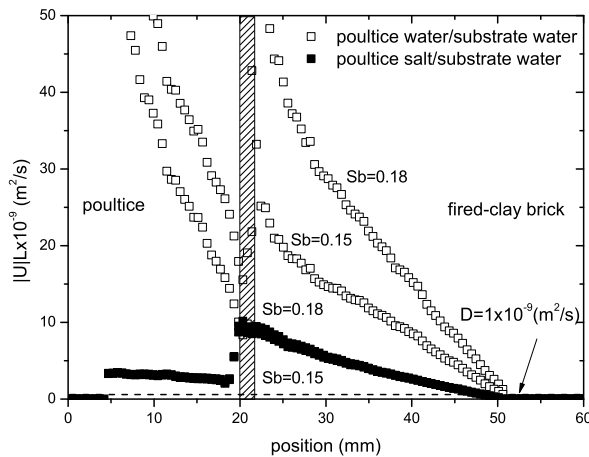


Fig. 5.7: Water velocity multiplied by the thickness of the substrate as a function of the position in the sample for several times of the drying process.

In order to investigate the influence of osmotic pressure on the efficiency of desalination by poultices, it is important to estimate the water velocity at various positions in the sample. These velocities can be calculated directly from the time evolution of the experimentally observed moisture profiles. Figure 5.7 and 5.8 show the position dependence of the absolute values of the

water velocity of the poultice(water)/substrate (water) and the poultice(saline solution)/substrate(water) systems multiplied by thickness of the substrate for several drying times.

The drying times of the plotted velocity profiles have been chosen in the region corresponding to the lower inflection point in figure 5.6, where the water saturation of the poultice (S_p) in the poultice(water)/substrate(water) system starts to drop below about 0.5. The S_p values of 0.4 and 0.2 correspond to a water saturation S_b of the fired-clay brick of 0.18 and 0.15, respectively. In case of the poultice(saline solution)/substrate(water) system the osmotic pressure significantly decreases the water saturation of the fired-clay brick in this region. The horizontal dashed line indicates the situation where $|U|L$ equals a Na diffusion constant of 10^{-9} m²/s. The water velocity profiles show that in both systems the Peclet number is above 1 in a large part of the sample and hence transport by advection dominates. Moreover, for the fully water saturated system the moisture velocity in the brick is significantly higher than for the poultice(saline solution)/ substrate(water) system. In comparing the velocities for these systems one should note that the drying time between $S_b=0.18$ and 0.15 for the fully water saturated system is about 30 times higher than for the poultice(saline solution)/substrate(water) system. The drying rate for both systems becomes equal when the water saturation of the brick is below 0.11. Figure 5.8 shows the position dependence of the absolute values of the water velocity for both systems multiplied by thickness of the substrate for drying times corresponding to $S_b=0.11$, 0.1, and 0.09. The water velocity profiles show that in case of the fully water saturated system Peclet number at the interface drops below 1 and diffusion transport starts to dominate. However, in case of the poultice(saline solution)/ substrate(water) system the Peclet number for the same moisture saturation values of the brick is still above 1 at the interface and advection dominates. Hence in the latter system desalination by advection can take place for a much longer time.

5.4.2 Poultice (water)/Substrate (saline solution)

Next, the experiments described in the previous section were repeated, but with the modification that now the substrate was saturated with a salt solution and the poultice materials were mixed with water, as it occurs in a real situation. The experimental procedure is the same as described above.

Both the theoretical derived and measured moisture content relation between the poultice and the substrate are shown in figure 5.9.

The drying of the system consisting of poultice mixed with water and a substrate saturated with a salt solution has a similar behavior as that shown in figure 5.6. However, the theoretical and measured curves do not correspond with each other. This is caused by the fact that during drying salt is transported from the substrate into the poultice, which correspondingly reduces the effective pore size of the poultice. At the same time, the effective pore size of the substrate increases. Accordingly, the relation between the moisture contents of the two materials at the interface shifts to favor increased moisture (and salt) transport from the substrate to the poultice. A similar behavior has been observed in

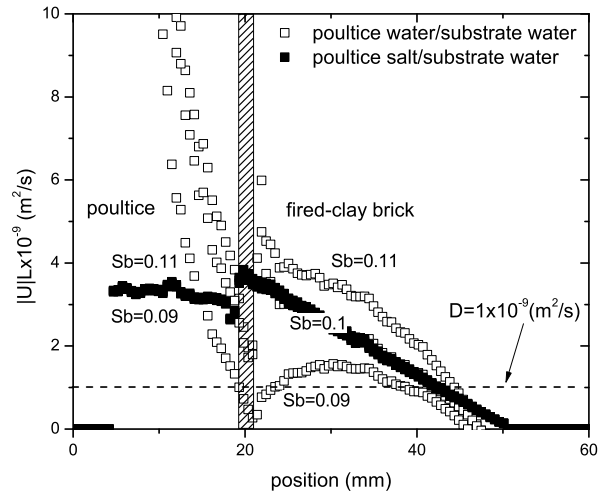


Fig. 5.8: Water velocity multiplied by the thickness of the substrate as a function of the position in the sample for several times of the drying process.

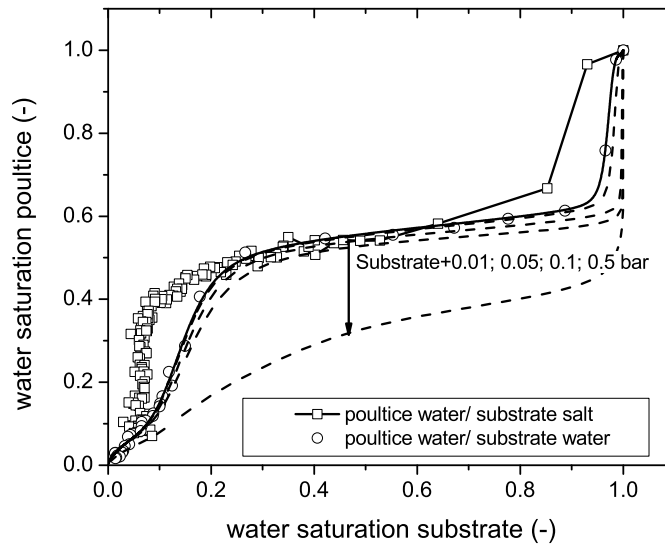


Fig. 5.9: Water saturation of the poultice as a function of water saturation of the substrate for the poultice(water) substrate(water) and the poultice(water)/substrate(saline solution) systems. The experimental results are compared with the theoretical model.

[Vor11].

Figure 5.10 shows the position dependence of the absolute values of the water velocity of the poultice(water)/substrate(water) and the poultice(water)/substrate(saline solution) systems multiplied by thickness of the substrate for drying times at

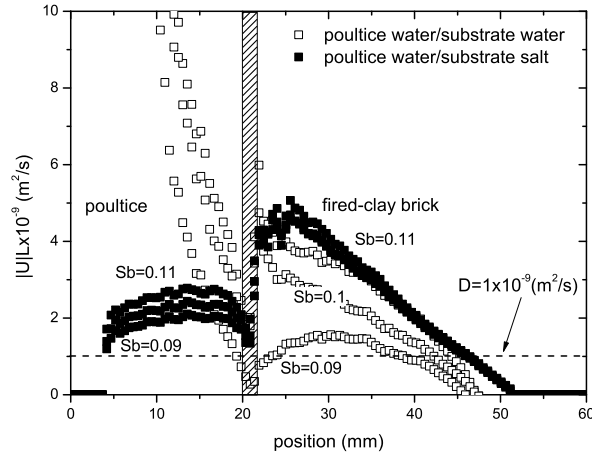


Fig. 5.10: Water velocity multiplied by the thickness of the substrate as a function of the position in the sample for several times of the drying process.

which the water saturations S_b of the brick are 0.11, 0.1, and 0.09. This figure reveals that for these values of S_b the Peclet number at the interface of the poultice (water)/substrate (saline solution) system is still above 1 and advection dominates, in contrast to the fully water saturated system.

5.4.3 Poultice (saline solution)/Substrate (saline solution)

In order to demonstrate the extreme effect of osmotic pressure on salt and moisture transport during poulticing treatments the experiments described in the previous section were repeated, but with the modification that the substrate was saturated with salt solution and the poultice was mixed with salt solution. The experimental procedure is the same as described in previous sections.

In figure 5.11 the results are given for both the theoretical derived and measured moisture content relation between the poultice and the substrate.

Because salt is transported from the substrate into the poultice while drying, we will expect that concentration in the interface will increase from the poultice side. As a result there is an immediate build up of osmotic pressure in the poultice. During first stage the poultice dries together with the substrate. It means that poultice correspondingly reduces its effective pore size and drying behavior of the poultice/substrate system does not reflect the pore size distribution of the poultice.

5.5 Discussion and Conclusions

In this study we have demonstrated the effect of osmotic pressure on moisture flow in a poultice/substrate system. The results show that osmotic pressure can reduce the effective pore size of the poultice, if salt is present there. These findings have a significant practical impact, since they can be used to improve

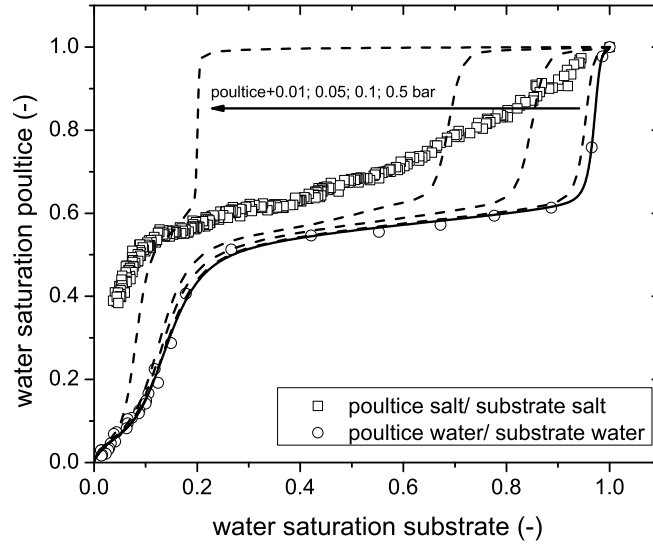


Fig. 5.11: The water saturation of the poultice as a function of water saturation of the substrate for the water mixed poultice/ water saturated substrate and solution mixed poultice/ solution saturated substrate systems. The experiment results compared with model described in the theory.

the salt extraction by poulticing. While the salt from the substrate accumulates in a poultice, its effective pore size decreases. Hence, the drying process extends in time and as a result the salt migration towards the poultice continues. Consequently, the pores of a poultice can have the same size as those of a substrate, although that is not suitable for capillary flow and advection to start. However, because the poultice stays in contact with the substrate, some salt will migrate by drying into the poultice. Once accumulated in the poultice, salt will build up an osmotic pressure and will effectively reduce the pore size of the poultice, thereby creating the requirements for advection.

In general a poultice consists of materials which shrink during drying. Consequently, the pore size distribution of the poultice varies with moisture content. Using the relation between the moisture contents of two different porous materials that are in hydraulic contact with each other we have shown that poultice based on kaolin clay and sand has mainly two dominant pore sizes: smaller pores in the diameter range below $3 \mu\text{m}$ and larger pores in the range above $10 \mu\text{m}$. During the first drying stage of a system where such a poultice is applied on a substrate, the larger pores of the poultice disappear due to shrinkage and only the smaller pores take part in the extraction of salt from the substrate by advection. Importantly, we have shown that as salt is transported from the substrate into the poultice, an osmotic pressure will build up within the poultice, thereby improving the salt extraction.

6. POULTICE COMPOSITION

This study aims to develop a better understanding of the working principle of salt extraction by poultices. The present research focuses on salt extraction by drying poultices when advection is the main mechanism for salt transport. In the case of advection based desalination the extraction efficiency depends on the difference of the pore size distributions of the poultice and the substrate. Therefore, a poultice has to be adapted to the pore size distribution of a substrate in order to create effective salt extraction by poultices. In practice, a poultice which includes shrinking materials is mixed with aggregates to reduce the shrinkage effect. The ratio between the mixed materials can influence the pore size distribution of a poultice. Therefore, we have investigated the effect of poultice mixture composition on the drying behavior and salt transport of a poultice/substrate system.

6.1 Introduction

The process of removing salt from a material by poultices can occur by a diffusion or an advection mechanism. In this study we focus on salt extraction by drying the poultice, during which advection is the main mechanism for salt removal, because advection is generally more rapid than diffusion.

If advection is the main desalination mechanism, dissolved salts will be transported by water flow from the substrate to the poultice driven by capillary forces. The water flow in the poultice/substrate system depends on the porous structures of the poultice and the substrate. Water will move from the large pores into the small pores. Therefore, a poultice working by the advection mechanism must have smaller pores than the substrate.

A common material used in practice for poultices is clay. The relatively small pores of clay make it an ideal ingredient of a poultice for a wide range of substrate materials. However, one of the main characteristics of clays is that they can shrink dramatically with decreasing moisture content. A poultice which shrinks too much during drying can detach from a substrate and hence destroy the water flow from the substrate into the poultice. However, the shrinkage of clay can be reduced by the use of non shrinking aggregates, such as sand. The shrinkage will depend on the composition of the poultice, i.e. on the components and the ratio between them.

Lubbeli [Lub10] measured the pore-size distribution of selected poultice mixture compositions by mercury intrusion porosimetry (MIP). These poultice materials and the ratio between the components were selected on the basis of a characterization survey, covering adhesion, workability, and application to vertical surfaces. The selected mixtures are given in Table 6.1. It has to be

noted that kaolin clay, which was chosen as poultice material, is not generally used in the field, because it can leave a white deposit on the substrate which is not acceptable. However, kaolin clay has been selected for this research because of its low shrinkage level. The sand used is siliceous sand (standard sand CEN-NORMSAND DIN-EN 196-1).

According to results of the experimental work conducted by [Lub10], the ratio between clay and sand can influence the pore size distribution of the poultice. However, measurements using MIP can only be carried out on dry poultice material. Hence, in order to validate whether varying the sand/clay ratio influences the pore size distribution of the poultice, drying experiments have been performed using the same poultice mixtures as Lubbeli.

Tab. 6.1: Composition and water content of the selected poultices

Kaolin / sand ratio (by weight)	Water content (by weight)
1:3	0.22
1:5	0.2
1:7	0.16

These poultices have been tested on two types of porous building materials: fired-clay brick and Dutch limestone (mergel). These two substrates were selected because of the significant differences of their pore size distributions. The pore-size distribution of both substrate materials measured by MIP is shown in figure 6.1. The pores of the fired-clay brick are in a range between 3'-8 μm in diameter. In contrast, the pores of the Dutch limestone are between 30 and 40 μm in diameter.

In our experiments cylindrical substrates were used with a diameter of 19 mm and a total length of 31 mm. Initially the substrates were fully saturated by immersing them in 3M NaCl solution for about 24 h. To be able to model the observed drying and salt transport as a 1D process, the substrates were sealed with teflon tape at all sides except for the top. In order to apply the poultice a cylindrical teflon holder is placed over the top of the sample. As a result there is a small difference in diameter between substrate and poultice. In some experiments it was observed that poultice material was leaking through this holder along the substrate. The top of the poultice was dried with dry air (at 5% RH). The hydrogen and sodium profiles have been measured with the NMR setup described in chapter 4.

6.2 *Results and discussions*

6.2.1 *Poultice/fired-clay brick*

First a system, consisting of a fired-clay brick substrate on which poultices were applied, was measured.

In figure 6.2 the moisture profiles of the systems measured by NMR are plotted for several times during drying. The bar with of the dashed region at

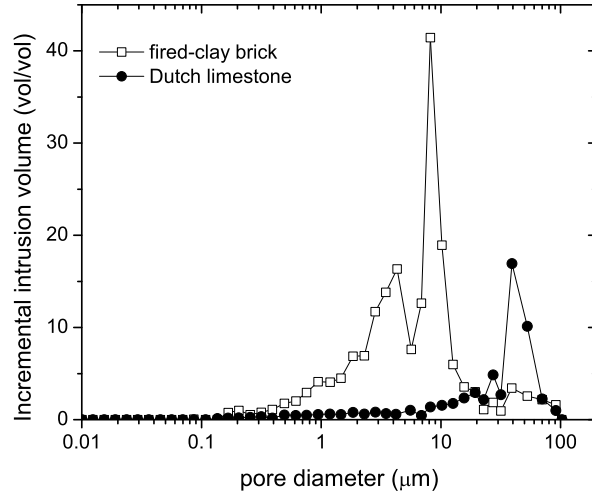


Fig. 6.1: Pore size distribution of fired-clay brick and Dutch limestone determined from MIP measurements.

the poultice/substrate interface shows the resolution of the measured profiles. The fluctuations in the moisture profiles near the interface are due to unwanted leakage of some poultice material.

As already outlined in previous chapters, during drying the largest pores empty first, because their capillary pressure (P_c) is lowest. In the present systems the same three drying stages can be observed as discussed in chapter 5. During the first stage the poultice dries significantly, whereas the substrate remains almost fully saturated. The substrate starts to dry during the second stage, whereas during the third stage the substrate is almost dry and the poultice still contains some water.

As can be seen from the moisture profiles, during drying the poultice starts to shrink. In figure 6.3 the thickness of each poultice determined from the moisture profiles is plotted as a function of the drying time. The figure shows that during the first drying stage the thickness of all poultices decreases. The poultices shrink at different rates and the shrinkage decreases with reducing amount of kaolin clay in the poultice. In chapter 5 it was assumed that the shrinkage is mainly associated with collapsing of the larger pores when they are emptied. This assumption was supported by the observation that the thickness of the 1:5 poultice decreased by about 5% corresponding to a volume shrinkage of about 15%. This fraction agreed well with the water loss of $0.15 \text{ m}^3/\text{m}^3$ of the poultice during the first drying stage. These findings also match the shrinkage of the other poultices. The thickness of the 1:3 poultice appears to decrease by about 6%, corresponding to a volume shrinkage of about 18%, whereas the water loss during the first drying stage is $0.2 \text{ m}^3/\text{m}^3$. The thickness of the 1:7 poultice appears to decrease by about 3%, corresponding to a volume shrinkage of about 9%, whereas the water loss during the first drying stage is $0.1 \text{ m}^3/\text{m}^3$. Therefore the amount of kaolin clay will determine the overall shrinkage of the

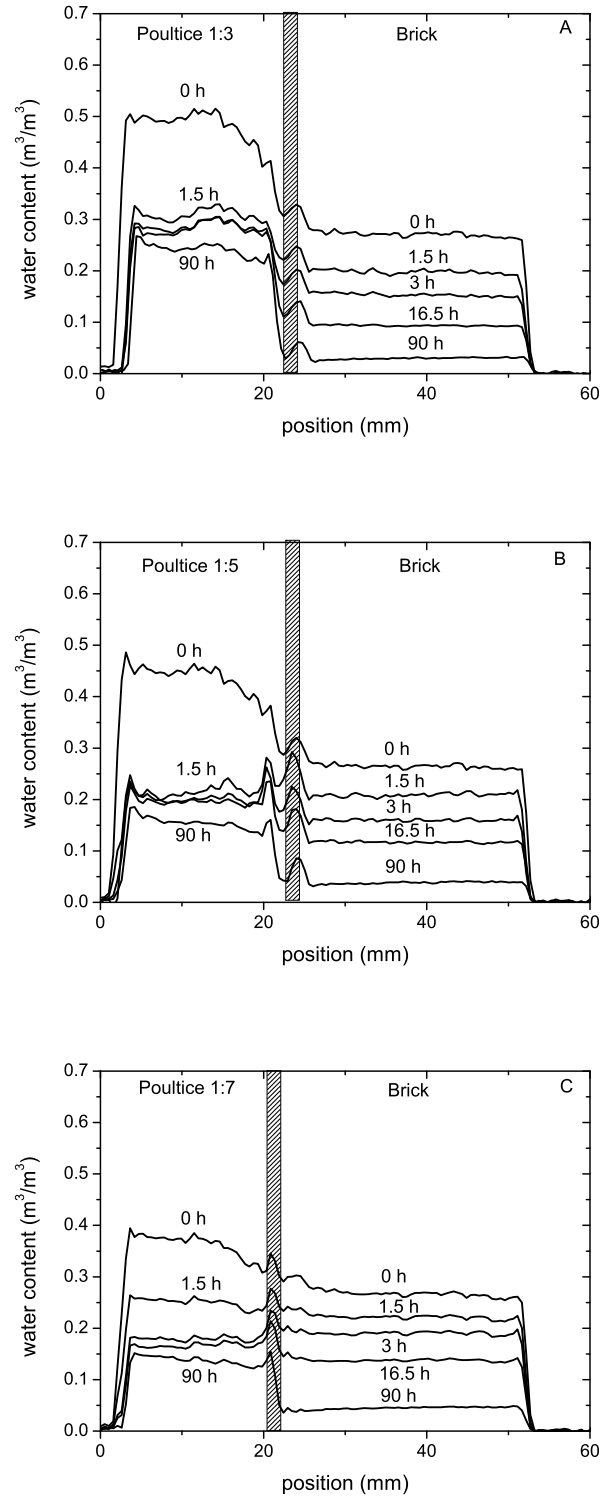


Fig. 6.2: Measured moisture profiles in the poultrice/fired-clay brick system during drying. The brick was initially saturated with 3M NaCl solution. Dry air is blown over the top of the system with a flow of 1.6 m/s. A. Poultrice with kaolin/sand ratio 1:3. B. Poultrice with kaolin/sand ratio 1:5. C. Poultrice with kaolin/sand ratio 1:7.

poultice.

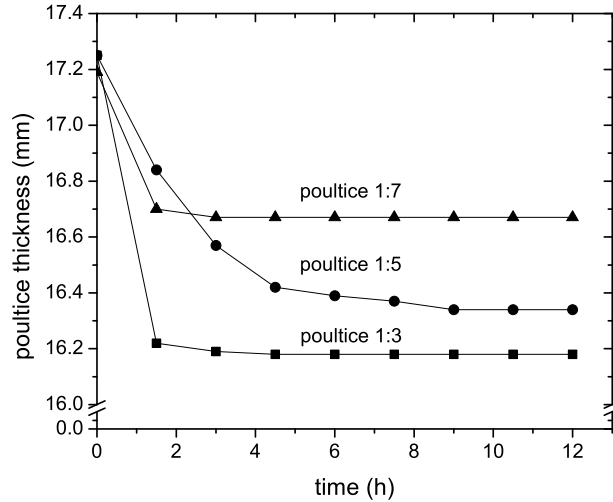


Fig. 6.3: Thickness of all poultices determined from the moisture profiles vs. drying time.

In figure 6.4 the measured salt profiles of these systems are plotted for several times during drying. In all experiments we see that the salt in the fired-clay brick remains uniformly distributed throughout the experiment. However, the salt distribution in the poultice is non uniform, and a salt peak evolves at the drying surface of the poultice.

As can be seen from figure 6.4 during drying salts migrate from the substrate to the poultice and a concentration gradient at the interface occurs. The presence of a concentration gradient in the poultice/substrate interface will create an osmotic pressure, which can influence the water flow in the system.

In figure 6.5 the observed relation between the moisture contents at both sides of the interface between fired-clay brick and 1:5 clay/sand poultice is given. In the same figure the experimental results are shown for composite samples that were saturated only with water. This figure shows that as the drying starts, the poultice loses moisture, while the substrate stays almost saturated. Once the moisture saturation of the poultice drops below 0.7, the substrate loses water while the saturation of the poultice remains almost constant.

As it was shown in chapter 2, the large pores of the poultice disappear due to the shrinkage during the first drying stage and their contribution can be neglected after the initial stage of drying process. Therefore, the osmotic pressure influences only the small pores of the poultice. As an example, in the inset of figure 6.5 the capillary pressure curve for 1:5 clay/sand poultice determined from drying experiments is shown. In figure 6.5 we have included the calculated relation between the moisture content of the poultice and that of the substrate at the interface (see chapter 5). The calculated relation includes only the influence of the osmotic pressure on the small pores of the poultice. The curve determined from the drying experiments corresponds rather well with

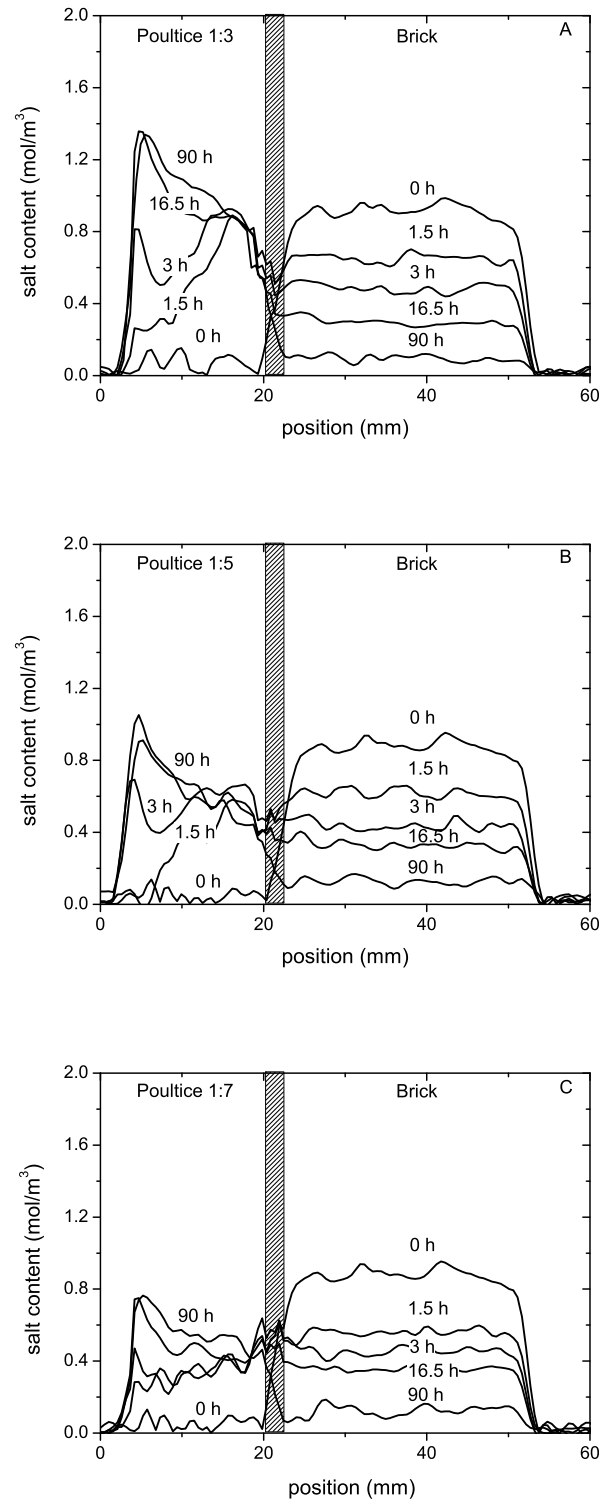


Fig. 6.4: Salt profiles in the poultice/fired-clay brick system during drying. The brick was initially saturated with 3M NaCl solution. Dry air is blown over the top of the system with a flow of 1.6 m/s. A. Poultice with kaolin/sand ratio 1:3. B. Poultice with kaolin/sand ratio 1:5. C. Poultice with kaolin/sand ratio 1:7.

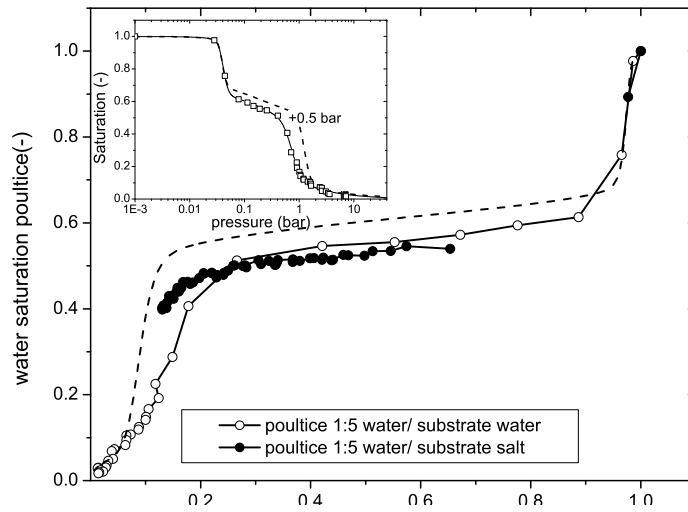


Fig. 6.5: Water saturation of a fired-clay brick as a function of the water saturation of a clay/sand poultice determined from the drying experiments. The dashed curve represents the predicted effect of the osmotic pressure. The inset shows the capillary pressure curve for clay/sand poultice determined from drying experiments. The dashed curve represents the relation for 0.01 mol NaCl salt content in the poultice.

the calculated behavior.

It has to be noted that the model completely neglects the effect of the osmotic pressure on the larger pores. However, the purpose of this model is not to yield an exact quantitative prediction. For instance, one can see that the calculated curve is slightly higher than the drying curve in the plateau region. Nevertheless, the model does reveal the mechanisms and drying behavior of the poultice/substrate system. As can be seen from figure 6.5, a significant osmotic pressure effect can be observed below 0.2 water saturation of the substrate. Above this value, the behavior for substrates saturated with water and those saturated with a saline solution is largely the same. Obviously, at these values of the saturation osmotic pressure effects are negligible.

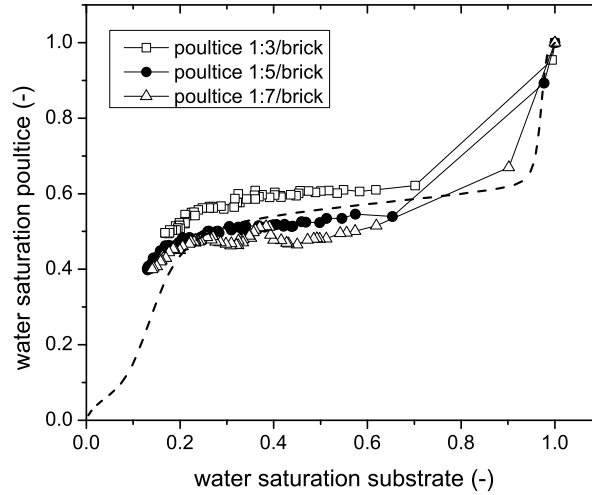


Fig. 6.6: Water saturation of a fired-clay brick as a function of the water saturation of a clay/sand poultrice determined from drying experiments. The dashed curve represents the relation derived from the capillary pressure curves.

In order to study the effect of the poultrice composition on the water flow in the poultrice/substrate system, the relation between the moisture contents at both sides of the interface between the fired-clay brick and the clay/sand poultrice is given in figure 6.6 for all poultrice/substrate combinations. The dashed curve represents the relation derived from the capillary pressure curves for a clay/sand ratio of 1:5. One should note that this relation does not include any osmotic pressure effects, which have been shown to be negligible above a substrate water saturation of 0.2.

The relation between the moisture content of the poultrice and the substrate for poultrices with clay/sand ratio 1:3 and 1:7 does not show significant changes with respect to the relation for the poultrice with ratio 1:5.

A small osmotic pressure effect can be observed for all combinations below a water saturation of the substrates of 0.2, where moisture content of the poultrice is slightly higher than the dashed curve. These results show that the amount of the sand does not have a large influence below a water saturation of about 0.6 on the relation between the water contents at the poultrice/substrate interface and therefore does not have a large influence on the pore-size distribution of the poultrice, except for the large pores.

In previous chapters the influence of the salt transport on the drying behavior was outlined. As at very low drying rates diffusion based transport becomes increasingly dominant, it is important to keep the drying rates sufficiently high. The drying rate of the poultrice/substrate system can be evaluated by the velocity of the moisture in the system. In order to check to what extent the drying rate in the poultrice depends on the amount of sand in the poultrice the water velocity profiles have been calculated from the experimentally observed moisture profiles. In figure 6.7 the absolute values of the water velocity of poul-

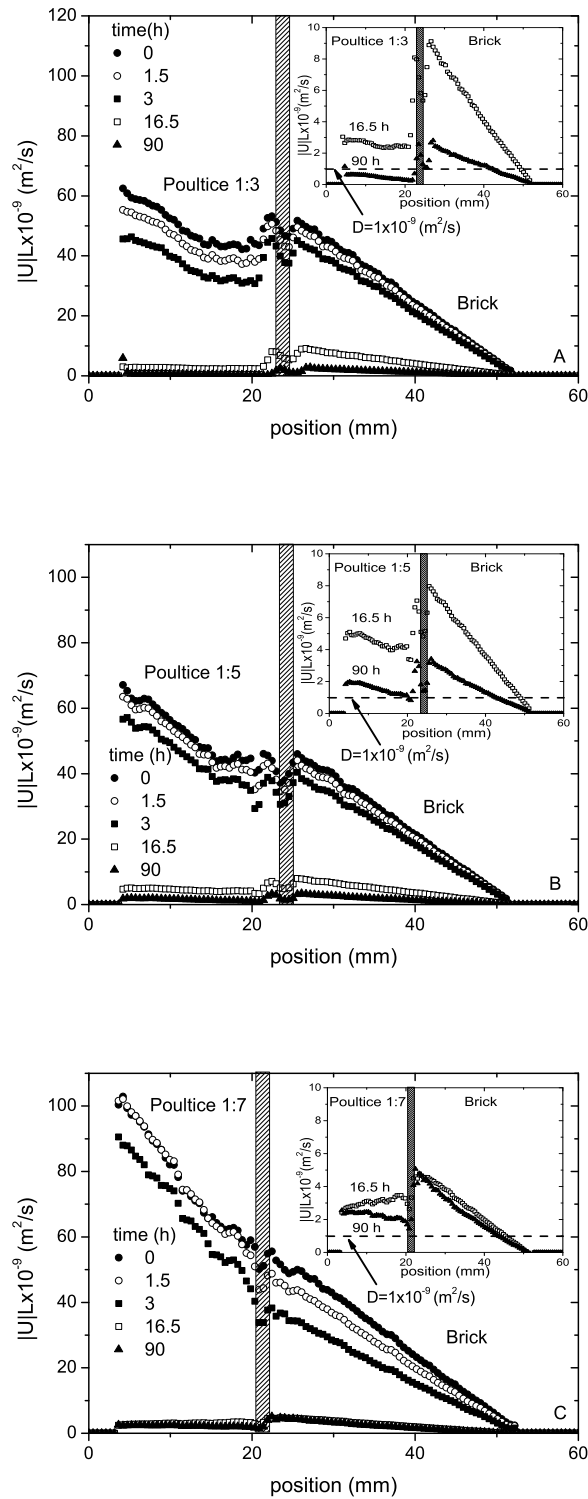


Fig. 6.7: Water velocity in the poultrice/fired clay brick system multiplied by the thickness of the substrate as a function of the position in the sample for every 1.5 hours of a drying process. A. Poultrice with kaolin/sand ratio 1:3. B. Poultrice with kaolin/sand ratio 1:5. C. Poultrice with kaolin/sand ratio 1:7.

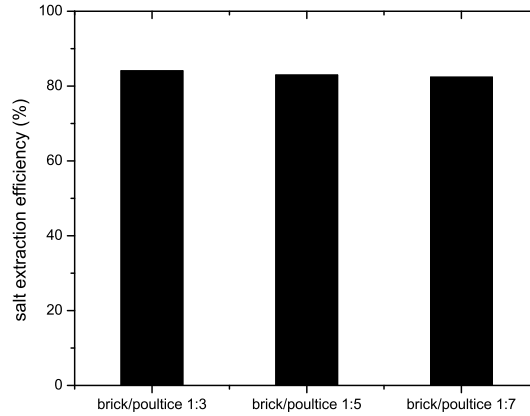


Fig. 6.8: Relative amount of salt extracted from the fired-clay brick by poultices with different kaolin/sand ratios. The results were obtained from Ion Chromatography.

tice/substrate systems are shown. The absolute value of the water velocity is multiplied by the thickness of the substrate ($|U|L$). The horizontal dashed line indicates the situation where $|U|L$ equals a Na diffusion constant of 10^{-9} m²/s, i.e. $Pe = 1$ (see chapter 2). The water velocity profiles show that in all cases the Peclet number is above 1 and transport by advection dominates. Moreover, in all cases we observe almost the same velocity of the brick for all drying times.

The salt accumulated in the poultice at the drying surface will crystallize and can not be determined by NMR. In order to validate the total amount of the salt which was extracted from the substrate into the poultice, the poultice/substrate systems were removed from the NMR setup after the drying experiments and each substrate was cut into three slices. Each slice was ground into powder and diluted in water and the total amount of sodium in this sample was measured quantitatively by ion chromatography (IC). The results of this analysis are shown in figure 6.8, which reveals that the degree of salt extraction was not affected by the amount of sand in the poultice.

6.2.2 *Poultice/Dutch limestone*

Next the system with Dutch limestone as a substrate was studied. Since the pores of Dutch limestone are significantly larger than those of fired-clay brick, we expect a better salt extraction. This point is illustrated in figure 6.9(A). In this figure the capillary pressure curves measured for Dutch limestone by a pressure plate and for a 1:5 poultice by a drying experiment are plotted. From these capillary pressure curves the relation between the moisture contents at both sides of the interface between the Dutch limestone and the poultice is shown in figure 6.9(B). The solid curve represents the same relation for fired-clay brick. Since the pores of Dutch limestone are significantly larger than those of fired-clay brick the poultice remains saturated during the first drying stage,

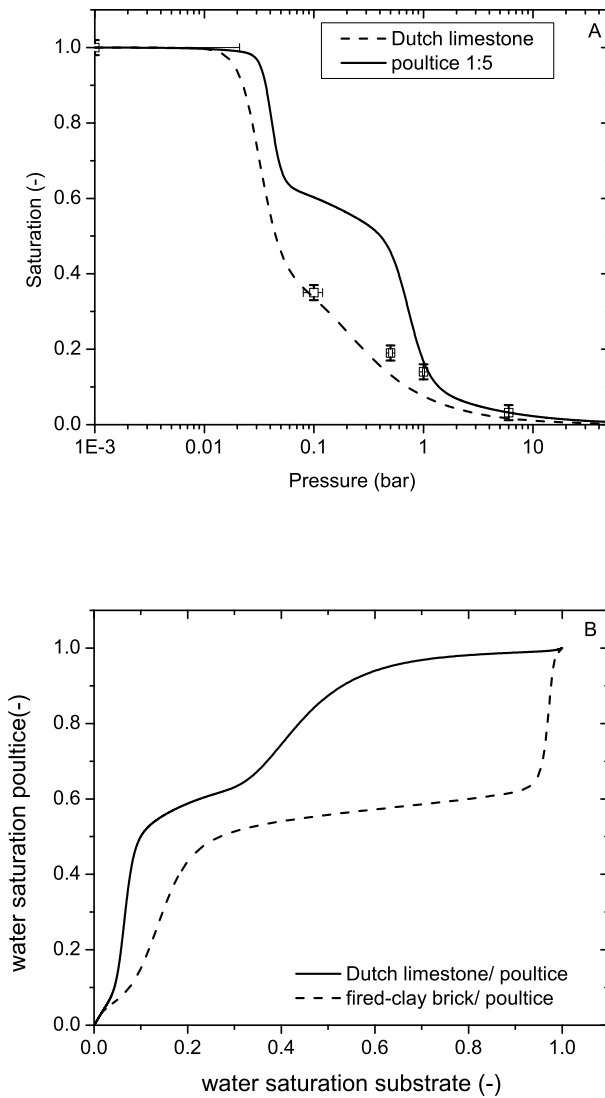


Fig. 6.9: A. Capillary pressure curve for Dutch limestone measured by a pressure plate and for a poultice 1:5 determined from a drying experiment. B. Water saturation of Dutch limestone and fired-clay brick as a function of the water saturation of a clay/sand poultice determined from the capillary pressure curves.

while the substrate dries. Hence we assume that the clay/sand poultice can be used on substrates which have larger pores than the fired-clay brick and it can even provide a faster water flow from the substrate into the poultice.

In order to study the potential effect of the pore-size distribution of the substrate on the salt extraction the drying experiments have been repeated using a Dutch limestone as substrate. The experimental procedure is the same as described in the previous section.

In figure 6.10 the water profiles of the poultice/substrate system are shown

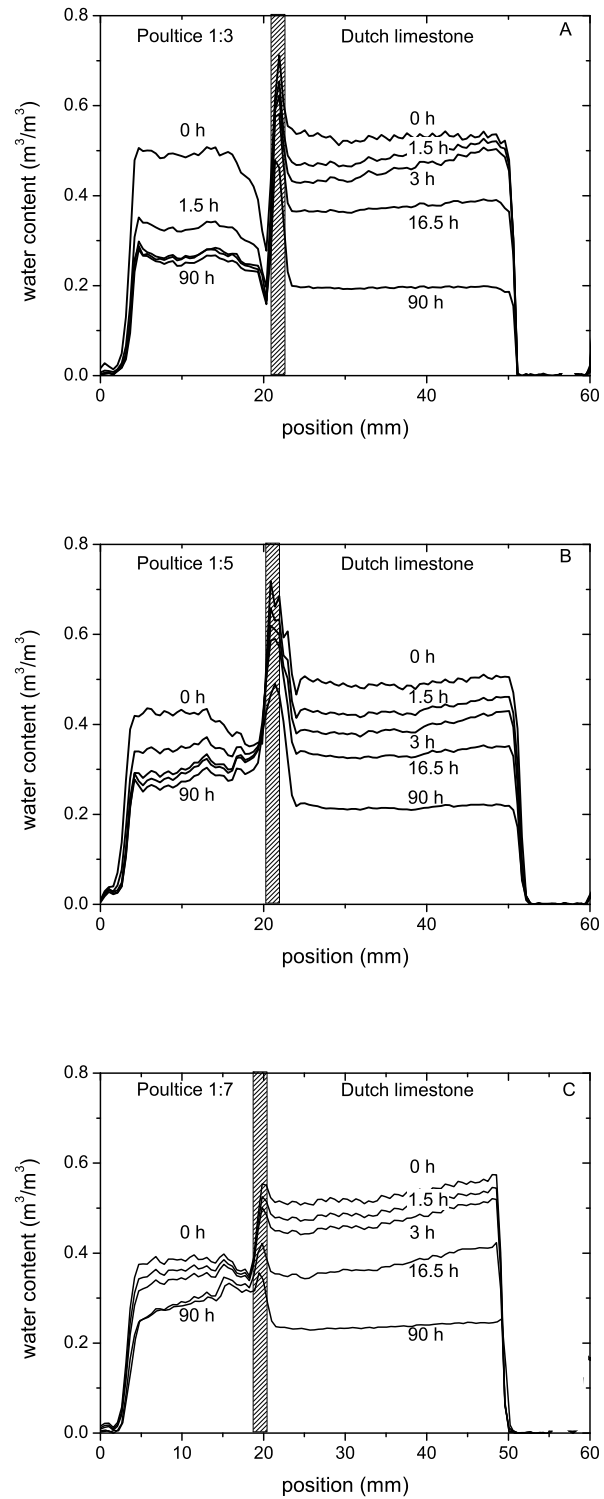


Fig. 6.10: Moisture profiles in the poutlice/Dutch limestone system during drying. The Dutch limestone was initially saturated with 3M NaCl solution. Dry air is blown over the top of the system with a flow of 1.6 m/s. A. Poutlice with kaolin/sand ratio 1:3. B. Poutlice with kaolin/sand ratio 1:5. C. Poutlice with kaolin/sand ratio 1:7.

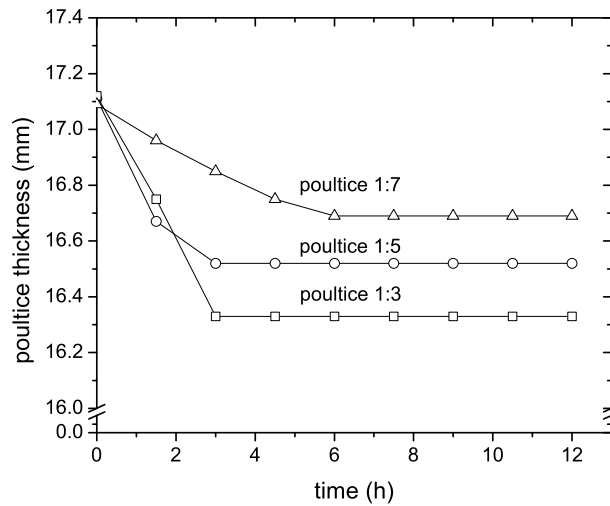


Fig. 6.11: Thickness of all poultrices determined from the moisture profiles vs. drying time.

for several times during drying process. The drying behavior of the poultrice/Dutch limestone system does not significantly differ from the drying of the poultrice/fired-clay brick system. At the beginning of the drying the poultrice dries significantly, whereas the substrate remains almost fully saturated. After some time the substrate starts to dry and the saturation of the poultrice remains almost constant. A similar shrinkage of the poultrices is observed. The thickness of the each poultrice is plotted as a function of the drying time in figure 6.11. As has been observed in the previous section the shrinkage decreases with reduction of the amount of kaolin clay in the poultrice.

In figure 6.12 the salt profiles are presented for several times during drying. Similar to previous section we can see that the salt in the limestone remains uniformly distributed and the salt distribution in the poultrice is non uniform, and a salt peak evolves at the drying surface of the poultrice.

In figure 6.13 we plotted both the theoretically derived and the measured moisture content relation at the poultrice/substrate interface for all systems. The dashed curve represents the theoretical relation between the moisture contents of the poultrice and the substrate which includes the contribution of all limestone pores. As can be seen this relation deviates significantly from the measured data. This deviation may be caused by the fact that a mixture of clay and sand produces a plastic substance that does not have a stable solid structure. Because of this, during application the poultrice may penetrate into the large pores of the substrate. When this occurs the surface pores become effectively smaller. Therefore, in the poultrice/substrate interface the part of the substrate made up of pores that are larger than the pores in the poultrice is eliminated and the water flow becomes slower.

In order to demonstrate the effect of a reduction of the effective pore size of

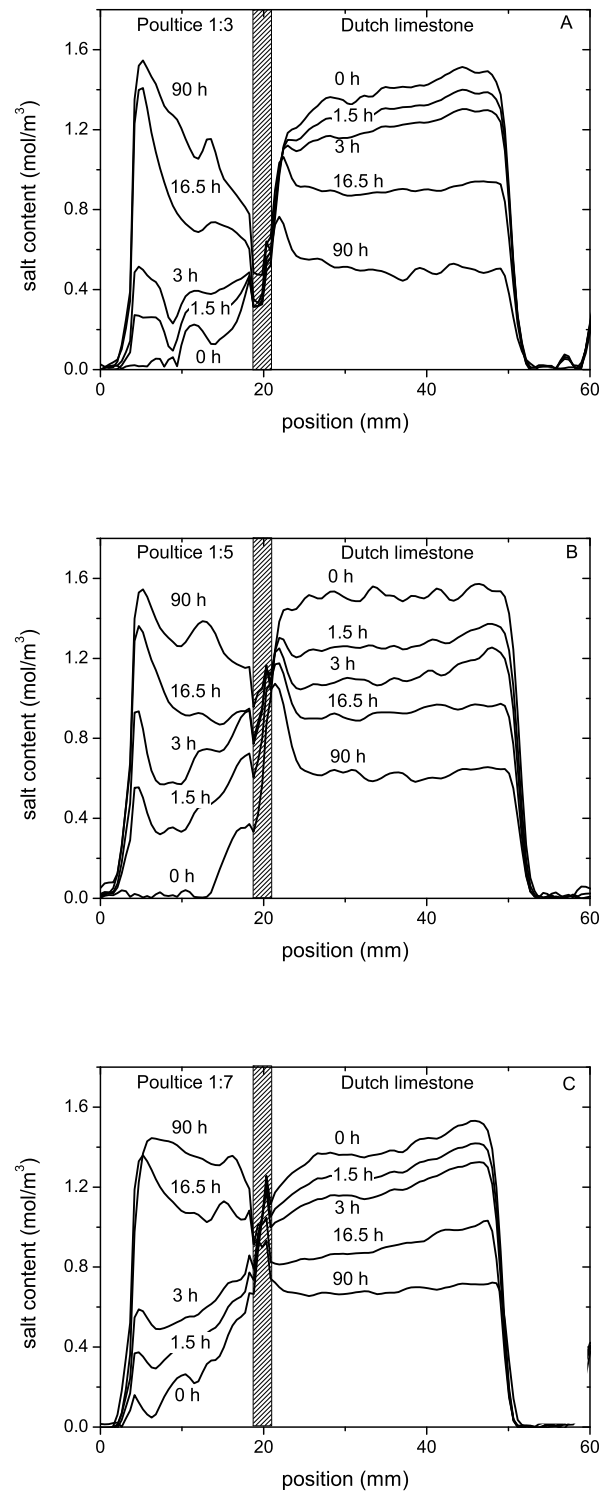


Fig. 6.12: Salt profiles in the poultice/Dutch limestone system during drying. The Dutch limestone was initially saturated with 3M NaCl solution. Dry air is blown over the top of the system with a flow of 1.6 m/s. A. Poutlice with kaolin/sand ratio 1:3. B. Poutlice with kaolin/sand ratio 1:5. C. Poutlice with kaolin/sand ratio 1:7.

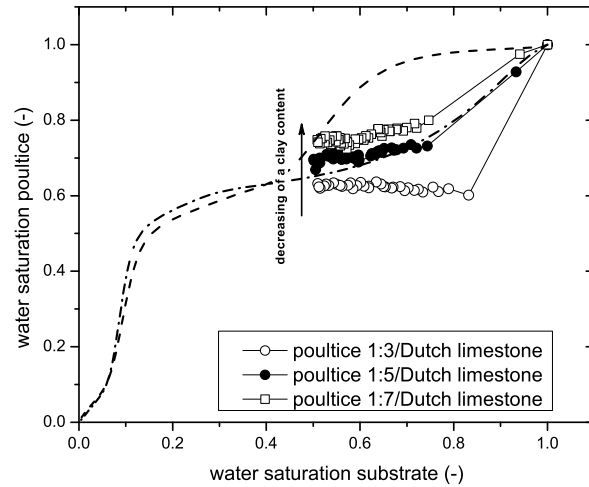


Fig. 6.13: Water saturation of a Dutch limestone as a function of the water saturation of a clay/sand poultice determined from by drying experiments. The dashed line represents the relation as determined by capillary pressure curves.

the substrate a simple model was used, which is illustrated in figure 6.14. This model contains only a shift of all pore sizes to smaller values, so no attempt is made to describe in detail the blocking of the larger pores. These results are reflected by the dashed-dotted curve in figure 6.13. Despite the simplicity of the model this curve appears to describe the experimental data very nicely.

In order to investigate the influence of the (effective) pore-size distribution of Dutch limestone on the efficiency of desalination by poultices it is important to estimate the water velocity profiles. In figure 6.15 the absolute values of the water velocity of the poultice/Dutch limestone systems multiplied by the thickness of the substrate are shown as a function of the position for several times during drying. The water velocity profiles show that the drying of the Dutch limestone is slower than the fired-clay brick. Moreover, the diffusive transport becomes more dominant.

The extraction efficiency results calculated from the Ion Chromatography measurements for all systems are shown in figure 6.16. It can be seen that the efficiency of salt extraction drops below 50% for the Dutch limestone, whereas for the fired-clay brick it reaches values above 80%.

6.3 Conclusions

Drying experiments have been performed to study the effect of the poultice composition on the water flow in the poultice/substrate system. It has been shown that the chosen amount of sand does not influence the pore-size distribution of the poultice. However, it may be difficult to use clay/sand poultices on substrates with large pores, like the Dutch limestone. As clay can penetrate into the large pores, the effective size of the pores at the surface of the sub-

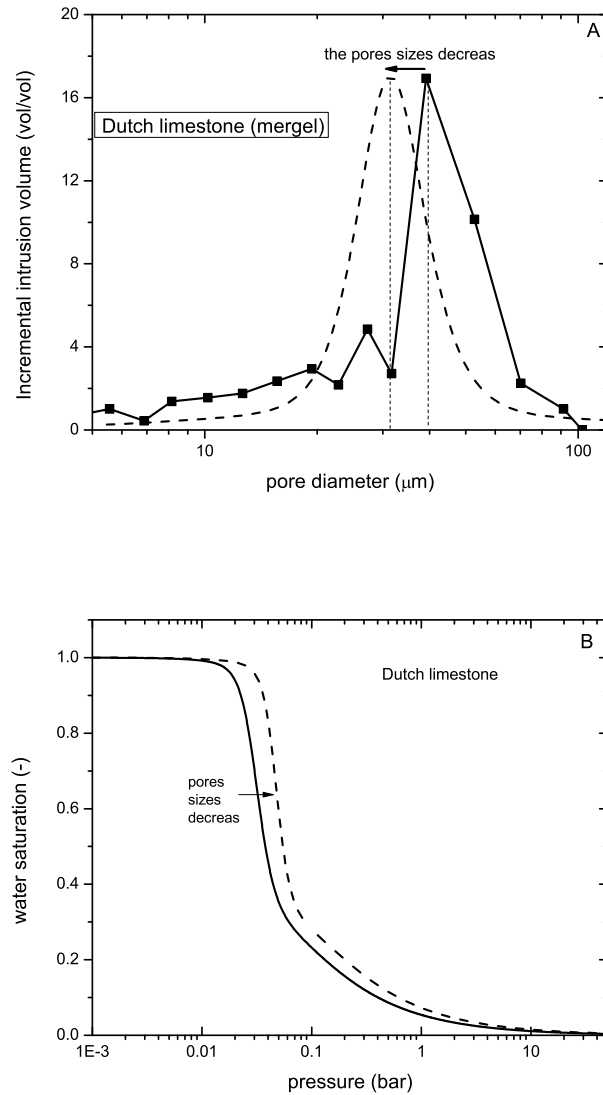


Fig. 6.14: A. The pore size distribution of Dutch limestone obtained by means of mercury intrusion porosimetry. The dashed curve schematically indicates the reduction of the effective pore size, due to the presence of kaolin clay in pores. B. Capillary pressure curve of Dutch limestone measured by pressure plate. The dashed curve reflects the effect of a reduction of the effective pore size.

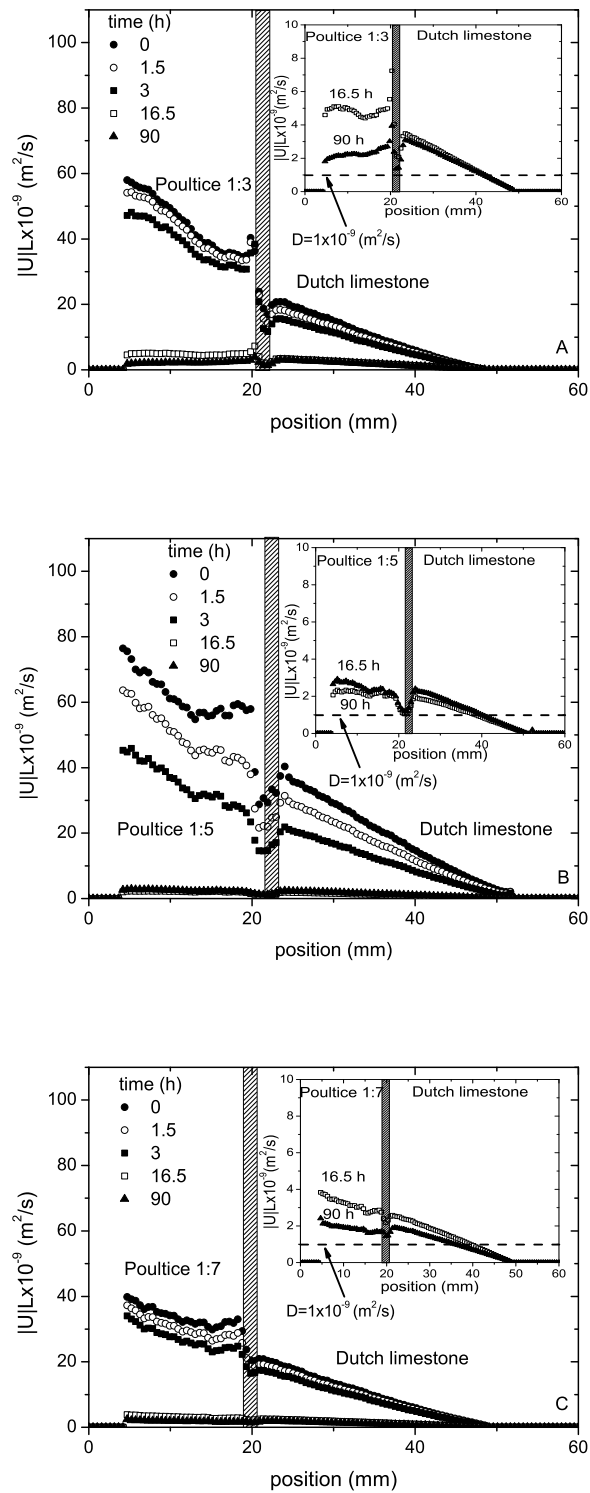


Fig. 6.15: Water velocity multiplied for the thickness of the substrate as a function of the position in the sample for every 1.5 hours of a drying process. A. Poultice with kaolin/sand ratio 1:3. B. Poultice with kaolin/sand ratio 1:5. C. Poultice with kaolin/sand ratio 1:7.

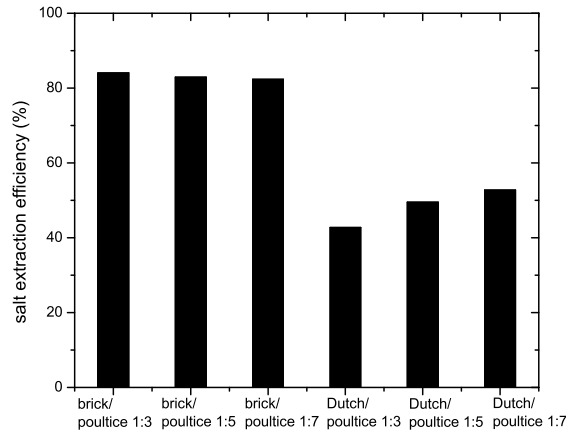


Fig. 6.16: Relative amount of salt extracted from the fired-clay brick and the Dutch limestone by poultices with different kaolin/sand ratios. The results were obtained from Ion Chromatography.

strate can be reduced. Therefore, the drying behavior of the poultice/substrate system changes significantly.

The pore-size distribution of the kaolin/sand poultice measured by Lubbeli using MIP cannot directly be related to the poultice/substrate drying behavior. This can be explained by the different arrangement of kaolin and sand particles in the wet and dry states. In the wet state all interstitial spaces between the sand grains are filled with kaolin particles which are suspended in water. As the poultice dries, the kaolin tends to agglomerate in the interstitial spaces between sand grains, thus partially filling the interstitial pores in the sand. This reduced interstitial porosity, was measured by MIP.

An other results of this study is that in the case of advection based salt extraction, the efficiency of salt extraction strongly depends on the pore-size range of the substrate and the poultice.

7. INTERVENTION LAYER

A significant problem connected to the use of poultices is the deposit of poultice material on surface substrate after the treatment. Moreover, when the substrate surface is very fragile or damaged, the application and removal of the poultice can result in physical damage of the surface. In order to protect the substrate surface an intervention layer between the poultice and the substrate should be used. This additional layer can protect the surface of the substrate from the mechanical disturbance during poultice application and removal. The present study assesses the effect of the use of an intervention layer between the substrate and the poultice on the penetration of clay from the poultice into the substrate.

7.1 Introduction

The extraction of salt from porous building materials by poultices is used in conservation of cultural heritage. Based on the ion transport process two salt extraction methods by poultices exist: diffusion and advection based methods. The diffusion based method uses the salt concentration gradient between the substrate and the poultice. In this case the salt ions diffuse from the substrate into the poultice. The advection based method is realized by capillary water flow from the substrate into the poultice (generally resulting from drying), which is accompanied by advection of ions within the solution. The present research focuses on salt extraction by the advection based method.

A poultice must be applied on a substrate with sufficient force to develop adhesion between the poultice material and the substrate. As the poultice is pressed onto a substrate, the poultice material fills up the irregularities of the substrate and will form a mechanical bond between poultice and substrate. In many cases one of the components of a poultice is clay, which consists of particles which have a plate-like shape of a certain size. When the pores of the substrate are larger than the size of a clay plate, these can penetrate in to the substrate.

In chapter 6 we observed that the application of a kaolin/sand poultice on a porous material with large pores (Dutch limestone) results in a water flow that was smaller during drying than for a porous material with smaller pores (fired-clay brick). As the typical size of the plate surface of kaolin clay is about $10\ \mu\text{m}$ squared and the pore size of Dutch limestone is about $30\ \mu\text{m}$, kaolin clay which is present in the poultice penetrates inside the open pore spaces of the substrate at the poultice/substrate interface. By this process the effective pore size of the substrate is reduced.

In order to demonstrate the potential effect of a changing pore size of the substrate the capillary pressure curve and pore size distribution measured for

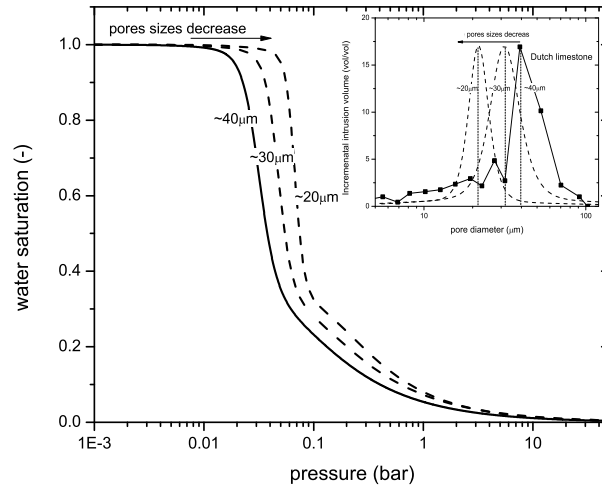


Fig. 7.1: Capillary pressure curve for Dutch limestone measured by a pressure plate (solid curve). In the inset, the pore size distribution as obtained by mercury intrusion porosimetry is plotted. The dashed curves illustrate the effect of a reduction of the effective pore size.

Dutch limestone are given in figure 7.1. The reduction of the effective pore sizes is illustrated by the various dashed line curves. These curves represent the water saturation vs. pressure relation for various effective pore sizes, which are smaller than the actual pores size of the Dutch limestone.

As a result the relation between the moisture contents at both sides of the interface between the poultice and the substrate will change. In figure 7.2 we have plotted the predicted relation between the moisture content of the poultice and that of the substrate. When the effective pore size of the substrate becomes smaller the moisture will have a tendency to remain in the substrate.

The objective of the present research is to investigate whether an intervention layer can prevent the poultice material to penetrate into the pores of the substrate, thereby increasing the water flow and salt extraction. To this end, drying experiments were performed on a series of poultice/substrate systems. In order to validate whether the amount of clay in the poultice influences the clay penetration, these experiments have been done using the same poultice mixtures as in chapter 6. Japanese paper was chosen as an interventional layer, because it is used in practice as protection of fragile surfaces [Mar10],[Avd03].

7.2 Results and Discussion

Experiments with poultices and an intervention layer were conducted on Dutch limestone (mergel) as it was seen in chapter 6 that for this substrate clay has a large influence (see chapter 6). The experimental procedure is the same as described in chapter 6, but now a single sheet of Japanese tissue is put on the top surface of the substrate, before application of the poultice layer.

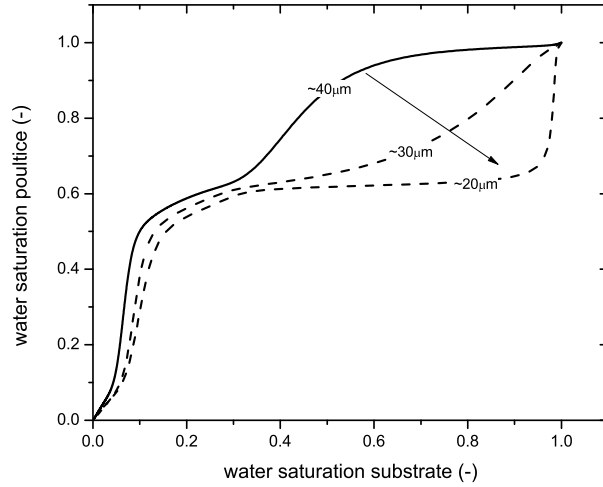


Fig. 7.2: The water saturation of a Dutch limestone as a function of the water saturation of a clay/sand poultice at the interface as determined from by capillary pressure curve. The dashed line represents the relation when the pores of the Dutch limestone become smaller.

In figure 7.3 the measured moisture profiles of the poultice/substrate systems are shown for several times during drying process. The same shrinkage of the poultice is observed as in the experiments discussed in chapter 6. Also the same irregular jump of the signal near the poultice/substrate interface is observed. Because it is difficult to control the leaking of the poultice material through the holder, the intensity of the signal jump can vary from one experiment to another. Moreover, as Japanese paper is present in the poultice/substrate interface, clay particles can also partly penetrate through the paper and affect the signal near the interface. One can see that the drying behavior is almost the same for all poultice/substrate combinations. The general drying behavior of the poultice/Dutch limestone systems with paper does not differ much from that of the systems without paper.

In figure 7.4 the corresponding salt profiles are presented for several times during drying. In all experiments that were performed it appeared that the salt in the brick remains uniformly distributed. However, the salt distribution in the poultice is non uniform.

In figure 7.5 we have plotted both the theoretically derived and the measured moisture content relation at the poultice/substrate interface for all systems with and without an intervention layer. It was expected that the use of Japanese paper would reduce the penetration of kaolin into the Dutch limestone substrate. However, as can be seen from the figure 7.5, the relation between the moisture contents at both sides of the interface of the system with Japanese paper is the same as for the system without paper, when poultice containing a low amount of kaolin clay was applied. The use of Japanese paper only results in a change in the moisture content relation when the poultice contains the largest amount

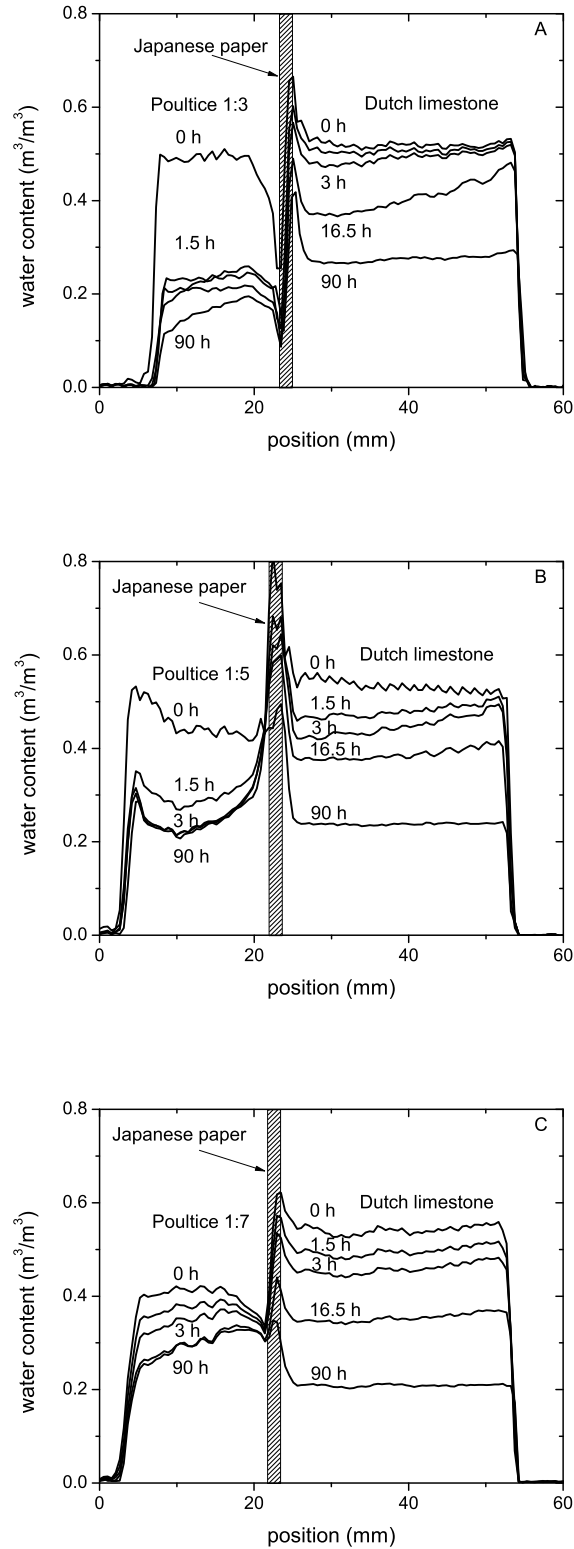


Fig. 7.3: Measured moisture profiles in the poultice/Dutch limestone system during drying. The Dutch limestone was initially saturated with 3M NaCl solution. Dry air is blown over the top of the system with a flow of 1.6 m/s. A. Poultice with kaolin/sand ratio 1:3. B. Poultice with kaolin/sand ratio 1:5. C. Poultice with kaolin/sand ratio 1:7.

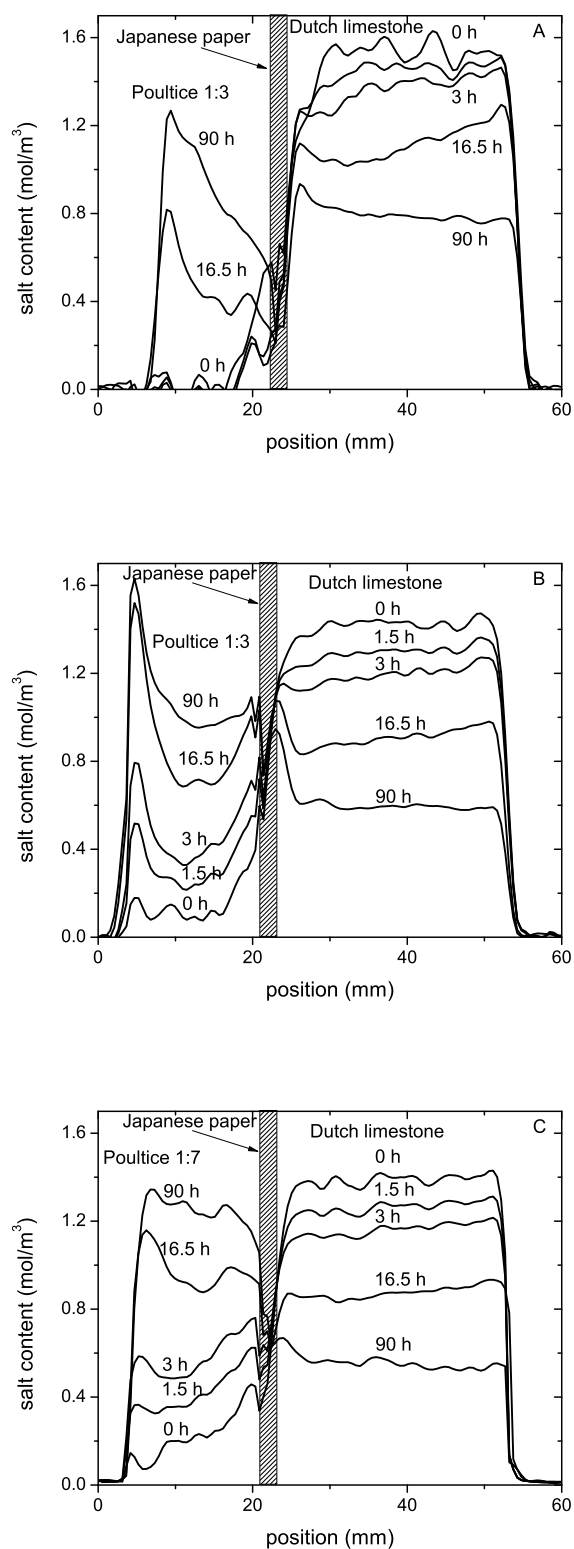


Fig. 7.4: Salt profiles in the poultice/Dutch limestone system during drying. The Dutch limestone was initially saturated with 3M NaCl solution. Dry air is blown over the top of the system with a flow of 1.6 m/s. A. Poultice with kaolin/sand ratio 1:3. B. Poultice with kaolin/sand ratio 1:5. C. Poultice with kaolin/sand ratio 1:7.

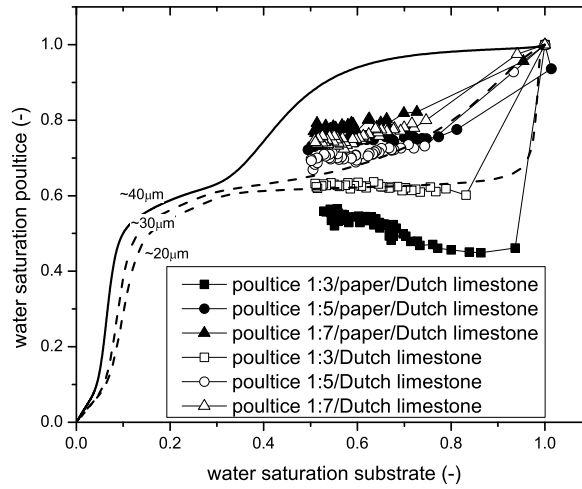


Fig. 7.5: Water saturation of a Dutch limestone as a function of the water saturation of a clay/sand poultice determined from drying experiments. The solid curve represents the relation determined from the capillary pressure curves. The dashed curves reflect the effect of a reduction of the effective pore size of the substrate.

of kaolin (1:3 kaolin/sand).

After the experiments the poultice/substrate systems were removed from the NMR set up and the poultice and the substrate were taken apart. Particles of kaolin were observed on the surface of the Dutch limestone substrate for each experiment. The Japanese paper was totally blocked with kaolin when the 1:3 poultice was applied, and partly blocked when poultices with a lower amount of kaolin were applied. What generally can be stated is that kaolin penetrates through the paper and blocks some pores in the same way as in the system without paper. Moreover, if a large amount of kaolin is present, also the pores of the paper are blocked and the paper start to act as a third porous layer with pore size comparable to that of kaolin. This layer hinders water to flow from the substrate to the poultice.

In order to confirm that the drying rate of the system does not change when paper is present between poultice and substrate for low amounts of kaolin in the poultice, the water velocity profiles have been calculated from the experimentally observed moisture profiles. In figure 7.6 the absolute values of the water velocity in the poultice/Dutch limestone system multiplied by the thickness of the substrate are shown as a function of the position for several times drying the drying process. The horizontal dashed line indicates the situation where $|U|L$ equals a Na diffusion constant of 10^{-9} m²/s. The water velocities for poultices containing a low amount of kaolin (poultice with clay/sand ratios 1:5 and 1:7) do not show any significant differences between systems with paper and those without it (see figure 6.15). However, changes in the water flow velocity can be observed for the 1:3 (kaolin/sand) poultice. In that case the inclusion of the

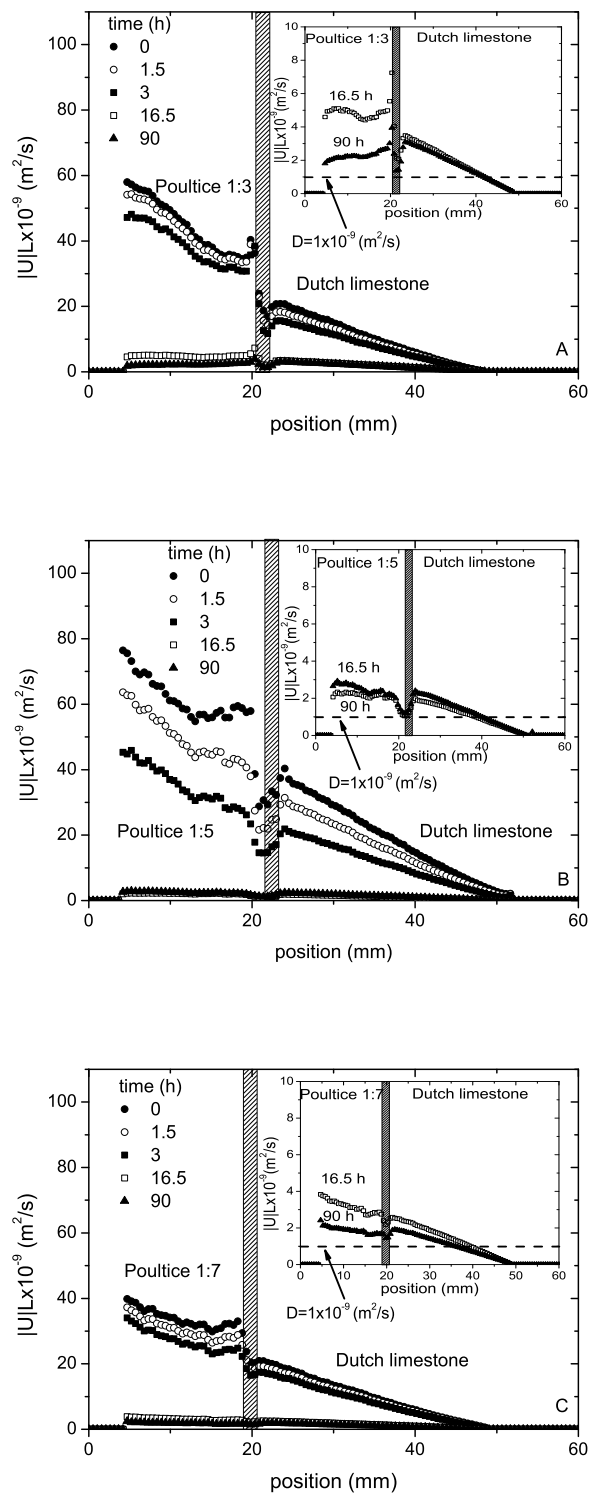


Fig. 7.6: Water velocity multiplied by the thickness of the substrate as a function of the position in the sample for every 1.5 hours during a drying process. A. Poultice with kaolin/sand ratio 1:3. B. Poultice with kaolin/sand ratio 1:5. C. Poultice with kaolin/sand ratio 1:7.

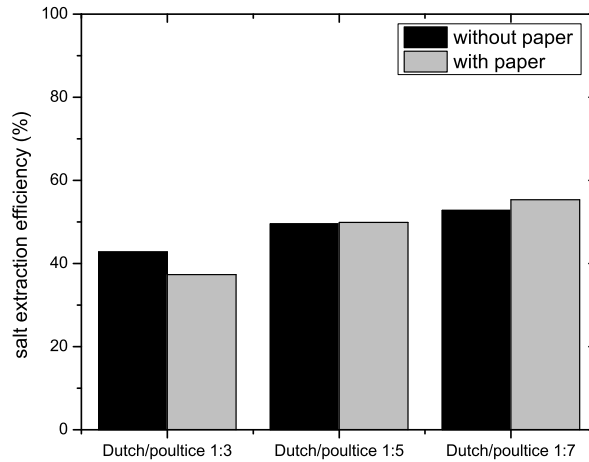


Fig. 7.7: Salt extraction efficiency for the Dutch limestone after treatments by different kaolin/sand poultices. The results are obtained from Ion Chromatography.

Japanese paper results in a lower drying rate.

The salt accumulated at the drying surface of the poultice will crystallize and can not be determined by NMR. In order to validate the total amount of the salt that was extracted from the substrate during the desalination each substrate was cut in three slices after the drying experiment and the total amount of sodium in these slices was measured quantitatively by ion chromatography (IC). The results of this analysis are shown in figure 7.7, which reveals that the uses of Japanese paper does not increase the efficiency of salt extraction. For the poultice with a clay/sand ratio of 1:3, the presence of the paper even seems to reduce the efficiency.

7.3 Conclusions

An intervention layer, such as Japanese paper is generally used by conservators to protect the treated object from leaving deposits on the surface. It was initially expected that Japanese paper would reduce the penetration of kaolin into the Dutch limestone substrate which would keep the effective pore size of the substrate large enough. However, the Japanese paper did not prove to be completely effective to protect penetration of kaolin into a substrate. The experiments have shown that the intervention layer does not increase the water flow from the poultice to the substrate. It should be noted, that for high amounts of kaolin present in the poultice the water flow in the poultice/substrate system is reduced. However, in our experiments a simple mixture was used for a poultice. Additional material in the poultice composition (for example cellulose) might change the water flow in the poultice/paper/substrate system.

8. CONCLUSIONS AND OUTLOOK

This chapter contains the main conclusions of the research described in this thesis. Also an outlook for future research on salt extraction by poulticing is given.

8.1 Conclusions

In this thesis it has been demonstrated that the extraction of salts from a substrate by a poultice can be realized by two different transport mechanisms, diffusion and advection. The advantages and disadvantages of both methods have been analyzed. The diffusion-based desalination methods theoretically can reach an efficiency of 100% and they are independent of the pore size distribution. However, these methods are rather slow; it will take weeks or months for these methods to be effective. Moreover, the poultice has to be renewed frequently, in order to maintain the salt extraction, and has to remain completely saturated with water for very long time. This could result in an additional damage, for example, due to dissolution of the substrate material. In contrast, the advection method is fast; the salt extraction can be conducted within days and less moisture can be introduced into the object. However, the main disadvantage of this method is that it is pore-size dependent. This method will work only if the poultice contains a significant quantity of pores that are smaller than those of the object. Therefore, the poultice has to be adapted to the material on which it will be used. If the object has rather small pores ($< 1\mu\text{m}$) it will be difficult to find a poultice material which has pores that are even smaller.

In this study we focused on a desalination by advection. Because of the presence of salt concentration differences, osmotic pressure gradients arise during the salt extraction. This in principle can change the drying behavior of the poultice/substrate system. With the help of drying experiments the effect of the osmotic pressure on the salt and moisture transport within porous materials was demonstrated. It has been shown that a saline solution in a porous material exerts an osmotic pressure which reduces the effective pore size of the material. These findings have potential practical implications for the optimization of poulticing treatments. As in practice salt is transported from the substrate to the poultice where it is accumulated, the effective pore size of the poultice will decrease. This will have a positive influence on the advection and hence improve the salt extraction process. Moreover, the longer a poultice stays in contact with the substrate, the more it will accumulate salt, and thereby the osmotic pressure is increased and the effective pore size of a poultice will become smaller.

The desalination poultice mixtures available on the market are predominantly based on materials (i.e. clay) which can shrink during drying and therefore may detach from the surface of the object to be desalinated. In order to reduce this effect a poultice is generally mixed with aggregates. Pore-size distribution measurements on clay/sand poultices by MIP showed that the ratio between the mixed materials may have an influence on the pore-size distribution. Since MIP measurements can be carried out only on a dry material, drying experiments has been performed on water saturated poultice. These experiments show that the chosen amount of sand does not influence the pore-size distribution of the poultice for clay/sand ratios between 1:3 and 1:7. The pore size distribution of the kaolin/sand poultice measured by MIP does not correspond to that inferred from the poultice/substrate drying behavior. The arrangement of kaolin and sand particles in the wet state differs from the dry state. In its wet state all interstitial spaces between the sand grains are filled with kaolin particles which are suspended in water. As the poultice dries, the kaolin tends to agglomerate in the interstitial spaces between sand grains thus partially filling the interstitial pores in the sand. This reduced interstitial porosity is measured by MIP.

Our study is also shown that it may be problematic to use clay/sand poultices on substrates with large pores, like Dutch limestone. Clay may penetrate into the large pores, which can reduce the effective pore sizes of the substrate in the region near surface. Therefore, the drying behavior of the poultice/substrate system changes significantly. In order to prevent the poultice from penetrating an intervention layer has be used. Our experiments have shown that an interventional layer of Japanese paper does not influence the water flow from the poultice to the substrate when the applied poultice contains a low amount of kaolin. When high amounts of kaolin are present in the poultice, a decrease of the water flow in the poultice/substrate system has been observed.

8.2 *Outlook*

Our research on moisture and salt transport in poultice/substrate systems has resulted in a lot of information that can be used in practice. Despite of these potential practical improvements there are still many open questions, which will be discussed in this section.

Firstly, this study focuses on a salt transport from a substrate into a poultice considering an advection process. However, in general a desalination treatment consists of two steps. In the first one, water penetrates from the poultice into the substrate and dissolves the salt. In the second one, the salt ions are transported from the substrate into the poultice. The present study has demonstrated that in order to make the salt accumulate in the poultice during the second step of desalination, the substrate has to dry prior to the poultice. This can be realized when the poultice has smaller pores than the substrate. However, to realize water penetration from a poultice into a substrate during the first step of the desalination process a different pore-size distribution of the poultice is required. In this case, the poultice must have pores larger than the substrate so that the substrate can absorb water from the poultice. When water will flow

from a poultice into a substrate there is a risk of transporting salts that are accumulated just below the surface of the substrate deeper into the substrate. In order to control the wetting of the substrate research should be done on moisture and salt transport during both steps of the desalination process. The investigation of the controlled wetting of the substrate by poultice which also is intended to act as a reservoir for water is required.

Secondly, in our study we have only investigated the transport and accumulation of NaCl, since it is a simple salt which, for instance, does not show supersaturation. It is obvious that other more complicated salts (like Na₂SO₄) also cause damages in building materials. Na₂SO₄ may show a supersaturation depending on temperature and relative humidity. It would be interesting to investigate transport and accumulation of these types of salt during a salt extraction treatment.

Thirdly, in our experiments we used only one type of poultice which consists of a kaolin/sand mixture. However, kaolin is not generally used in the field, since it leaves a white deposit on the desalinated object, which is usually not acceptable. Nevertheless, this type of clay was selected because of the fact that the shrinkage of kaolin during drying is relatively low. An alternative may be bentonite clay. The advantage of this clay is that it does not leave any deposit. A significant disadvantage is that bentonite shrinks a lot during drying. Moreover, a clay/sand poultice is not the only combination of materials which is used in the field. The investigation of the effect of other combinations of poultice materials (as for instance, a mixture containing cellulose) is required.

Finally, we used Japanese paper as an intervention layer. This paper is generally used by conservators to protect the object which has to be treated from deposits on the surface. However, in the literature no references were found about the penetration of clays through paper. It should be noted, that in our experiments a simple mixture for the poultice was used without additional materials which can change the water flow in the poultice/paper/substrate system. It may be worthwhile to investigate the moisture and salt transport in such systems in the presence of additional materials in the poultice.

APPENDIX A. BOLTZMANN'S TRANSFORMATION

The diffusion of ions can be generally described using the following non-diffusion equation:

$$\frac{\partial C}{\partial t} = \frac{\partial}{\partial x} \left(D \frac{\partial C}{\partial x} \right) \quad (8.1)$$

with the boundary conditions $C = 0$ at $x = 0$, $C = C_0$ for $x \rightarrow \infty$, $t > 0$ and initial conditions $C = C_0$ at $x > 0$ and $t = 0$. If D is constant, this gives rise to equation 2.2, Fick's second law of diffusion. Here we will assume that within the experimental time the sample can be regarded as semi-infinite.

One can now introduce the so-called Boltzmann-Matano transformation by introducing a new variable [Mat32]:

$$\lambda = \frac{x}{\sqrt{t}}. \quad (8.2)$$

Accordingly, we obtain the spatial derivative:

$$\frac{\partial C}{\partial x} = \left(\frac{\partial C}{\partial \lambda} \right) \left(\frac{\partial \lambda}{\partial x} \right) = \frac{1}{\sqrt{t}} \frac{\partial C}{\partial \lambda}. \quad (8.3)$$

and the corresponding time derivative:

$$\frac{\partial C}{\partial t} = \left(\frac{\partial C}{\partial \lambda} \right) \left(\frac{\partial \lambda}{\partial t} \right) = -\frac{x}{2t^{3/2}} \frac{\partial C}{\partial \lambda}. \quad (8.4)$$

Hence equation 8.1 can be rewritten as:

$$-\frac{\lambda}{2} \frac{dC}{d\lambda} = \frac{d}{d\lambda} \left(D \frac{dC}{d\lambda} \right). \quad (8.5)$$

With the new boundary conditions $C = 0$ at $\lambda = 0$, $C = C_0$ for $\lambda \rightarrow \infty$, $t > 0$ and initial conditions $C = C_0$ at $\lambda > 0$ and $t = 0$. Since equation 8.5 is an ordinary differential equation with fixed boundary conditions, it has only one solution. Hence all concentration profiles can be scaled with λ , which as stated in equation 8.2 is proportional to the square root of time.

APPENDIX B. WATER VELOCITY

In the case of a porous material the conservation of mass can be written as:

$$\frac{\partial \theta}{\partial t} = -\frac{\partial}{\partial x} (\theta U) \quad (8.6)$$

where U is the water velocity. If the moisture content is known as a function of the position and time, the velocity can be derived directly after integration:

$$U(x) = \frac{1}{\theta(x)} \frac{\partial}{\partial t} \int_x^l \theta(x') dx'. \quad (8.7)$$

In this formula l is length of the sample and $\int_x^l \theta(x') dx'$ is the integral of the moisture content over the sample from position x to l . Here we have assumed the end of the sample is closed and there is no drying.

In the case of the constant drying rate one can approximate the moisture content in the sample during the constant drying rate period by:

$$\theta = \theta_0 - \alpha t \quad (8.8)$$

Hence the velocity is given by:

$$U(x) = -\frac{\alpha}{\theta_0 - \alpha t} (l - x). \quad (8.9)$$

REFERENCES

- [Ahl04] J. Ahl, Salt diffusion in brick structures, *Journal of Material Science*, 39:247-4254, 2004 9
- [Arn91] A. Arnold and K. Zehnder, Monitoring wall paintings affected by soluble salts, *The Conservation of Wall Paintings* S. Cather (ed), The Getty Conservation Institute, Los Angeles, 1991 23, 53
- [Aun01] K.K. Aung, H. Rahardjo, E.C. Leong and D. G. Toll, Relationship between porosimetry measurement and soil-water characteristic curve for an unsaturated residual soil, *Geotechnical and Geological Engineering*, 19:401-416, 2001 50
- [Aur08] M. Auras, Poultrices and mortars for salt contaminated masonry and stone objects, *Salt Weathering on Buildings and Stone Sculptures, Proceedings from the International Conference, The National Museum Copenhagen*, pp. 197-217, 22-24 October 2008 24
- [Alb87] R.A. Alberty, *Physical chemistry*, 7th ed. John Wiley and Sons, New York, 1987
- [And84] E.R. Andrew, A historical review of NMR and its clinical applications, *British Medical Bulletin*, 40:115-119, 1984 6
- [Avd03] N.P. Avdelidis, A. Moropoulou, Applications of infrared thermography for the investigation of historic structures, *Journal of Cultural Heritage*, 5:119-127, 2004 88
- [Bea90] J. Bear and Y. Bachmat, *Introduction to Modeling of Transport Phenomena in Porous Media*. Kluwer, Dordrecht, 4, 1990 9, 13, 17, 60
- [Ber04] M.A. Bernstein, K. F. King and X.J. Zhou, *Handbook of MRI pulse sequences*, Elsevier Academic Press, London, 2004 44
- [Bou08a] A. Bourges, V. Verges-Belmin, Comparison and optimization of five desalination systems on inner walls of Saint Philibert church in Dijon, France, *Salt Weathering on Buildings and Stone Sculptures, Proceedings from the International Conference, The National Museum Copenhagen*, pp. 29-41, 22-24 October 2008 13, 20
- [Bou08b] A. Bourges, V. Verges-Belmin, A new methodology to determine rheologic behaviour and mechanical properties of desalination poultrices, *Proceedings from the 11th International Congress on deterioration and conservation of stone, Torun*, 15-20 September 2008 4

- [Bou08c] E. Bourguignon, F. Bertrand, A. Bourges, P. Coussot and N. Shahidzadeh-Bonn, Poulitice characterization and MRI study of desalination of model stones, Salt Weathering on Buildings and Stone Sculptures, Proceedings from the International Conference, The National Museum Copenhagen, pp. 329339, 22-24 October 2008 20
- [Bow75] M.J. Bowley, Desalination of stone: A case study, Building Research Establishment Current Paper CP46/75, Watford, 1975 3
- [Bro79] K.R. Brownstein, and C.E. Tarr, Importance of classical diffusion in NMR studies of water in biological cells, Physical Review A, 19:24462453, 1979 46
- [Cal91] P.T. Callghan, Principles of Nuclear Resonance Microscopy, Oxford Science Publications, New York, 1991 41, 44
- [Cam85] G.S. Campbell, Soil Physics with Basic, Transport Models for Soil-Plant Systems, Elsevier, Amsterdam, 1985
- [Car54] H.Y. Carr and E.M. Purcell, Effects of diffusion on free precession in nuclear magnetic resonance experiment, Physical Review, 94:630-638, 1954 45
- [Clo91] A. Cloutier and Y. Fortin, Moisture content-water potential relationship of wood from saturated to dry conditions, Wood Science and Technology, 25:263-280, 1991 48
- [Cor47] C.W. Correns, Growth and dissolution of crystals under linear pressure, Faraday Discussion Society, 5: 267-271, 1949
- [Dul91] Dullien, Porous media: fluid transport and pore structure, Academic Press, London, 1991 9, 13
- [Eij05] J.C.T. Eijkel and A. Berg, Water in micro- and nanofluidics systems described using the water potential, The Royal Society of Chemistry, 5: 1202-1209, 2005
- [Eng88] P. Englezos and P.R. Bishnoi, Prediction of gas hydrate formation conditions in aqueous electrolyte solutions, AIChE Journal, 34: 1718-1721, 1988 28
- [For79] Y. Fortin, Moisture content-matric potential relationship and water flow properties of wood at high moisture contents, Ph.D. thesis, The University of British Columbia, pp. 187, 1979. 48
- [Gal01] C. Gallé, Effect of drying on cement-based materials pore structure as identified by mercury intrusion porosimetry. A comparative study between oven-, vacuum-, and freeze-drying, Cement and Concrete Research, 31: 1467-1477, 2001
- [Gou97] A. Goudie and H. Viles, Salt weathering hazard, Wiley, Chichester, 1997 1, 23, 53

- [Hah50] E.L. Hahn, Spin echoes, *Physical review*, 80: 580-594, 1950 44
- [Hal02] C. Hall and W.D. Hoff, *Water transport in brick, stone and concrete*, Spon, London, 2002
- [Her420] Herodotus, *History*, 420BC 1
- [Her08] A. Heritage, A. Sawdy, A. Funke, F. Vergès-Belmin, A. Bourgès, How do conservators tackle desalination? Proceedings from the 8th European Conference on Research for Protection, Conservation and Enhancement of Cultural Heritage, Ljubljana, 10-12 November 2008 3, 8, 24
- [Hui02] H.P. Huinink, L. Pel and M.A.J. Michels, How ions distribute in a drying porous medium - A simple model, *Phys. Fluids*, 14:1389-1395, 2002 17, 61
- [Kro99] B. Kroes, *The influence of material properties on drying kinetics*, PhD Thesis, Eindhoven University of Technology, 1999 50
- [Kru97] M. Krus, K. Kießl, Determination of the moisture storage characteristics of porous capillary active materials, *Materials and Structures*, 31:522-529, 1998 49
- [Lar90] E.S. Larsen, C.B. Nielsen, Decay of bricks due to salt, *Materials and Structures*, 23:1625, 1990
- [Lav53] M. Lavalle, Recherches sur la formation de cristaux á la température ordinaire, *Les Comptes rendus de l'Académie des sciences*, 34:493-495, 1853 1
- [Let69] J. Letey, W.D. Kemper and L. Noonan, The effect of osmotic pressure gradients on water movment in unsaturated soil, *Soil Science Society of America Journal*, 33:15-18, 1969 5, 24
- [Lew80] S.Z. Lewin, *The mechanism of masonry decay through crystallization, conservation of hystoric stone buildidings and monumnets*, National Academic Press, Washington, 1980 1, 23, 53
- [Lub10] B. Lubelli R.P.J. van Hees, Desalination of masonry structures: Fine tuning of pore size distribution of poultices to substrate properties, *Journal of Cultural Heritages*, 11:10-18, 2010 24, 62, 69, 70
- [Man03] M.D. Mantle and A.J. Sederman, Dynamic MRI in chemical process and reaction engeneering, *Progress in Nuclear Magnetic Resonance Spectroscopy*, 43:3-60, 2003 6
- [Mat32] C. Matano, On the relation between the diffusion coefficients and concentrations of solid metals (the nickel-copper system), *Japan J Phys*, 8: 109-113, 1932 99

- [Mar10] I. Martnez-Arkarazo, A. Sarmiento, M. Maguregui, K. Castro, J. M. Madariaga, Portable Raman monitoring of modern cleaning and consolidation operations of artworks on mineral supports, *Anal Bioanal Chem*, 397(7):2717-2725, 2010 88
- [Mor33] H. Mortensen, Die "Salzsprengung" und ihre bedeutung fur die regional-klimatische gliederung der wusten, *Petermanns Geographische Mittheilungen* 5: 130-135, 1933
- [Nas89] I.N. Nassar and R. Horton, Water transport in unsaturated nonisothermal salt soil: I. Experimental results, *Soil Science Society of America Journal*, 53: 1323-1329, 1989 5, 24
- [Ngu08] T.Q. Nguyen, J. Petkovic, P. Dangla, V. Baroghel-Bouny, Modelling of coupled ion and moisture transport in porous building materials, *Construction and Building Materials*, 22: 2185-2195, 2008 5, 24
- [Nob83] P.S. Nobel, *Biophysical plant physiology and ecology*, W.H. Freeman and Co., San Francisco, 1983
- [Pel95] L. Pel, *Moisture Transport in Porous Building Materials*, Ph.D. thesis, Eindhoven University of Technology, 1995 30, 62
- [Pel00] L. Pel, K. Kopinga, E.F. Kaasschieter, Saline absorption in calcium-silicate brick observed by NMR scanning, *Journal of Physics D*, 33: 1380-1385, 2000 6, 46, 62
- [Pel02] L. Pel, H. Huinink, K. Kopinga, Ion transport and crystallization in inorganic building materials as studied by nuclear magnetic resonance, *Applied Physics Letters* 81: 2893-2895, 2002 30, 62
- [Pel10] L. Pel, A. Sawdy, and V. Voronina, Physical principles and efficiency of salt extraction by poulticing, *Journal of Cultural Heritage*, *Journal of Cultural Heritage*, 11: 59-67, 2010 5, 18, 24, 28, 33, 53, 54
- [Pet05] J. Petkovic, *Moisture and ion transport in layered porous building materials: a Nuclear Magnetic Resonance study*, PhD Thesis, Eindhoven University of Technology, 2005 14, 16, 19
- [Pet07] J. Petkovic, H.P. Huinink, L. Pel, K. Kopinga and R.P.J. van Hees, Salt transport in plaster/substrate layers, *Materials and structures*, 40: 475-490, 2007 14, 16, 30
- [Poz99] Po-Zen Wong, *Methods in the physics of porous media*, Academic press, London, 1999
- [Rat15] F. Rathgen, *Die Konservierung von Altertumsfunden*, Berlin, 1915 2
- [Rod08] C. Rode, K. Grau, Moisture Buffering and its Consequence in Whole Building Hygrothermal Modeling, *Journal of Building Physics*, 31: 333-360, 2008

- [Ric48] L.A. Richards, Porous plate apparatus for measuring moisture retention and transmission by soil, *Soil Science*, 66:105-109, 1948 48
- [Rij04] L. Rijniers, Salt crystallization in porous materials: an NMR study, Ph.D. thesis, Technical University of Eindhoven, 2004
- [Rit45] H.L. Ritter and L.C. Drake, Pressure Porosimeter and Determination of Complete Macropore-Size Distributions. Pressure Porosimeter and Determination of Complete Macropore-Size Distributions, *Industrial and Engineering Chemistry Analytical Edition*, 17: 782-786, 1945 49
- [Saw08] A. Sawdy, A. Heritage and L. Pel, A review of salt transport in porous media, assesment methods and salt reduction treatments, Proceedings from the Internetenal Conference, Salt Weathering on Buildings and Stone Sculptures, The National Museum Copenhagen, 22-24 October 2008 3, 5, 8
- [Saw10] A. Sawdy, B. Lubelli, V. Voronina, F. Funke and L. Pel, Optimising the extraction of soluble salts from porous materials by poultices, *Studies in Conservation*, 55: 26-40, 2010 5, 24, 33
- [Sch99] G.W. Scherer, Crystallization in pores, *Cement and Concrete Research*, 29:13471358, 1999
- [Sma75] H. Small, T.S. Stevens, W.C. Baumann, Novel ion exchange chromatographic method using conductimetric detection, *Analytical Chemistry*, 47: 1801-1809, 1975 50
- [Ott07] L. M. Ottosen, I. Rørig-Dalgård, Electrokinetic removal of $Ca(NO_3)_2$ from bricks to avoid salt-induced decay, *Electrochimica Acta*, 52: 3454-3463, 2007
- [Uem87] Y. Uemura, Y. Hatate, A. Ikari, Formation of nickel concentration profile in nickel/alumina catalyst during post-impregnation drying, *Journal of Chemical Engineering of Japan*, 20: 117-123, 1987 27
- [Ver05] F. Vergès-Belmin and H. Siedel, Desalination of masonries and monumental sculptures by poulticing: A review, *Restoration of Building and Monuments*, 11: 1-18, 2005
- [Vor11] V. Voronina, L. Pel, A. Sawdy, K. Kopinga, The influence of osmotic pressure on poulticing treatments for cultural heritage objects, submitted in *Journal of Materials and Structures*, 2011 3, 8, 24, 53
- [Was21] E.W. Washburn, Note on a method of determining the distribution of pore sizes in a porous material, *Proceedings of the National Academy of Sciences of the USA*, 7: 115-116, 1921 54, 58, 66
- [Web97] P.A. Webb and C. Orr, *Analytical Methods in Fine Particle Technology*, Micromeritics Instrument Corporation, Norcross, 1997 49
50

- [Whe25] L.C. Wheeting, Certain relationship between added salts and the moisture of soils, *Soil Science*, 19:287-299, 1925 5, 24
- [Wil88] C.R. Wilke, Diffusion in Gases and Liquids, Physical chemistry source book, McGraw-Hill, London, 122-128, 1988
- [Won99] Po-Zen Wong, Methods in the Physics of porous media, Academic press, San Diego, 1999 48
- [Woo00] C. Woolfitt and G. Abrey, The true or plain poultice and the cleaning and desalination of historic masonry and sculpture, *The Building Conservation Directory*, 2000

LIST OF PUBLICATIONS

The influence of osmotic pressure on poulticing treatments of cultural heritage objects, V.Voronina, L.Pel, A.Sawdy and K.Kopinga, *Construction and Building Materials*, submitted 2011

Physical principles and efficiency of salt extraction by poulticing, L. Pel, A. Sawdy, and V. Voronina, *Journal of Cultural Heritage*, 11: 59-67, 2010

Optimising the extraction of soluble salts from porous materials by poultices, A. Sawdy, B. Lubelli, V. Voronina, F. Funke and L. Pel, *Studies in Conservation*, 55: 26-40, 2010

L .Pel, V. Voronina and K.Kopinga, Desalination of historical objects as studied by NMR, *The Book of Proceedings of 9 th International Bolonga Conference on Magnetic Resonance in Porous Media (MRPM9)*, Cambridge, 2008

De fysische principes achter en de effectiviteit van het ontzoutingsmethoden, L. Pel, N. van Gils, and V. Voronina, *WTA*, Bergen op Zoom, The Netherlands, 2008

ACKNOWLEDGEMENT

This book would not be in your hands without the support of a lot of people over the past years. At the end of the thesis I would like to thank all people who directly or indirectly contributed to this thesis. First I would like to express my gratitude to my professor and promoter, Prof. Klaas Kopinga, who gave me the opportunity to do this PhD in his group and provided me with inspiration for my research. I would like to thank my copromotor and direct supervisor dr.ir. Leo Pel, for his help to carry on ideas for experiments. Also, the way that this thesis is written has a strong influence of the valuable comments of Dr. ir. Leo Pel. I would also like to express my gratitude to the members of the committee for their time and energy in reading this document: Prof. Fulvio Zezza, Prof. Norman Tennet, and Prof. David Smeulders.

I would like to show my gratitude to the whole TPM and BTM group for creating an excellent research friendly atmosphere, for group activities and birthday cakes and for valuable discussions during meetings. Henk, I would like to thank you for the generosity in sharing your time and the broad knowledge in theoretical aspects. Bart, I appreciate your help with the Comsol. Olaf, thank you for giving me a lot of delighted comments and remarks during our group meetings. Hans, thank you for helping me a lot in a chemical lab with the sample preparation, the fast ordering and with all innumerable ion chromatography measurements. Jef, without your engineering talent I would never cope to reanimate the NMR set up, I would like also to thank you for your great soul. Larry, Jo, Jeanine, Gustav, Desiree thank you for your interest to my life and work.

During my PhD I shared the office with Gijs, Kashif, Paul and Pim. I can't help says that it was pleasure pure for me. Gijs, I would like to thank you for being a great room-mate and as you were sitting next to me you contributed a lot by answering all my questions and helping me with NMR set-up beyond your own work. Kashif, I will never forget all the scientific and non-scientific chats, your thoughtful words and support. Pim, I have never possessed the special batch for Van der Waals bar, without you I would never join such nice parties that happen every Thursday. Tamerlan and Victor thank you for unforgettable lunch discussions whether they were about political issues or they were scientific related, anyway they have made a major influence upon my vision and work. Mirjam, Nick, Paul thank you for our interesting research-related discussions and for your company. Sonia, and Nico thank you for agreeing to be my paranimfs. I had also the opportunity to guide students during IFP project together with Jan Botman and Prof.dr ir Frans Sluijter. It was a great experience, thank you.

I would like to express my gratitude to our very efficient secretaries: Ria Groenendijk Marlouke Creemers-Samuels and Hedwig for dealing perfectly with

all administrative work and also for organizing group meetings, BBQ's and special events. Karin, special thanks to you for finding gaps in a very busy Klaas schedule and for being so friendly and kind to me.

I would like to express my gratitude to all the people who were involved in Desalination project, in particular Alison Heritage, Barbara Lubelli, Eloisa Dispio, Friederike Funke, Rob van Hees, Vronique Vergs-Belmin, Ann Bourgs, Eric Doehne, and Adrian Heritage for continuously generating new ideas and suggestions.

I would like to thank Research department: Jos, Ramin, Michel, Tamara, Andriy, Andrei, Paul, Nico, Niek, Diederik, Raymond, Rogier, Yogesh, Frits, Hein, Sander, Jim, Laurens, Rob, Daniel, Mirjam, Bas, Irina for warm welcome in a team, for the support and confidence revealed during the last year of my work on the thesis.

Also thanks to all other many people who came across during the past 5 years, it was pleasure for me to work with you.

Going back in time, I would like to thank my former supervisor in the Saint-Petersburg State University, Dr. Grigory Druzhinin for the wonderful work, for the pleasant cooperation and the advice he gave me. Svetlana Vladimirovna, thank you for your kindness and being so nice to me. Thank you for coming to visit us in Eindhoven!

Natalia you are my best friend, always supporting and caring about me. You often helped me see things in a new light and gave me needed energy at times when, I was depressed. I would like to thank you for everything, for all the nice evenings, dinners and "evening readings". Pino, I remember all the fun we had in Switzerland. Thank you for the special way you took good care of me. We have to schedule our next meeting, I promise to avoid "penguin falling" next time. Heico, thank you for being the best ear during all time I know you. Tamara, thank you for being a great twin-friend. Thank you very much for all tips you gave me during the most stressful time, for your support, for helping me in the design of my thesis and of course for your delicious jam. I would like to thank Dana for his advises in writing important letters. Roland and Mirjam I will never forget the most exciting time I spent at your shop (especially before my wedding), wonderful wine contest and your visit in Saint-Petersburg. Oleksii, thank you for sharing the university life with me over the last year and for your friendship. Stella and Ruud, thank you for for a great host at your place and great time we spent together. Paulin, I am happy to have such a great Dutch teacher. During our lessons you patiently were listening to all my dramatic stories. Thank you very much to be so kind to me. Masha, thank you for all your visits which you paid to Eindhoven during past 5 years. Alex, I know you so long that I am even afraid to say how long. Thank you for being there when I needed you the most, for being such a good friend no matter what I did. Johan, thank you for keeping speak Dutch to me. Andriy, I will never forget your moral support. Tanja, Yurii, Anja, Robert you are the first friends I met in Eindhoven. I remember all the good time we spent together and hopefully much more will come! Keep in touch. Andrei, thank you for the advice you gave me, coffee breaks talks often helped dealing with PhD issues.

Finally, a big Thank you goes to my family. Loec, Wim, Angelique, April,

Rachil, thank you that you have become my Dutch family. Papa and Mama, I want to thank you for raising me with a love. Your strong faith and confidence and trust in me have are created me to be the person I am today. Thank you for all the support and opportunities you gave me over the all years. My dear Granny Victoria, thank you for all your love and support in all my pursuits. I always looked up to you and try to live by such a great example. Maikel, words fail me to express my appreciation of your love, confidence in me and faithful support.

CURRICULUM VITAE

Victoria Voronina was born on May 6, 1982, in Saint-Petersburg (Russia). After finishing the secondary education in 1999 at General Secondary School N 242, she started her study at the Saint-Petersburg State University (Russia). In 2006 Victoria obtained Master degree in Applied Physics under supervision of Docent G. Druzhinin. The work of the master program was focused on oscillating gas bubble heat exchange. In 2006 she started a PhD project at the Eindhoven University of Technology in the group Transport in Permeable Media. The most important results of the PhD work are described in this thesis.

